

**SYNTHESIS AND CHARACTERIZATION OF NORBORNENE-
FUNCTIONALIZED SIDE-CHAIN MONOMERS FOR POTENTIAL
USE AS TRANSPORT MATERIALS IN ORGANIC LIGHT-
EMITTING DIODES**

A Thesis
Presented to
The Academic Faculty

by

LaKeisha Michelle McClary

In Partial Fulfillment
of the Requirements for the Master's Degree
Chemistry in the
School of Chemistry and Biochemistry

Georgia Institute of Technology
December 2007

COPYRIGHT BY LAKEISHA MICHELLE MCCLARY

**SYNTHESIS AND CHARACTERIZATION OF NORBORNENE-
FUNCTIONALIZED SIDE-CHAIN MONOMERS FOR POTENTIAL
USE AS TRANSPORT MATERIALS IN ORGANIC LIGHT-
EMITTING DIODES**

Approved by:

Dr. Seth Marder, Advisor
School of Chemistry and Biochemistry
Georgia Institute of Technology

Dr. Jean-Luc Brédas
School of Chemistry and Biochemistry
Georgia Institute of Technology

Dr. Laren Tolbert
School of Chemistry and Biochemistry
Georgia Institute of Technology

Date Approved: November 12, 2007

I dedicate this thesis to my mother and my grandparents whose prayers, support, and motivation are my foundation.

ACKNOWLEDGEMENTS

I wish to thank Dr. Seth Marder for his patience, his support, and his guidance. I would like to express gratitude and appreciation for members of the Marder group who challenged me, helped me, and encouraged me. I especially appreciate Dr. Stephen Barlow, Dr. Jian-Yang Cho, and Dr. Simon Jones. Lastly, I want to acknowledge my friends who grounded me, especially Jennifer Barber-Brown, Peter Hotchkiss, Ejae John, and Susan Odom.

TABLE OF CONTENTS

	Page
ACKNOWLEDGEMENTS	iv
LIST OF TABLES	vii
LIST OF FIGURES	viii
LIST OF SYNTHETIC SCHEMES	x
LIST OF ABBREVIATIONS	xi
SUMMARY	xiii
<u>CHAPTER</u>	
1 INTRODUCTION TO ORGANIC LIGHT-EMITTING DIODES	1
Historical Background of OLEDs	1
Structure of OLEDs	1
Operation of OLEDs	3
Characteristics of OLEDs that Affect Electroluminescence	4
Advantages of OLEDs to Other Display Technologies	7
Side-Chain Polymers: A Method to Improve OLEDs	8
Previous Work on Side-Chain Polymers by Our Group	9
Current Direction of Our Work	10
References	10
2 SYNTHESIS AND CHARACTERIZATION OF NORBORNENE-FUNCTIONALIZED TPD MONOMERS	19
Introduction	19
Results and Discussion	22
Experimental Details	31

References	43
3 SYNTHESIS AND CHARACTERIZATION OF NORBORNENE-FUNCTIONALIZED 1,10-PHENANTHROLINE MONOMERS	49
Introduction	49
Results and Discussion	54
Experimental Details	74
References	82
4 CONCLUSIONS	85
APPENDIX: ^1H AND ^{13}C SPECTRA OF NOVEL TPD ESTERS	87

LIST OF TABLES

	Page
Table 2.1: Redox Potentials of TPD Derivatives	31
Table 3.1: Redox Potentials of 1,10-Phenanthroline Derivatives	70
Table 3.2: Redox Potentials of 1,10-Phenanthroline Derivatives	73

LIST OF FIGURES

	Page
Figure 1.1: Diagram of a Typical Bilayer OLED	2
Figure 1.2: Structures of Commonly Used Transport Materials	2
Figure 1.3: Diagram of EL in a Bilayer OLED under Applied Voltage	3
Figure 1.4: Schematic Representation of a Hopping Mechanism in TPD	3
Figure 1.5: Exciplex Formation in <i>m</i> -MTDATA and Alq ₃	6
Figure 1.6: Structures of DEC and TNF	6
Figure 2.1: Structures of Target Norbornene-Functionalized TPD Monomers	21
Figure 2.2: Proposed Mechanism to Form <i>N</i> -(<i>m</i> -Tolyl)- <i>N</i> -phenyl-4-bromo-1,1'-biphenyl-4'-amine	23
Figure 2.3: Structure of Side Product, <i>N</i> -(<i>m</i> -Tolyl)- <i>N</i> -phenyl-1,1'-biphenyl-4'-amine	24
Figure 2.4: Structures of Target <i>exo</i> -Norbornene Bromides	28
Figure 3.1: Structures of Commercially Available 1,10-Phenanthrolines	48
Figure 3.2: AM1 Theoretical Energy Values for 1,10-Phenanthroline Derivatives	51
Figure 3.3: Structure of 1,10-Phenanthroline Derivatives for Electrochemical Studies	52
Figure 3.4: Structures of Norbornene-Functionalized 1,10-Phenanthrolines	53
Figure 3.5: Structures Related to the Synthesis of a 2-Substituted-phenanthroline Monomer	57
Figure 3.6: Expected Products Formed by Reacting a Grignard Reagent with Benzyl Bromide or Benzaldehyde	60
Figure 3.7: Reactions to Reduce or to Esterify 2-Carboxy-1,10-phenanthroline	61
Figure 3.8: Structure of 5,6-Dihydro-5,6-diol-1,10-phenanthroline	63
Figure 3.9: Structures of Starting Materials Used to Synthesize 5-Methoxy-1,10-phenanthroline	66
Figure 3.10: Cyclic Voltammogram of 2-Cyano-1,10-phenanthroline in THF	69

Figure 3.11: Graph of First Reduction Potentials of 1,10-Phenanthroline Derivatives in Acetonitrile and THF.

71

LIST OF SYNTHETIC SCHEMES

	Page
Scheme 2.1: Synthesis of <i>N</i> -(<i>m</i> -Tolyl)- <i>N</i> -phenyl-4-bromo-1,1'-biphenyl-4'-amine	22
Scheme 2.2: Synthesis of <i>N</i> , <i>N'</i> -(<i>m</i> -Tolyl)- <i>N</i> -[4 -(bicyclo[2.2.1] hept-2-enylpentoxy)-phenyl]- <i>N'</i> -phenyl-1,1'-biphenyl amine	25
Scheme 2.3: Modified Synthesis of <i>N</i> , <i>N'</i> -(<i>m</i> -Tolyl)- <i>N</i> -[4 -(bicyclo[2.2.1] hept-2-enylpentoxy)-phenyl]- <i>N'</i> -phenyl-1,1'-biphenyl amine	26
Scheme 2.4: Synthesis of <i>exo</i> -3-(4-((4'-(Phenyl (<i>m</i> -tolyl) amino) biphenyl-4-yl) (<i>m</i> -tolyl amino) phenoxy) propyl bicyclo[2.2.1] hept-5-ene-2-carboxylate	29
Scheme 2.5: Synthesis of <i>endo/exo</i> -3-(4-((4'-(Phenyl (<i>m</i> -tolyl) amino) biphenyl-4-yl) (<i>m</i> -tolyl amino) phenoxy) propyl bicyclo[2.2.1] hept-5-ene-2-carboxylate	30
Scheme 3.1: Synthesis of 2-Carbinol-1,10-phenanthroline and 4-(1,10-Phenanthroline-5-yloxy) butan-1-ol	54
Scheme 3.2: Synthesis of Pentyl phenanthroline ketone	57
Scheme 3.3: Synthesis of 2-Substituted Norbornene Monomers	60
Scheme 3.4: Synthesis of 5-Ethoxy-1,10-phenanthroline	66
Scheme 3.5: Synthesis of 5-Substituted Norbornene Monomers	66

LIST OF ABBREVIATIONS

Alq ₃	tris(8-oxyquinolato)aluminum
anh.	anhydrous
BCP	2,9-dimethyl-4,7-diphenyl-1,10-phenanthroline, bathocuproine
Bphen	4,7-diphenyl-1,10-phenanthroline, bathophenanthroline
BPS	(<i>tert</i> -butyl)diphenylsilane
DCC	dicyclohexylcarbodiimide
DMAP	<i>N,N</i> -dimethylaminopyridine
DMF	<i>N,N</i> -dimethylformamide
DMSO	dimethyl sulfoxide
DPPF	1,1'-bis(diphenylphosphino)ferrocene
ETM	electron transport material
GC-MS	gas chromatography-mass spectroscopy
HBL	hole blocking layer
HOMO	highest occupied molecular orbital
HTM	hole transport material
LUMO	lowest unoccupied molecular orbital
NMR	nuclear magnetic resonance
NPB	4,4'-bis(1-naphthyl-phenylamino)biphenyl
Pd ₂ (dba) ₃	tris(dibenzylideneacetone)dipalladium (0)
PDI	polydispersity index
SEC	size exclusion chromatography
TBAF	tetrabutyl ammonium fluoride

THF	tetrahydrofuran
TPD	4,4'-bis(phenyl- <i>m</i> -tolylamino)biphenyl
tol	toluene
TLC	thin liquid chromatography

SUMMARY

We have synthesized norbornene-functionalized side-chain monomers for potential use as hole transporting and electron transporting/hole blocking materials in organic light-emitting diodes. TPD-norbornenes were prepared. The monomers demonstrated similar electrochemical and absorbance spectra to the parent TPD small-molecule. The similarity is promising for their use in OLEDs because TPD is a known blue-emitter with relatively high hole mobility in amorphous thin films.

1,10-Phenanthroline small molecules and monomers were synthesized to explore their potential as hole blocking materials in multilayer devices. We had difficulty purifying the monomers; however, the small molecules were slightly easier to reduce than commonly used hole blocking materials 2,9-dimethyl-4,7-diphenyl-1,10-phenanthroline (BCP) and 4,7-diphenyl-1,10-phenanthroline (Bphen).

Work on these projects continues, and we hope to discover the utility these compounds have for use in OLEDs and other opto-electronic devices.

CHAPTER 1

INTRODUCTION TO ORGANIC LIGHT-EMITTING DIODES

Historical Background of OLEDs

Electroluminescence (EL) is the emission of photons when an electron and a hole recombine to give an excited molecule that then radiatively relaxes to the ground state. Helfrich and Schneider first reported the phenomenon of EL from single crystals of anthracene when they observed fluorescence after applying an external voltage using electrodes.¹ In the late 80s, Tang and VanSlyke and Adachi *et al.* independently developed an operational organic light-emitting diode (OLED) using EL organic dyes.^{2,3} The devices required lower drive voltages and produced brighter light than previous research reported. In 1990, Burroughes *et al.* documented EL in conjugated polymers.⁴ With these key discoveries, scientists were able to propel OLED research from pure academic interest into a viable field for consumer products.

Structures of OLEDs

OLEDs are multi-component devices that emit light when voltage is applied (Figure 1.1). While the structure of the devices can vary, typically an OLED has thin layers of organic materials sandwiched between a high work function, transparent anode (*e.g.*, indium tin oxide) and a low work function metal cathode (*e.g.*, aluminum). For single layer devices, the organic film is either an emissive electron transport material (ETM) like tris(8-oxyquinolato)aluminum (Alq₃) or an emissive hole transport material

(HTM) like 4,4'-bis(phenyl-*m*-tolylamino)biphenyl (TPD) (Figure 1.2).⁵ Likewise, an ETM and a HTM can be mixed or covalently bound to one another to form a single layer.⁶ In a single layer OLED, the transport material must act not only as a semi-

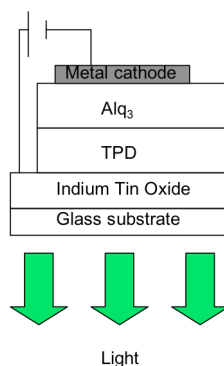
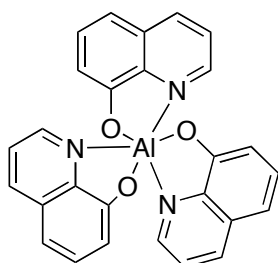
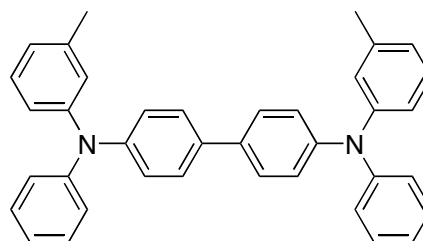


Figure 1.1 Diagram of a typical bilayer OLED structure with common charge transporting materials.



Alq₃



TPD

Figure 1.2. Structures of commonly used charge transport materials.

conducting material, but it must also effectively transport both charges.⁵

Sometimes, a thin layer of insulating material or conducting material is deposited between the anode and the emissive layer to help balance injection of holes and electrons.⁷⁻⁸ Bilayer OLEDs have both an electron transport layer and a hole transport layer. Multilayer devices can include injection layers and blocking layers to further tune the balance of electrons and holes. Generally, multiple layers in an OLED lead to higher

efficiencies and lower turn-on voltages because the additional layers can facilitate charge injection, charge transport, recombination of holes and electrons, and emission of light.⁹

Operation of OLEDs

Under an applied voltage, the ETM and HTM in a bilayer OLED accept either an electron or a hole into the lowest unoccupied molecular orbital (LUMO) or the highest occupied molecular orbital (HOMO), respectively (Figure 1.3). For the injection

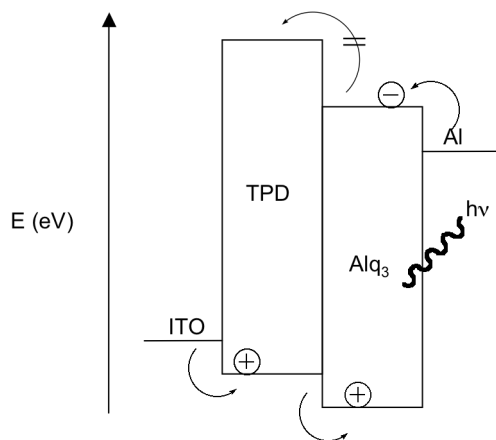


Figure 1.3. Diagram of EL in a bilayer OLED under applied voltage.

process to occur efficiently, the energy levels of the organic materials should closely match those energy levels of the electrodes to lower the energy barrier. The second process that occurs in an OLED is charge transport, which occurs by a hopping mechanism in these disordered organic systems (Figure 1.4).¹⁰⁻¹¹ Finally, when an excited hole and an excited electron recombine on the same molecule, radiative relaxation (*i.e.*, electroluminescence) can occur.

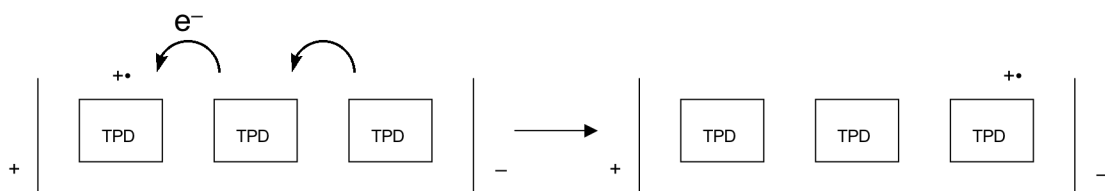


Figure 1.4. Schematic representation of charge transport by hopping mechanism under the influence of an electric field.¹¹

Characteristics of OLEDs that Affect Electroluminescence

Several factors adversely affect electroluminescence; consequently, device efficiencies and lifetimes can suffer. Poor alignment of energy levels impedes the EL process because charges cannot efficiently inject into transport materials and transport through them.^{10–15} Larger energy barriers require higher voltages to successfully attain light output suitable for commercialization (*i.e.*, $>100 \text{ cd/m}^2$). Finding organic molecules and electrodes with comparable energy levels remains an issue for charge injection.¹⁶ The lack of complementarity between organic/electrode^{15,17–18} and organic/organic interfaces^{19–23} further contributes to device degradation. Introduction of injection layers or modification of electrodes has proven to be a useful alternative for closer energy matching and for better compatibility of interfaces.^{19–23}

Charge transport can be hindered because generally, hole mobilities (μ_h) are on the order of 1–2 magnitudes higher than electron mobilities.²⁴ Intrinsically, however, electron mobilities and hole mobilities are generally comparable. Mobilities are typically measured by the time-of-flight (TOF) technique and are reported with units $\text{cm}^2/\text{V}\cdot\text{s}$.²⁵ In general, mobilities are dependent on the temperature, the electric field, and the measurement technique. Charge mobilities are an indication of how well a material transports charges. For example, TPD has a hole mobility on the order of $10^{-3} \text{ cm}^2/\text{V}\cdot\text{s}$,

while common electron transport materials bathocuproine (BCP) and Alq₃ have electron mobilities on the order of 10⁻⁷ cm²/V·s and 10⁻⁵ cm²/V·s, respectively.^{24,26-28}

The lower mobilities of electrons in ETMs, in some cases, are due to the instability of the radical anions toward oxygen and water.^{10,29-31} As a consequence of this phenomenon, extrinsic electron traps can be created.³⁰ The traps tend to lower electron mobility and require higher voltages than if fewer traps were present. The development of ETMs with mobilities similar to HTMs will be necessary to improve device performances since the imbalance of charge can adversely affect the device lifetime.³²

EL can also be affected by the formation of exciplexes and charge transfer complexes.³¹ Exciplexes are transient donor-acceptor complexes formed between the excited state of one organic material and the ground state of the other organic material (Figure 1.5).³³ Bound by Coulombic forces, exciplexes form only at organic interfaces.^{9,33-36} Formation of exciplexes can be determined spectroscopically by measuring emission, excitation, and/or absorbance spectra. A shift in the wavelength of emission from the device relative to a single thin layer of the emissive material is usually evidence of exciplex formation. For color purity, an unwanted shift of emission is detrimental. However, exciplexes can be used to tune the color of emission by judiciously selecting HTM-ETM pairs. Exploiting this phenomenon, OLEDs have been fabricated with emissions spanning the entire visible spectrum.³⁵⁻³⁷

Similar to exciplexes, charge transfer (CT) complexes affect the emission of light produced in OLEDs.^{38,39} CT complexes occur when an electron in the HOMO of a Lewis-basic donor molecule transfers to the LUMO of a Lewis-acidic acceptor molecule.⁴⁰ The complexes are typically detected by optical spectroscopy, but

characterization has been demonstrated using differential scanning calorimetry (DSC).^{41–}

⁴⁴ Rather than measuring absorption bands and molar extinction coefficients,

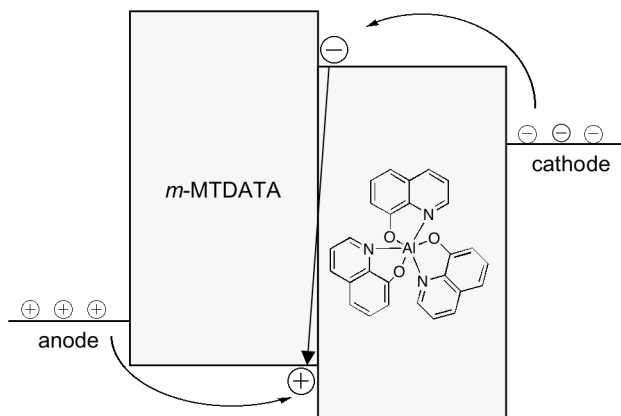


Figure 1.5. Exciplex formation between 1,3,5-tris-(3-methylphenylphenylamino)triphenylamine (*m*-MTDATA) and Alq₃.

characterizing CT complexes by DSC rely on the displacement of the fusion peak of the donor. For example, Rocquin and Chevot detected the CT complex of DEC and TNF by observing in the thermograms of DEC and DEC-TNF complex a fusion peak shift from 186 °C to 206 °C.

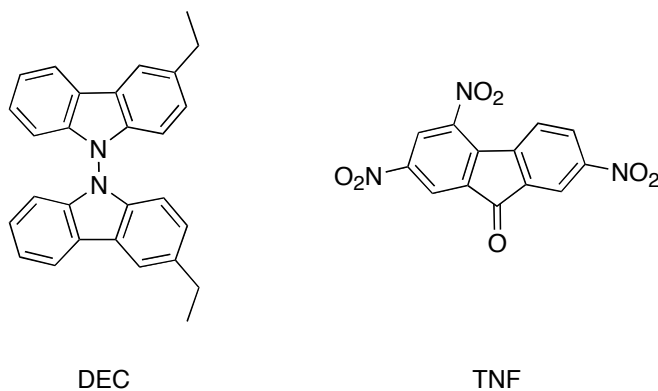


Figure 1.6. Structures of donor 3,3'-diethyl-9,9'-dicarbazole (DEC) and acceptor 2,4,7-trinitro-9-fluorenone (TNF).

As mentioned before, color purity is an important component of OLEDs, especially for full color display applications. Currently, red and green emitters with

lifetimes of at least 10,000 hours are known.^{45–48} However, stable blue emitters remain a challenge.^{47–50} Long-term stability of OLEDs is essential for commercial applications; moreover, red, green, and blue emitters should have similar lifetimes to prevent color shift occurring in displays.

OLED technology is also limited by physical size of the multicolor display.⁵¹ Samsung reported developing a 21-inch screen, but this is noticeably smaller than the 50- and 60-inch screen sizes available in other display formats.⁵² Likewise, EPSON developed a 40-inch OLED television screen. Still, this is 2.0 times smaller than the best plasma screen in the marketplace.⁵³ Typically, manufacturing OLED displays is not complementary to other displays; therefore, separate production plants/lines are required.^{54–55} Thus, production costs currently are not ideal for OLEDs.

Advantages of OLEDs to Other Display Technologies

Kraft *et al.* cite many of the benefits of OLEDs compared to older and more ubiquitous technologies based on cathode ray tubes (CRT) and liquid crystals (LCD).¹⁵ OLEDs are better suited for large-area displays because the small organic films can be solution processed and chemical modifications permit tuning the light emission across the entire visible spectrum. Solution processing itself leads to other benefits for OLEDs. For example, it is cheaper than the vapor deposition or sublimation techniques used for earlier technologies. Flexible displays^{56–58} and inkjet printing^{59–61} also become possible with the use of solution processible organic materials because materials besides glass can be used as substrates to fabricate OLED displays.

Devices based on small organic molecules are expected to be brighter and more efficient than displays currently on the market.^{62–63} OLEDs are brighter than other

displays because most organic molecules have extremely high quantum efficiencies.² Incorporating fluorescent or phosphorescent dopants also increases the luminance of the devices.^{64–70} Efficiencies are further improved in OLEDs because removing the need for a backlight (as in liquid crystalline displays) reduces power consumption.⁷¹

Because of the potential OLEDs have for commercial applications, scientists are actively pursuing research that can address many of the problems OLEDs present so that light-emitting devices based on small organic molecules can flourish in the mainstream global marketplace.

Side-Chain Polymers: A Method to Improve OLEDs

One strategy to improve the use of small organic molecules in OLEDs involves side-chain polymers. The use of side-chain polymers has been reported in the literature.^{72–76} Compared to main-chain polymers, having pendant groups connected to the polymer backbone improves solubility, and therefore solution processibility.^{72,76} A variety of pendant groups can be attached at various intervals as a side chain to enable chemical tuning.⁷² Attaching a large planar moiety to a polymer backbone as a side-chain has also been demonstrated to minimize their aggregation, which in turn minimizes quenching of emission.^{11,77–78} Moreover, compared to main-chain polymers, the synthesis of side-chain polymers is simplified, and the use of these polymers can prevent crystallization of the chromophore.^{76,78}

In his review article on electroluminescent polymers,⁷⁸ Akcelrud provides numerous literature examples of side-chain polymers using a variety of polymerized backbones including polystyrene,^{79–81} PPV,⁸² poly(methylmethacrylate) (PMMA),⁷⁶ and polynorbornene.⁸³ Carbazole,⁷⁶ stilbene,⁷⁹ N-methylnaphthalimide,⁷⁷ and pyrene⁷⁶ were

used as chromophores. Grafting,⁸⁴⁻⁸⁵ doping,^{72,86} and co-polymerization⁸⁷⁻⁸⁸ were techniques used by several groups to obtain blue-emitting polymers.

Previous Work on Side-Chain Polymers by Our Group

Considerable effort in our group has been focused on synthesizing charge transport materials that are pendant groups for side-chain polymers.⁸⁹⁻⁹⁵ We began using norbornene as the polymerizable group when we observed higher mobilities compared to acrylate derivatives.⁹² The polar acrylate groups broadened the energy distribution of states as described by the disorder formalism; thus, we observed lower hole mobilities compared to the non-polar norbornene derivatives.⁹⁶⁻⁹⁸ The presence of norbornene provides the opportunity to employ ring opening metathesis polymerization (ROMP). ROMP is useful because we can obtain monodisperse, low molecular weight polymers and copolymers in a living manner.⁹⁹⁻¹⁰¹ Living polymerization is vital to preparing well-defined block copolymers of interest. Finally, literature precedent has demonstrated that polynorbornenes allow crystalline molecules to be used as pendant groups in forming amorphous materials.⁸³

Incorporating cross-linking groups like oxetane into copolymers is also of keen interest to us. Cross-linking provides a method to fabricate multi-layer devices using solution-processible materials. It is important to use solution-processing techniques because the cost is cheaper than vapor deposition and large area displays can be easily fabricated (*vide supra*). However, because one layer is soluble, it makes deposition of a subsequent solution-cast film difficult. By cross-linking a layer, one can effectively make it insoluble and thereby allow the casting of the next layer.⁹²

With a library of ROMP monomers, our group plans to co-polymerize interesting polymers for a variety of opto-electronic applications including OLEDs, organic field effect transistors, and photovoltaics.

Current Direction of Our Work

This thesis describes the synthesis and characterization of norbornene-functionalized side-chain monomers. We prepared three TPD-derivatives for potential use as hole transport materials in OLEDs to exploit the properties of TPD that make it a good choice for hole transport. Specifically, we wanted to take advantage of the tendencies TPD has to form amorphous, thin films, to emit blue light efficiently ($\Phi_{\text{PL}} = 0.35 \pm 0.03$),¹⁰² and to form relatively stable radical cations. Our synthetic modifications were aimed at increasing the morphological and thermal stability of TPD while maintaining its electrochemical and spectroscopic properties.

We also synthesized 1,10-phenanthroline small molecules and monomers to evaluate their potential as electron transport materials and hole blocking materials. BCP, a 1,10-phenanthroline derivative, has been used to transport electrons in OLEDs, but it has a lower electron mobility than Alq₃ (*vide supra*). Important advantages BCP has over Alq₃ are that it has a relatively deep HOMO level (6.7 eV) compared to Alq₃ (5.7 eV), and it is non-emissive. Therefore, BCP confines holes to the emissive layer without affecting the emission color.

From the efforts reported herein, we hope to move toward our ultimate goal of fabricating an entirely solution-processible efficient OLED for commercial applications.

References

(1) Helfrich, W.; Schneider, W. *Phys. Rev. Lett.* **1965**, *14*, 229–231.

- (2) Tang, C.W.; VanSlyke, S.A. *Appl. Phys. Lett.* **1987**, *51*, 913–915.
- (3) Adachi, C.; Tokito, S.; Tsutsui, T.; Saito, S. *Jpn. J. Appl. Phys. Part 2* **1988**, *27*, L269–L271.
- (4) Burroughes, J.H.; Bradley, D.D.C.; Brown, A.R.; Marks, R.N.; Mackay, K.; Friend, R.H.; Burns, P.L.; Holmes, A.B. *Nature* **1990**, *347*, 539–541.
- (5) Nabatova-Gabain, N.; Wasai, Y.; Tsuboi, T. *Curr. Appl. Phys.* **2006**, *6*, 833–838.
- (6) Bugatti, V.; Concilio, S.; Ianneli, P.; Piotto, S.P.; Bellone, S.; Ferrara, M.; Neitzert, H.C.; Rubino, A.; Della Sala, D.; Vacca, P. *Synth. Met.* **2006**, *156*, 13–20.
- (7) Gao, Y.; Wang, L.; Zhang, D.; Duan, L.; Dong, G.; Qiu, Y. *Appl. Phys. Lett.* **2003**, *82*, 155–157.
- (8) Lane, P.A.; Kushto, G.P.; Kafafi, Z.H. *Appl. Phys. Lett.* **2007**, *90*, 023511-1–023511-3.
- (9) Shirota, Y. *J. Mater. Chem.* **2000**, *10*, 1–25.
- (10) Murata, H.; Mallarias, G.G.; Uchida, M.; Shen, Y.; Kafafi, Z.H. *Chem. Phys. Lett.* **2001**, *339*, 161–166.
- (11) Thelakkat, M. *Macromol. Mater. Eng.* **2002**, *287*, 442–461.
- (12) Sano, T.; Nishio, Y.; Hamada, Y.; Takahashi, H.; Usuki, T.; Shibata, K. *J. Mater. Chem.* **2000**, *10*, 157–161.
- (13) Rajagopal, A.; Kahn, A. *Adv. Mater.* **1998**, *10*, 140–144.
- (14) Bellmann, E.; Shaheen, S.E.; Thayumanavan, S.; Barlow, S.; Grubbs, R.H.; Marder, S.R.; Kippelen, B.; Peyghambarian, N. *Chem. Mater.* **1998**, *10*, 1668–1676.
- (15) Kraft, A.; Grimsdale, A.C.; Holmes, A.B. *Angew. Chem. Int. Ed.* **1998**, *37*, 402–428.
- (16) Chun, M.S.; Teraji, T.; Ito, T. *Appl. Surf. Sci.* **2003**, *216*, 106–112.

- (17) Bradley, D.D.C.; Friend, R.H. *J. Phys.:Condens. Matter* **1989**, *1*, 3671–3678.
- (18) Ziemelis, K.E.; Hussain, A.T.; Bradley, D.D.C.; Friend, R.H.; Ruhe, J.; Wegner, G. *Phys. Rev. Lett.* **1991**, *66*, 2231–2234.
- (19) Barth, S.; Muller, P.; Riel, H.; Seidler, P.F.; Riess, W.; Vestweber, H.; Bäessler, H. *J. Appl. Phys.* **2001**, *89*, 3711–3719.
- (20) Chen, C.W.; Cho, T.Y.; Wu, C.C.; Yu, H.L.; Luh, T.Y. *Appl. Phys. Lett.* **2002**, *81*, 1570–1572.
- (21) Ichikawa, M.; Shibata, H.; Nukada, K.; Sato, K.; Koyama, T.; Taniguchi, Y. *Mol. Cryst. Liq. Cryst. Sci.* **2002**, *377*, 65–68.
- (22) Mazhari, B. *Solid-State Electron.* **2005**, *49*, 311–315.
- (23) Mazhari, B. *Org. Electron.* **2005**, *6*, 229–236.
- (24) Naka, S.; Okada, H.; Onnagawa, H.; Tsutsui, T. *Appl. Phys. Lett.* **2000**, *76*, 197–199.
- (25) Martin, E.H.; Hirsh, J. *Solid State Commun.* **1969**, *7*, 783–786.
- (26) Fong, H.H.; Lun, K.C.; So, S.K. *Mater. Res. Soc. Symp. Proc.* **2002**, *725*, P8.1.1–P8.1.6
- (27) Ben Khalifa, M.; Vaufrey, D.; Tardy, J. *Org. Electron.* **2004**, *5*, 187–198.
- (28) Chen, L.L.; Li, W.L.; Li, M.T.; Chu, B. *J. Lumin.* **2007**, *122–123*, 667–670.
- (29) Risko, C.; Zojer, E.; Brocorens, P.; Marder, S.R.; Brédas, J.L. *Chem. Phys.* **2005**, *313*, 151–157.
- (30) Palilas, L.C.; Uchida, M.; Kafafi, Z.H. *IEEE J. Sel. Top. Quantum. Electron.* **2004**, *10*, 79–88.
- (31) Yamaguchi, S.; Endo, T.; Uchida, M.; Izumizawa, T.; Furukawa, K.; Tamao, K. *Chem. Eur. J.* **2000**, *6*, 1683–1692.

- (32) Tamao, K.; Uchida, M.; Izumizawa, T.; Furukawa, K.; Yamaguchi, S. *J. Amer. Chem. Soc.* **1996**, *118*, 11974–11975.
- (33) Liang, C.J.; Zhao, D.; Hong, Z.R.; Li, R.G.; Li, W.L.; Yu, J.Q. **2000**, *371*, 207–210.
- (34) Tao, X.T.; Zhang, Y.D.; Wada, T.; Sasabe, H.; Suzuki, H.; Watanabe, T.; Miyata, S. *Appl. Phys. Lett.* **1997**, *71*, 1921–1923.
- (35) Itano, K.; Ogawa, H.; Shiota, Y. *Appl. Phys. Lett.* **1998**, *72*, 636–638.
- (36) Ogawa, H.; Okuda, R.; Shiota, Y. *Appl. Phys. A* **1998**, *67*, 599–602.
- (37) Shiota, Y.; Noda, T.; Ogawa, H. *Proc. SPIE Int. Soc. Opt. Eng.* **1999**, *3797*, 158–169.
- (38) Goliber, T.E.; Perlstein, J.H. *J. Chem. Phys.* **1984**, *80*, 4162–4167.
- (39) Domercq, B.; Grasso, C.; Maldonado, J.-L.; Halik, M.; Barlow, S.; Marder, S.R.; Kippelen, B. *J. Phys. Chem. B* **2004**, *108*, 8647–8651.
- (40) Schreiber, A.; Zilker, S.J.; Haarer, D. *J. Chem. Phys.* **2000**, *112*, 7190–7194.
- (41) Yang, H.; Natansohn, A. *Chem. Mater.* **1994**, *6*, 1842–1844.
- (42) Rocquin, O.; Chevrot, C. *Synth. Met.* **1997**, *89*, 119–123.
- (43) Sadki, S.; Kham, K.; Chevrot, C. *Synth. Met.* **1999**, *101*, 477–478.
- (44) Paraschuk, D.Y.; Elizarov, S.G.; Khodarev, A.N.; Shchegolikhin, A.N.; Arnautov, S.A.; Nechvolodova, E.M. *JETP Lett.* **2005**, *81*, 467–470.
- (45) Liu, T.-H.; Iou, C.-Y.; Chen, C.H. *Appl. Phys. Lett.* **2003**, *83*, 5241–5243.
- (46) Meerheim, R.; Walzer, K.; Pfeiffer, M.; Leo, K. *Appl. Phys. Lett.* **2006**, *89*, 061111-1–061111-3.

- (47) Wu, W.; Inbasekaran, M.; Hudack, M.; Welsh, D.; Yu, W.; Cheng, Y.; Wang, C.; Kram, S.; Tacey, M.; Bernius, M.; Fletcher, R.; Kiszka, K.; Munger, S.; O'Brien, J. *Microelectron. J.* **2004**, *35*, 343–348.
- (48) Lee, J.Y.; Kwon, J.H.; Chung, H.K. *Org. Electron.* **2003**, *4*, 143–148.
- (49) Kulkarni, A.; Gifford, A.P.; Tonzola, C.J.; Jenekhe, S.A. *Appl. Phys. Lett.* **2005**, *86*, 061106-1–061106-3.
- (50) Divayana, Y.; Sun, X.W.; Chen, B.J.; Lo, G.Q.; Jiang, C.Y.; Sarma, K.R. *Appl. Phys. Lett.* **2006**, *89*, 173511-1–173511-3.
- (51) Sturm, J.C.; Wilson, W.; Iodice, M. *IEEE J. Sel. Top. Quantum Electron.* **1998**, *4*, 75–82.
- (52) Samsung, “Samsung Develops the World’s Largest 21-inch OLED for TVs”, www.samsung.com/Products/TFTLCD/News/category_TFTLCD_20050105_0000090476.htm (Accessed March 11, 2006).
- (53) Epson, “Epson Creates World’s First Large Full-Color OLED Display Using Original Inkjet Technology”, www.epson.co.jp/e/newsroom/news_2004_05_18.htm (Accessed September 26, 2007).
- (54) Kelley, T.W.; Baude, P.F.; Gerlach, C.; Ender, D.E.; Muyres, D.; Haase, M.A.; Vogel, D.E.; Theiss, S.D. *Chem. Mater.* **2004**, *16*, 4413–4422.
- (55) Sheats, J.R. *J. Mater. Res.* **2004**, *19*, 1974–1989.
- (56) Allen, K.J. *Proc. IEEE* **2005**, *93*, 1394–1399.
- (57) Gu, G.; Burrows, P.E.; Venkatesh, S.; Forrest, S.R.; Thompson, M.E. *Opt. Lett.* **1997**, *22*, 172–174.

- (58) Zhou, L.; Wanga, A.; Wu, S.-C.; Sun, J.; Park, S.; Jackson, T.N. *Appl. Phys. Lett.* **2006**, *88*, 083502-1–083502-3.
- (59) Ikegawa, M.; Azuma, H. *JSME Int. J. Ser. B* **2004**, *47*, 490–496.
- (60) Okada, H.; Naka, S.; Satoh, R.; Shibata, M.; Miyashita, T.; Matsushita, Y.; Ooe, M.; Shimada, H.; Arisawa, T.; Hyodo, T.; Yangai, J.; Nagai, T.L.; Onnagawa, H.; Takemura, H.; Kakumoto, H.; Miyabayashi, T.; Inoue, T. *J. Photopolym. Sci. Technol.* **2005**, *18*, 79–82.
- (61) Shibusawa, M.; Kobayashi, M.; Hanari, J.; Sunohara, K.; Ibaraki, N. *IEICE Trans. Electron.* **2003**, *E86-C*, 2269–2274.
- (62) Shaheen, S.E.; Jabbour, G.E.; Kippelen, B.; Peyghambarian, N.; Anderson, J.D.; Marder, S.R.; Armstrong, N.R.; Bellmann, E.; Grubbs, R.H. *Appl. Phys. Lett.* **1999**, *74*, 3212–3214.
- (63) Kanno, H.; Hamada, Y.; Nishimura, K.; Okumoto, K.; Saito, N.; Mameno, K.; Shibata, K. *Jpn. J. Appl. Phys. Part 2* **2006**, *45*, L947–L950.
- (64) Kaur, A.; Cazeca, M.J.; Sengupta, S.K.; Kumar, J.; Tripathy, S.K. *Synth. Met.* **2002**, *126*, 283–288.
- (65) Ikai, M.; Tokito, S.; Sakamoto, Y.; Suzuki, T.; Taga, Y. *Appl. Phys. Lett.* **2001**, *79*, 156–158.
- (66) Kan, S.D.; Liu, X.D.; Shen, F.Z.; Zhang, J.Y.; Ma, Y.G.; Zhang, G.; Wang, Y.; Shen, B.C. *Adv. Funct. Mater.* **2004**, *13*, 603–608.
- (67) Kim, J.H.; Nam, E.J.; Hong, S.Y.; Kim, B.O.; Kim, S.M.; Yoon, S.S.; Suh, J.H.; Ha, Y.Y.; Kim, Y.K. *Mater. Sci. Eng.* **2004**, *24*, 167–171.
- (68) Liu, S.Y.; Feng, J.; Zhao, Y. *Jpn. J. Appl. Phys. Part 1* **2004**, *43*, 2320–2322.

- (69) Ramos-Ortiz, G.; Oki, Y.; Domercq, B.; Kippelen, B. *Phys. Chem. Chem. Phys.* **2002**, *4*, 4109–4114.
- (70) Stampor, W.; Mezyk, J.; Kalinowski, J.; Cocchi, M.; Virgili, D.; Fattori, V.; Di Marco, P. *Macromol. Symp.* **2004**, *212*, 509–514.
- (71) Pribat, D.; Plais, F. *Thin Solid Films* **2001**, *383*, 25–30.
- (72) Bouché, C.-M.; Berdagué, P.; Facoetti, H.; Robin, P.; Le Barny, P.; Schott, M. *Synth. Met.* **1996**, *81*, 191–195.
- (73) Son, J.M.; Sakaki, Y.; Ogino, K.; Sato, H. *IEEE Trans. Electron Devices* **1997**, *44*, 1307–1314.
- (74) Yu, L.-S.; Chen, S.-A. *Synth. Met.* **2002**, *132*, 81–86.
- (75) Beiner, M.; Huth, H. *Nature Mater.* **2003**, *2*, 595–599.
- (76) Bisberg, J.; Cumming, W.J.; Gaudiana, R.A.; Hutchinson, K.D.; Ingwall, R.T.; Kolb, E.S.; Mehta, P.G.; Minns, R.A.; Peterson, C.P. *Macromolecules* **2005**, *28*, 386–389.
- (77) Cacialli, F.; Friend, R.H.; Bouché, C.-M.; Le Barny, P.; Facoetti, H.; Soyer, F.; Robin, P. *J. Appl. Phys.* **1998**, *83*, 2343–2356.
- (78) Akcelrud, L. *Prog. Polym. Sci.* **2003**, *28*, 875–962.
- (79) Aguiar, M.; Akcelrud, L.; Karasz, F.E. *Synth. Met.* **1995**, *71*, 2189–2190.
- (80) Aguiar, M.; Hu, B.; Karasz, F.E.; Akcelrud, L. *Macromol. Chem. Phys.* **1998**, *199*, 1255–1261.
- (81) Aguiar, M.; Fugihara, M.C.; Hummelgen, I.A.; Peres, L.O.; Garcia, J.R.; Gruber, J.; Akcelrud, L. *J. Lumin.* **2002**, *96*, 219–225.
- (82) Chung, S.J.; Jin, J.I.; Kim, K.K. *Adv. Mater.* **1997**, *9*, 551–554.

- (83) Rubner, M.F. *Macromolecules* **1997**, *30*, 3553–3559.
- (85) Heseman, P.; Vestweber, H.; Pommerehne, J.; Mahrt, R.F.; Greiner, A. *Adv. Mater.* **1995**, *7*, 388–390.
- (85) Sander, R.; Stumpflen, V.; Wendorff, J.H.; Greiner, A. *Macromolecules* **1996**, *29*, 7705–7708.
- (86) Cacialli, F.; Bouché, C.-M.; Le Barny, P.; Friend, R.H.; Facoetti, H.; Soyer, F.; Robin, P. *Opt. Mater.* **1998**, *9*, 163–167.
- (87) Lee, J.K.; Hwang, D.H.; Hwang, J.H.; Jung, H.K.; Zyung, T.Y.; Park, S.Y. *Synth. Met.* **2000**, *111*, 489–491.
- (88) Tarkka, R.M.; Zhang, X.J.; Jenekhe, S.A. *J. Amer. Chem. Soc.* **1996**, *118*, 9438–9439.
- (89) Domercq, B.; Hreha, R.D.; Zhang, Y.D.; Haldi, A.; Barlow, S.; Marder, S.R.; Kippelen, B. *J. Polym. Sci. Part B* **2003**, *41*, 2726–2732.
- (90) Domercq, B.; Hreha, R.D.; Zhang, Y.D.; Larribeau, N.; Haddock, J.N.; Schultz, C.; Marder, S.R.; Kippelen, B. *Chem. Mater.* **2003**, *15*, 1491–1496.
- (91) Hreha, R.D.; George, C.P.; Haldi, A.; Domercq, B.; Malagoli, M.; Barlow, S.; Brédas, J.-L.; Kippelen, B.; Marder, S.R. *Adv. Funct. Mater.* **2003**, *13*, 967–973.
- (92) Hreha, R.D.; Haldi, A.; Domercq, B.; Barlow, S.; Kippelen, B.; Marder, S.R. *Tetrahedron* **2004**, *60*, 7169–7176.
- (93) Zhan, X.W.; Risko, C.; Amy, F.; Chan, C.; Zhao, W.; Barlow, S.; Kahn, A.; Brédas, J.-L.; Marder, S.R. *J. Amer. Chem. Soc.* **2005**, *127*, 9021–9029.

- (94) Zhang, Y.D.; Hreha, R.D.; Jabbour, G.E.; Kippelen, B.; Peyghambarian, N.; Marder, S.R. *Abstracts of Papers of the American Chemical Society* **2001**, 221, U406–U406.
- (95) Zhang, Y.D.; Hreha, R.D.; Jabbour, G.E.; Kippelen, B.; Peyghambarian, N.; Marder, S.R. *J. Mater. Chem.* **2002**, 12, 1703–1708.
- (96) Borsenberger, P.M.; Pautmeier, L.; Richert, R.; Bäessler, H. *J. Phys. Chem.* **1991**, 94, 8276–8281.
- (97) Bäessler, H. *Phys. Status Solidi (b)* **1993**, 175, 15–56.
- (98) Van der Auweraer, M.; De Schryver, F.C.; Borsenberger, P.M.; Fitzgerald, J.J. *J. Phys. Chem.* **1993**, 97, 8808–8811.
- (99) Abd-El-Aziz, A.S.; May, L.J.; Edel, A.L. *Macromol. Rapid Commun.* **2000**, 21, 598–602.
- (100) Grubbs, R.H. *J. Macromol. Sci.-Pure Appl. Chem.* **1994**, A31, 1829–1833.
- (101) Slugov, C.; Demel, S.; Riegler, S.; Hobisch, J.; Stelzer, F. *Macromol. Rapid Commun.* **2004**, 25, 475–480.
- (102) Mattoussi, H.; Murata, H.; Merritt, C.D.; Iizumi, Y.; Kido, J.; Kafafi, Z.H. *J. Appl. Phys.* **1999**, 86, 2642–2650.

CHAPTER 2

SYNTHESIS AND CHARACTERIZATION OF NORBORNENE-FUNCTIONALIZED TPD MONOMERS

Introduction

4, 4'-Bis(phenyl-*m*-tolylamino)biphenyl (TPD) is an aromatic amine with properties that make it well suited for use as a hole transport material (HTM) in OLEDs.¹⁻⁴ The compound can form amorphous thin, colorless films by vacuum deposition.^{5,6} Polymers containing TPD, however, can be used to form thin films using solution processing techniques. Solution processing of materials, rather than vapor deposition, could potentially allow for the fabrication of electroluminescent devices at lower cost.⁷

One feature that makes TPD attractive as a hole transport material is its charge mobility ($\mu_h \cong 2-3 \times 10^{-3} \text{ cm}^2/\text{V}\cdot\text{s}$).^{5,8} While $\mu_h(\text{TPD})$ is orders of magnitude lower than state of the art hole transport materials like rubrene and pentacene (with mobilities reported as high as 20 and 35 $\text{cm}^2/\text{V}\cdot\text{s}$, respectively),⁹⁻¹⁰ thermally stable amorphous materials like TPD polymers and more robust triarylamine (e.g., NPB) are better suited for OLEDs than crystalline materials such as rubrene and pentacene (*vide infra*).¹¹ Triarylamine tends to be blue-emitting, making them useful for blue emissive devices.¹² The radical cation ($\text{TPD}^{+\bullet}$) is relatively stable and can form reversibly.¹³ The radical cations act as stable spin centers which are partially responsible for hole transport in a device.¹⁴ The low ionization potential (IP) of TPD facilitates charge injection.⁴ The IP is positioned between the work function of ITO ($\sim 4.7 \text{ eV}$) and the IP of many emissive

materials.¹ Altering substituents on TPD can impact many device characteristics such as device lifetime, operational voltage, quantum efficiency, and luminance efficiency.^{13, 15–16}

The solid-state ionization potential of TPD is reportedly between 5.1 eV and 5.4 eV.¹⁷ Adding an electron-withdrawing group to TPD increases the IP. Alternatively, introducing an electron-donating group decreases the IP. The ability to tune the IP of TPD makes it possible to improve device performance.¹⁶ The better alignment of the energy with those energies of the anode and the adjacent material (*e.g.*, Alq₃) can facilitate charge injection and transport of holes across interfaces within the device.

Another property of a transport material that impacts its performance in devices is glass transition temperature.⁹ During device operation, Joule heating can occur, and the low T_g (63–65 °C) of TPD can result in crystallization and lead to phase separation.^{11,16} Ultimately, these defects contribute to device failure.¹⁸ To increase the glass transition of TPD, researchers have prepared main chain polymers,^{19–26} side chain polymers,^{13,16, 27–31} and cross-linkable polymers.³² Mixing TPD with another hole transport material or with a high T_g transparent host polymer to prevent the morphological changes has also been reported.^{18,33}

Our group used the side-chain polymer approach to improve the stability of TPD and to facilitate its solution processability.^{13,16,27,34} We found lower hole mobilities in TPD-polyacrylates than in TPD-polynorbornenes, which was consistent with the disorder formalism developed by Bässler and Borsenberger.³⁴ According to the formalism, the presence of polar groups broadens the energy distribution of states; consequently, lower charge mobilities are observed.^{35–37} Another reason to use norbornene as the polymerizable group was because the strained olefin is ideal for ring–opening metathesis

polymerization (ROMP).^{38–39} The ROMP technique allows for the possibility to obtain polymers with low polydispersity indices, to obtain well-defined block co-polymers, and to incorporate a variety of chemical functionalities into polymers.^{39–40}

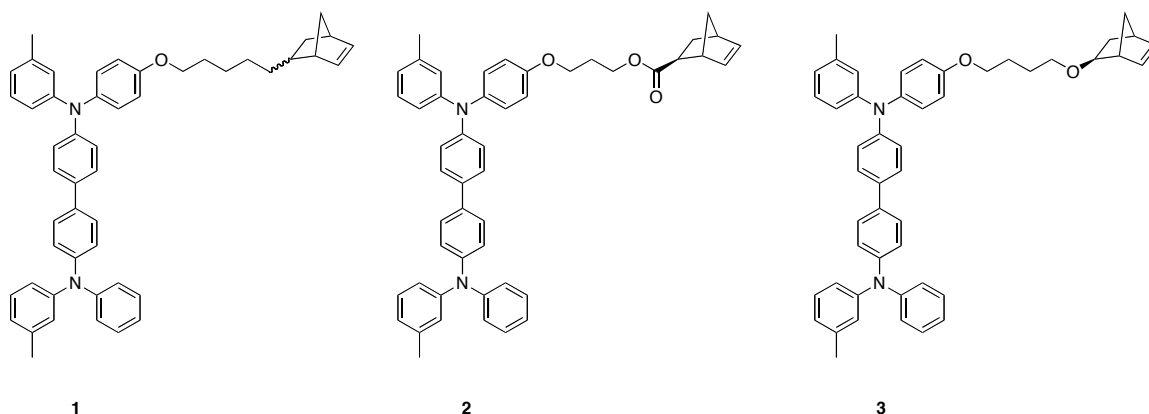


Figure 2.1. Structures of target norbornene – functionalized monomers.

Based on our previous research, we set out to synthesize TPD-norbornenes with different linkages for the following reasons (Figure 2.1):

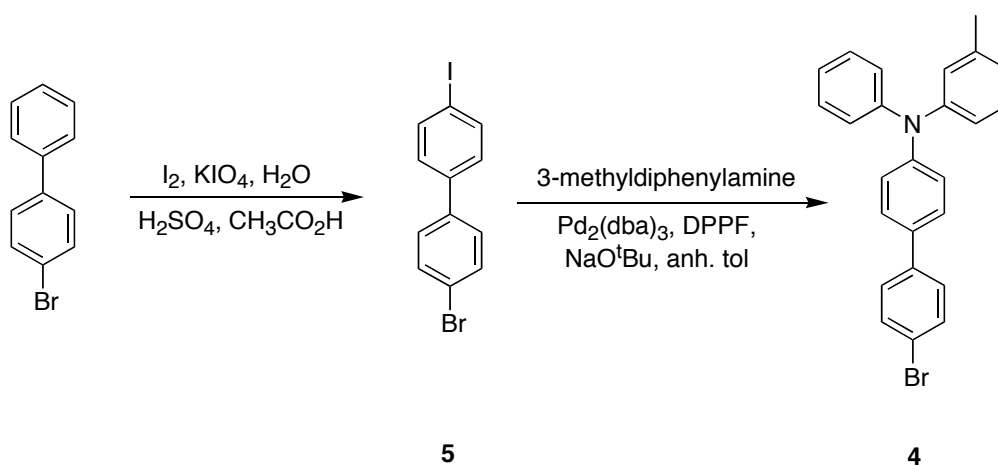
- To compare the rates of initiation and the rates of propagation for the polymerizations. The functional group adjacent to the norbornene is expected to affect the kinetics of polymerization.⁴⁰
- To compare the polydispersity indices. Narrow PDIs can be indicative of living polymerization.⁴¹ By being able to control the polymerizations, one can better design specific copolymer templates.
- To compare the hole mobilities of different polymers. Based on the disorder formalism, we expect that the ester would have a lower mobility than the ether, which would have a lower mobility than the pure alkyl. The magnitude of these differences is hard to predict, however.

- To evaluate the polymers based on the relative change in mobility. Our goal is to develop copolymers with narrow PDIs and increased mobility. With norbornenes, however, we must find a suitable balance between polydispersity and hole mobility.

Results and Discussion

Synthesis

The initial target was *N, N'*-(*m*-tolyl)-*N*-[4-(bicyclo[2.2.1] hept-2-enylpentoxy)-phenyl]-*N'*-phenyl-1,1'-biphenyl amine (**1**). We prepared *N*-(*m*-tolyl)-*N*-phenyl-4-bromo-1,1'-biphenyl-4'-amine (**4**). 4-bromobiphenyl was iodinated using acetic acid, aqueous sulfuric acid, iodine, and potassium periodate (Scheme 2.1). The reaction mixture changed from clear, dark purple to cloudy light pink during the 24 hour reaction time. Pouring the mixture into a beaker of water quenched the reaction. The powdery solid was filtered and washed repeatedly with water. 4-Bromo-4'-iodobiphenyl (**5**) was purified further by heating the crude material in warm ethanol and filtering the solid product.



Scheme 2.1. Synthetic route to prepare *N*-(*m*-tolyl)-*N*-phenyl-4-bromo-1,1'-biphenyl-4'-amine, **4**.

4 was prepared using a palladium-catalyzed coupling of **5** and 3-methyldiphenylamine. Likely, the catalytic cycle to form **4** was similar to the one proposed by Wolfe *et al.* whereby 4-bromo-4'-iodobiphenyl was inserted via oxidative addition and the desired product was expelled in the reductive elimination step (Figure 2.2).⁴²

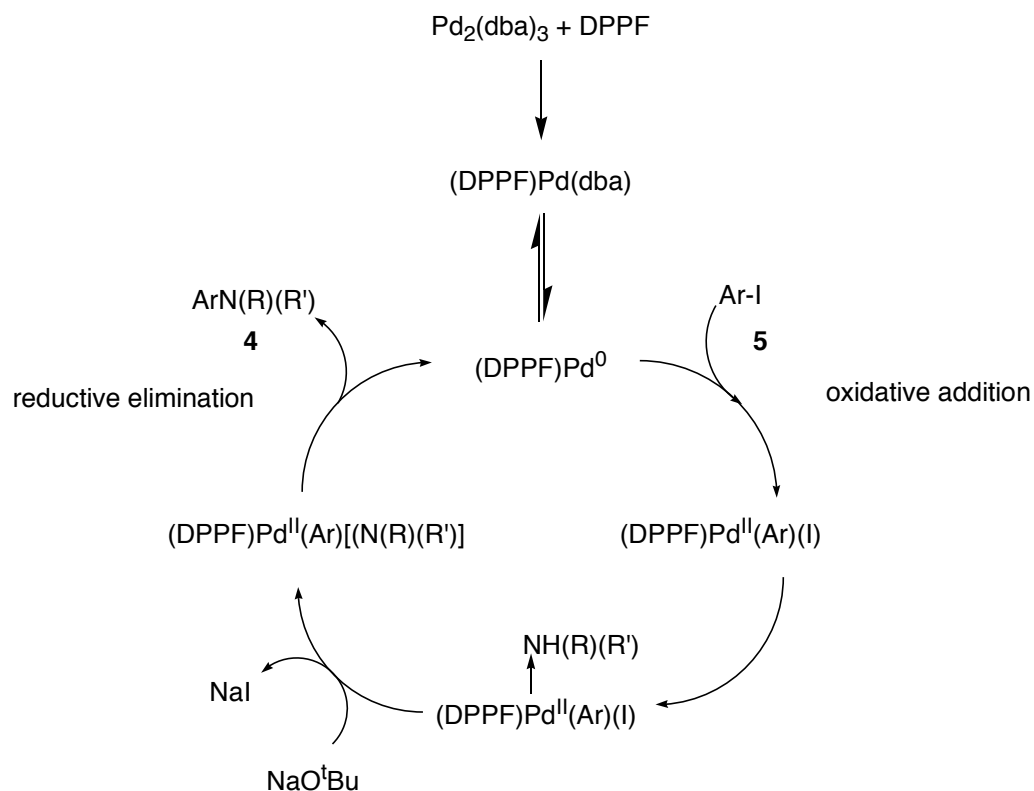
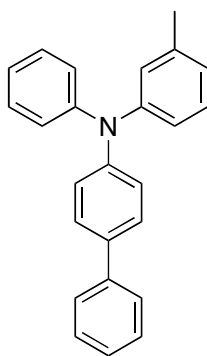


Figure 2.2. Proposed mechanism to form **4**.

The reaction was heated at 95 °C for 24 hours. At higher temperatures and on larger scales, yields were lower and side product *N*-(*m*-tolyl)-*N*-phenyl-1,1'-biphenyl-4-amine (Figure 2.3) was formed. The side product was difficult to separate from **4** by column chromatography. Thus, **4** either was isolated by column chromatography or was recovered with side product. Fortunately, the side product did not interfere with the next amination reaction because it lacked the reactive bromine (*vide infra*).



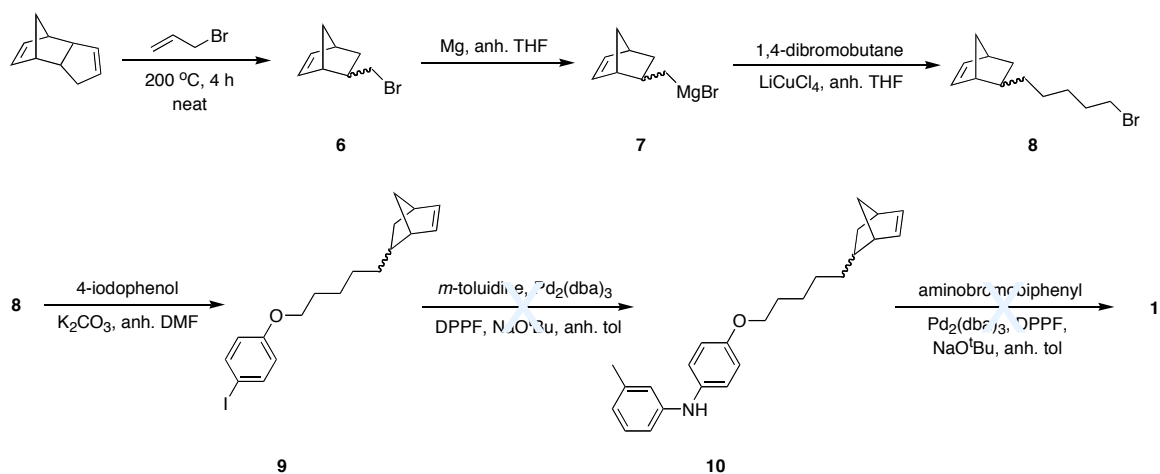
N-(*m*-tolyl)-*N*-phenyl-1,1'-biphenyl-4-amine

Figure 2.3. Structure of a side product in the amination of 4-bromo-4'-iodobiphenyl and 3-methyldiphenylamine.

To synthesize a norbornene-functionalized moiety for coupling to **4**, a Diels-Alder reaction of dicyclopentadiene with allyl bromide was performed in an autoclave heated at 200 °C for 4 hours (Scheme 2.2).⁴³ The reaction was repeated four times. Low boiling point starting materials were distilled at 175 °C at 1 atmosphere pressure. 5-(Bromomethyl) bicyclo[2.2.1] hept-2-ene (**6**) was distilled twice at 91–94 °C at 75 mmHg. The viscous, colorless liquid was recovered in 44% yield.

Following the procedure of Meyers and Weck,⁴⁴ the Grignard reagent derived from 5-bromomethyl norbornene was prepared in anhydrous THF. The reaction was completed when the solution became grey and cloudy. Meanwhile, 1,4-dibromobutane and catalytic lithium tetrachlorocuprate (II) were dissolved in anhydrous THF, and the flask was cooled to 0 °C. The Grignard reagent (**7**) was slowly transferred by cannula to the copper (II) solution. The reaction mixture remained clear; however, the color changed from orange to dark brown. Upon complete transfer of Grignard reagent, the reaction was stirred for 24 hours at room temperature.

The reaction mixture was poured into a separatory funnel. Diethyl ether and



Scheme 2.2. Synthetic route to prepare target pentylnorbornene monomer, **1**.

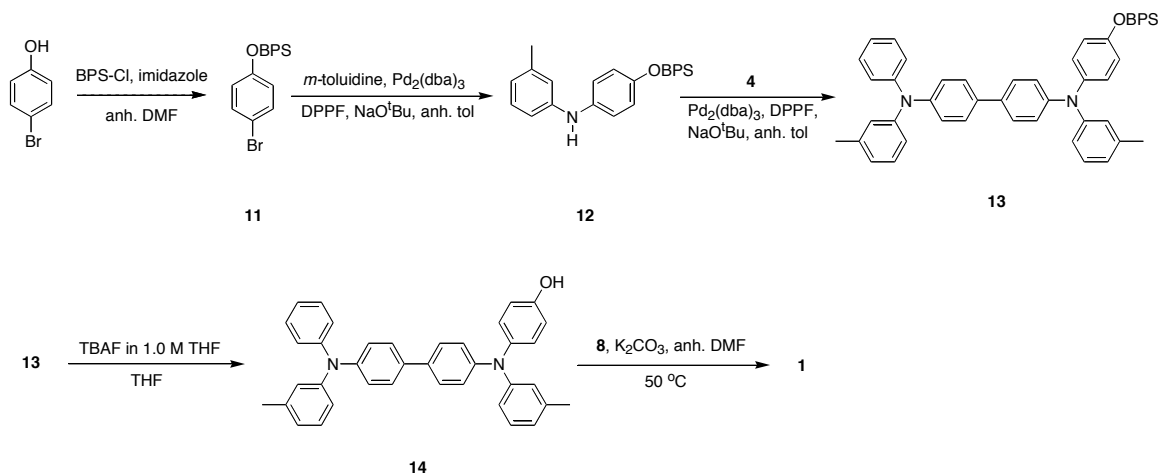
saturated aqueous NH_4Cl were added to the reaction flask to transfer all the reaction mixture. The organic products were extracted into ether twice. The first organic layer was blue-green, and it was washed with both saturated aqueous NaCl and water until it became yellow. The combined organic phases were washed with saturated aqueous NaCl and dried over MgSO_4 . The solvent was removed by rotary evaporation. A clear, yellow oil remained.

The reaction was repeated twice; a total of 87 g of 5-(bromomethyl)-bicyclo[2.2.1] hept-2-ene (**6**) was converted to a Grignard reagent (**7**) to synthesize 5-(5-bromopentyl)-bicyclo[2.2.1] hept-2-ene (**8**). The combined crude oils were purified by distillation. Excess 1,4-dibromobutane was removed at 70 °C. **8** was collected as a clear, colorless oil at 140 °C in good yield (56%).

Williamson ether synthesis conditions were used to prepare 5-(5-(4-iodophenoxy)pentyl bicyclo[2.2.1] hept-2-ene (**9**) from 4-iodophenol in good yield (62%). Attempts to couple *m*-toluidine to **9** with a palladium-catalyzed reaction repeatedly failed. A modified Ullmann coupling was also unsuccessful.⁴⁵ ^1H NMR spectra of the worked-up reaction

mixtures did not have the characteristic alkenyl peaks of norbornene. It is possible that the reaction conditions were leading to decomposition of the alkene.

An alternative route was devised to couple a norbornene moiety as the final step (Scheme 2.3). First, 4-bromophenol was protected with *tert*-butyldiphenylsilyl chloride (BPS) using Williamson ether conditions.⁴⁶ The completed reaction mixture was diluted with water, and (4-bromo-phenoxy)-*tert*-butyldiphenylsilane (**11**) was extracted into



Scheme 2.3. Modified synthetic route to form target pentyl norbornene TPD monomer, **1**.

hexanes. The solvent was removed, and the crude oil was purified on a silica gel plug. Then, the protected bromophenol was coupled to *m*-toluidine in a palladium-catalyzed amination reaction. The fragrant brown viscous liquid, [4-(*tert*-butyldiphenylsilyloxy)-phenyl]-*m*-tolyl amine (**12**) was routinely isolated in excellent yields (80–90 %) after column chromatography. It should be noted that a silica plug was run to remove impurities and catalyst prior to the column.

A second amination reaction was used to form the TPD skeleton. Initial efforts to synthesize **13** produced yields lower than 40%. Large quantities of intermediate

compounds were required to synthesize the target monomer (**1**) on a gram scale. To be a more efficient route, it was critical to improve the synthesis and the purification of **13**.

12 was coupled with **4** under very rigorous Schlenk conditions. Unlike with other palladium-DPPF reactions in this project, the catalyst system was reacted in a separate Schlenk vessel before being transferred to **4**. The reaction was heated overnight then worked up with a Celite plug and extraction. **13** was purified by column chromatography. Yields ranged from 52–85% yield depending on the scale of the reaction. Removing traces of oxygen and water and reacting the palladium and DPPF separately most likely contributed to the increase recovered yields.

13 was easily deprotected using *tetra-n*-butyl ammonium fluoride.⁴⁶ **14** decomposed under ambient conditions over extended periods; accordingly it was found desirable to deprotect quantities immediately prior to use. The phenol was highly viscous, so the recovered yield was greater than 100% even after attempts to remove residual solvent under high vacuum.

The etherification to synthesize **1** used standard conditions. The reaction required heating to go to completion. The monomer was extracted into ethyl acetate and purified by column chromatography. It was consistently recovered in good yield (55%) as a glassy white solid.

With the large-scale synthesis of BPS-protected TPD completed, we tried to synthesize isomerically pure norbornene-functionalized monomers **2** and **3**. *endo/exo* Mixtures of norbornene can lead to non-living polymerizations since *exo* isomers react significantly faster than *endo* isomers.³⁶ Achieving living polymerization is important because the absence of chain termination can produce well-defined block copolymers

with controllable molecular weights (*vide supra*). We hoped to lower the PDI of our monomers, so we introduced polar groups at the 5-position of norbornene to slow the rate of propagation (k_p).^{36,47} We wanted to synthesize the norbornene-functionalized ester and ether to couple with **14** (Figure 2.4). The norbornenes were designed to contain six



exo-3-bromopropylbicyclo[2.2.1]hept-5-ene-2-carboxylate

exo-5-(4-bromobutoxy)bicyclo[2.2.1]hept-2-ene

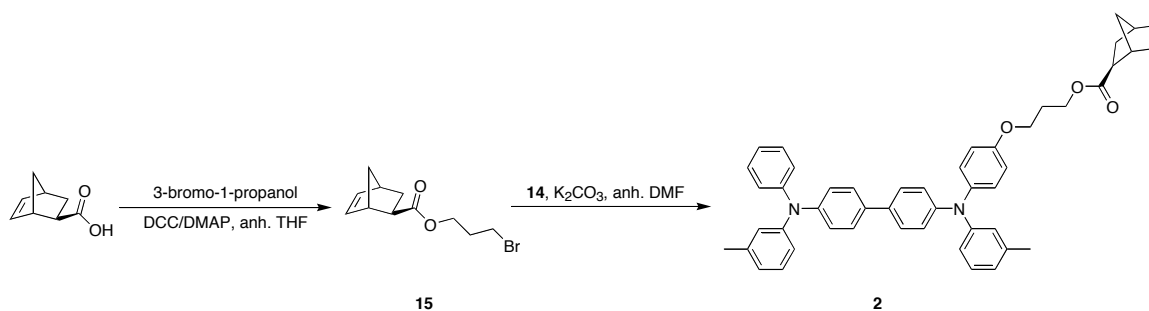
Figure 2.4. Structures of target *exo*-norbornenes for coupling to **14**.

atoms in the side chain to maintain consistency among the three TPD target monomers.

We were unsuccessful in our attempts to synthesize our target *exo*-norbornene ether.

Most intermediates of the *exo*-norbornene ether were isolated according to procedures by Mayo and Tam.⁴⁸

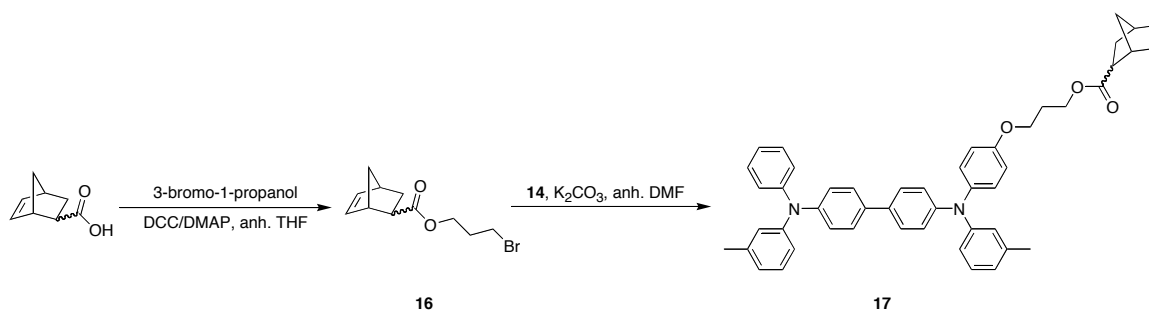
exo-3-Bromopropyl norbornene carboxylate (**15**) was prepared from *exo*-norbornene carboxylic acid and 3-bromopropanol using the (DCC/DMAP) protocol (Scheme 2.4).⁴⁹ The reaction was stirred at 50 °C until all the starting carboxylic acid was consumed. The urea precipitate was filtered before the desired ester was extracted into ether. The combined organic layers were washed with water, saturated aqueous NaHCO₃, and saturated aqueous NaCl. The carboxylate was purified by column chromatography, and it was recovered as white, crystalline solid. The yield was about 17%. The reaction was repeated using *endo/exo*-norbornene carboxylic acid, but the reaction was stirred at room temperature. The recovered yield was approximately five times the yield recovered for the *exo*-isomer (*vide supra*).



Scheme 2.4. Synthetic route to *endo/exo*-propylester norbornene TPD.

The synthesis of **2** was similar to that of **1**. *exo*-3-Bromopropyl norbornene carboxylate and TPD-OH were coupled in a Williamson ether synthesis reaction at room temperature. The desired monomer was extracted into ethyl acetate. The combined organic layers were washed with saturated aqueous NaCl. The monomer was purified by column chromatography. **2** was recovered in good yield (47%) as a light brown crystalline solid.

Our focus shifted to synthesizing the *endo/exo* analogue of **2**. The route toward **16** began with an esterification of commercially available *endo/exo*-norbornene carboxylic acid (Scheme 2.5). DCC was added to a cooled flask containing a solution of reactants, and the reaction was stirred at room temperature for 24 hours. Clear, colorless liquid (**16**) was recovered after column chromatography. The norbornene ester was coupled to **14** using Williamson etherification conditions. While some of the desired monomer was isolated by column chromatography, most of the crude material still contained a mixture of excess starting material and **17**. Thus, size exclusion chromatography (SEC) was used to further purify the monomer.



Scheme 2.5. Synthetic route to *endo/exo*-propylester norbornene TPD.

Interestingly, **17** was thermally unstable at moderate temperatures. Some of the material decomposed during rotary evaporation at 60 °C. Also, the *endo* and *exo* isomers were separated to a great extent by SEC. ¹H NMR confirmed the recovery of pure *exo*-**17**; however, *endo*-**17** decomposed before solvent could be removed by rotary evaporation. It was not clear if the *endo* isomer was unstable to SEC conditions or if it was unstable without its *exo* counterpart.

Electrochemical Studies

TPD and its derivatives have been used often in fabricating OLED devices. We wanted to understand the electrochemistry of our TPD monomers, especially because we have an oxygen atom directly attached to our skeletons. Our intention was not to significantly change the electronic properties of TPD with our modifications.

Cyclic voltammograms of pentylnorbornene TPD (**1**) and *exo*-propylester norbornene TPD (**2**) were collected using 0.1 M Bu₄NPF₆ as electrolyte in anhydrous CH₂Cl₂. The cobaltocene/cobaltocenium couple (−1.32 V vs. FeCp₂⁺⁰) was used as the internal standard, but the potentials were reported versus the ferrocene/ferrocenium couple (Table 2.1).

The target monomers had reversible oxidations. The monomers were only slightly easier to oxidize than TPD. Likewise, the absorbance maxima of the three compounds were similar. Thus, using cyclic voltammetry and ultraviolet-visible spectroscopy, we

Table 2.1. Redox potentials of TPD derivatives vs. $\text{FeCp}_2^{+/0}$ using 0.1 M Bu_4NPF_6 in CH_2Cl_2 as electrolyte at a scan rate of 50 mV s^{-1} and spectroscopic data in CH_2Cl_2 .

Compound	$E_{1/2}^{(1)}$ [a] [V]	$E_{1/2}^{(2)}$ [b] [V]	$\Delta E_{1/2}$ [c] [V]	λ_{max} [nm]
TPD	0.26	0.51	0.25	354
1	0.22	0.47	0.25	355
2	0.24	0.49	0.25	354

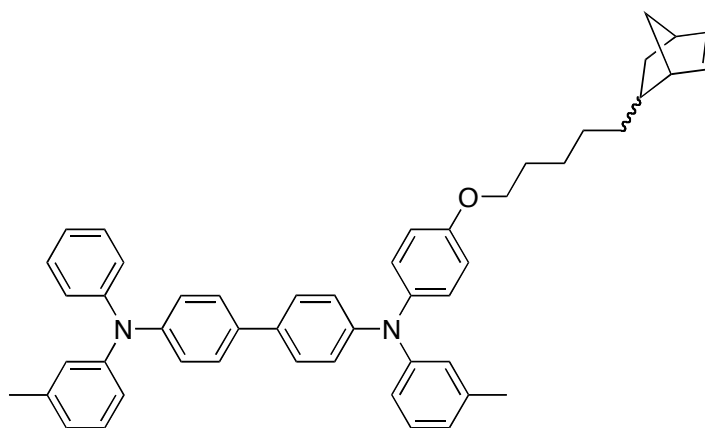
[a] Half-wave redox potential for the M^+/M couple. [b] Half-wave redox potential for the M^{2+}/M^+ couple. [c] $\Delta E_{1/2} = E_{1/2}^{(2)} - E_{1/2}^{(1)}$.

determined that the phenoxy functionality of our monomers did not significantly affect the electronic or spectroscopic properties of the TPD backbone. Because our monomers are electrochemically and spectroscopically similar to TPD, we expect them to be good candidates for hole transport materials in OLEDs. Further studies on morphology, thermal stability, and carrier mobility will help better demonstrate the usefulness of our monomers in devices.

Experimental

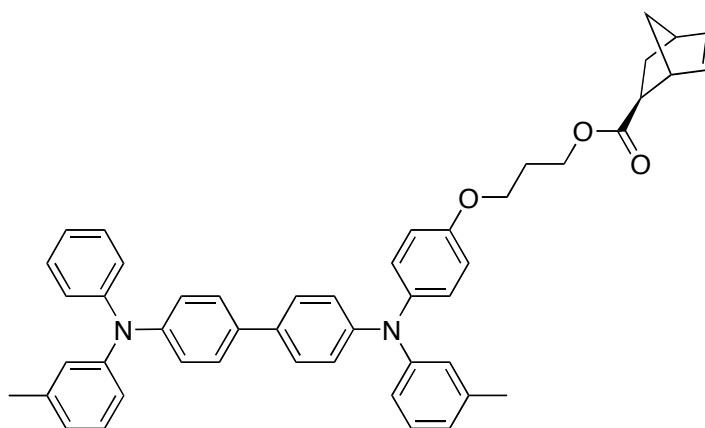
All reagents were purchased from Sigma/Aldrich, Acros, or EM Science and were used without further purification unless otherwise noted. Air sensitive reactions were conducted under a nitrogen atmosphere using Schlenk and vacuum line techniques. Schlenk flasks were oven dried overnight at 120°C and cooled on a vacuum line by pump-filling prior to use. Anhydrous solvents were taken from our solvent purification system⁵⁰ or transferred from sealed containers via cannula. ^1H , ^{13}C , and COSY nuclear magnetic resonance spectra of pure compounds were recorded on either a Varian 300

MHz or a Bruker 500 MHz NMR spectrometer and referenced to residual proton solvent peaks. All mass spectra were obtained from the Georgia Institute of Technology BioAnalytical Mass Spectrometry Facility. Elemental Analyses were conducted at Atlantic Microlab, Inc. in Norcross, Georgia. Electrochemical measurements were performed under nitrogen using deoxygenated dichloromethane and 0.1 M Bu₄NPF₆ as electrolyte. A BAS potentiostat, a glassy carbon working electrode, a platinum auxiliary electrode, and a non-aqueous AgCl/Ag pseudoreference electrode were used.



***N, N'*-(*m*-Tolyl)-*N*-[4-(bicyclo[2.2.1] hept-2-enylpentoxy)-phenyl]-*N'*-phenyl-1,1'-biphenyl amine (**1**).** Anhydrous DMF (3.6 mL), **6** (2.010 g, 3.773 mmol), potassium carbonate (0.672 g, 4.86 mmol), and **7** (0.762 g, 3.13 mmol) were added to a 50 mL round bottom flask. The reaction was capped, stirred, and heated to 50 °C until all **7** reacted. The reaction mixture was diluted with ethyl acetate, and DMF was extracted into the aqueous layer. The organic layer was washed with 3 × 20 mL portions of water, and the solvent was removed from the combined organic layers. The light brown oil was dissolved in warm ethyl acetate and vacuum filtered to remove white solid that formed when the organic layer was reduced under pressure. Column purification was performed on silica gel with 200:1 hexanes: ethyl acetate as eluent. A white glassy/yellow rock-like

solid was obtained (0.982 g, 45%). ^1H NMR (500 MHz, CD_2Cl_2): δ 7.22 – 7.04 (m, 11H), 6.98 (br s, 1H), 6.94 – 6.87 (m, 6H), 6.84 (d, $J = 7.5$ Hz, 1H), 6.15 (dd, $J = 5.5$ Hz, 3.0 Hz, 1H), 5.97 (dd, $J = 5.8$ Hz, 2.8 Hz, 1H), 3.98 (t, $J = 6.5$ Hz, 2H), 2.81 (br s, 1H), 2.78 (br s, 1H), 2.04 (m, 1H), 1.89 (m, 1H), 1.80 (m, 2H), 1.43 (m, 8H), 1.15 (m, 2H), 0.54 (ddd, $J = 11.3$ Hz, 4.3 Hz, 2.5 Hz, 1H). ^{13}C NMR (125 MHz, CD_2Cl_2): δ 156.4, 148.3, 148.2, 148.0, 147.7, 147.1, 140.8, 139.7, 139.5, 137.2, 135.0, 133.9, 132.7, 129.6, 129.4, 129.3, 127.8, 127.4 [2], 125.5, 124.5, 124.4, 124.3, 124.2, 123.4, 123.0, 122.9, 122.0, 120.8, 115.7, 68.7, 49.9, 45.8, 43.0, 39.1, 35.1, 32.8, 29.7, 28.8, 26.7, 21.5 [2]. EI-MS (70eV) m/z : M^+ 694 (100), 628 (48), 531 (38), 148 (80). Anal. Calcd for $\text{C}_{50}\text{H}_{51}\text{N}_2\text{O}$: C, 86.41; H, 7.25. Found: C, 86.18; H, 7.30.



***exo*-3-(4-((4'-(Phenyl (*m*-tolyl) amino) biphenyl-4-yl) (*m*-tolyl amino) phenoxy)**

propyl bicyclo[2.2.1] hept-5-ene-2-carboxylate (2). 14 (0.252 g, 0.473 mmol) was

added to a pump-filled Schlenk tube and dissolved in anhydrous DMF (3.0 mL). K_2CO_3

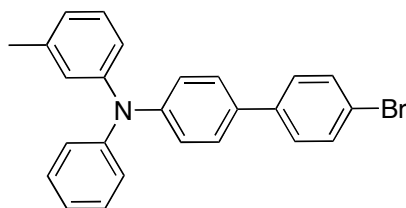
(0.100 g, 0.724 mmol) and *exo*-3-bromopropyl-5-norbornene-2-carboxylate (0.275 g,

1.06 mmol) then were added to the flask. The reaction was stirred at room temperature

for 22 h. The desired product was extracted into ethyl acetate, and the combined organic

layers were washed (brine) and dried (MgSO_4). The desired monomer was isolated by

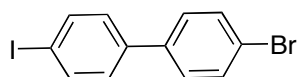
column chromatography on silica gel (15:1 hexanes: ethyl acetate), and the residual solvent was removed under reduced pressure. A brown, glassy solid was recovered (0.158 g, 47%). ^1H NMR (500 MHz, CD_2Cl_2): δ 7.45 – 7.42 (m, 4 H), 7.27 – 7.24 (m, 2 H), 7.17 – 7.06 (m, 9 H), 7.06 – 7.00 (m, 3 H), 6.94 (br s, 1 H), 6.89 – 6.84 (m, 5 H), 6.81 (d, J = 7.0 Hz, 1 H), 6.12 (m, 2 H), 4.26 (t, J = 6.4 Hz, 2 H), 4.05 (t, J = 6.3 Hz, 2 H), 3.01 (br s, 1 H), 2.90 (br s, 1 H), 2.26 (s, 3 H), 2.25 (s, 3 H), 2.22 (dd, J = 1.0 Hz, 1 H), 2.12 (quint, J = 6.3 Hz, 2 H), 1.90 (dt, J = 11.5 Hz, 4.0 Hz, 1 H), 1.49 (d, J = 8.5 Hz, 1 H), 1.38 – 1.33 (m, 2 H). ^{13}C NMR (125 MHz, CD_2Cl_2): δ 176.3, 156.0, 148.2, 147.2, 141.1, 139.7, 139.5, 138.4, 136.1, 135.0, 134.0, 129.6, 129.4, 129.3, 127.7, 127.4, 125.5, 124.5, 124.4, 124.2, 123.5, 123.0 [2], 122.0, 120.8, 115.7, 65.2, 61.6, 47.0, 46.7, 43.5, 42.1, 30.7, 29.2, 21.5 [2]. EI-MS (70eV) m/z : M^+ 710 (46), 644 (100), 531 (36), 113 (13).



***N*-(*m*-Tolyl)-*N*-phenyl-4-bromo-1,1'-biphenyl-4'-amine (4).**⁵¹ To a Schlenk tube, **9** (14.36 g, 40.01 mmol), DPPF (0.638 g, 1.15 mmol), sodium *tert*-butoxide (3.989 g, 41.50 mmol), and $\text{Pd}_2(\text{dba})_3$ (0.529 g, 0.578 mmol) were added. Anhydrous toluene (40 mL) was added, and then 3-methyldiphenylamine (5.8 mL, 33 mmol) was added by syringe. The reaction was stirred and heated at 90 °C under nitrogen for 24 h. The mixture was allowed to cool to room-temperature, then crude reaction mixture was passed through a silica plug eluting with dichloromethane. The solvent was removed under reduced pressure to give a dark brown oil that crystallized at room temperature. Boiling the solid in hexanes removed the colored impurities. Column chromatography on silica gel eluting

with 30: 1 hexanes: dichloromethane further purified the solid to give white flakes

(10.758 g, 77%). ^1H NMR (500 MHz, CD_2Cl_2): δ 7.59 (d, J = 8.9 Hz, 2 H), 7.51 (d, J = 9.0 Hz, 2 H), 7.50 (d, J = 9.0 Hz, 2 H), 7.32 (dd, J = 8.5 Hz, 7.4 Hz, 2 H), 7.21 (t, J = 7.3 Hz, 1 H), 7.14 (d, J = 8.1 Hz, 2 H), 7.13 (d, J = 8.7 Hz, 2 H), 7.09 (t, J = 7.1 Hz, 1 H), 7.00 (s, 1 H), 6.94 (d, J = 8.4 Hz, 1 H), 6.94 (d, J = 7.1 Hz, 1 H), 2.32 (s, 3 H). ^{13}C NMR (125 MHz, CD_2Cl_2): δ 148.2, 148.1, 147.9, 140.0, 139.8, 133.7, 132.2, 129.7, 129.5, 128.5, 127.8, 125.8, 124.9, 124.6, 123.9, 123.4, 122.3, 121.1, 21.5.

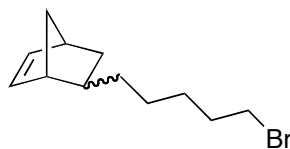


4-Bromo -4'-iodobiphenyl (5).⁵² 4-Bromobiphenyl (28.86 g, 123.8 mmol), iodine (15.74 g, 62.01 mmol), KIO_4 (14.25 g, 61.93 mmol), acetic acid (90 mL), distilled water (7 mL), and H_2SO_4 (3 mL) were added to a 250 mL flask equipped with reflux condenser and stir bar. The reaction mixture was stirred for 24 h at 70 °C and then cooled to room temperature. The mixture was poured into 1 L of water, and the solid was collected by vacuum filtration. Impurities were removed by heating the solid in ethanol, and white powder (39.37 g, 89%) was recovered after vacuum filtration. ^1H NMR (500 MHz, CD_2Cl_2): δ 7.83 (d, J = 8.5 Hz, 2 H), 7.62 (d, J = 8.6 Hz, 2 H), 7.50 (d, J = 8.5 Hz, 2 H), 7.37 (d, J = 8.5 Hz, 2 H).⁵³

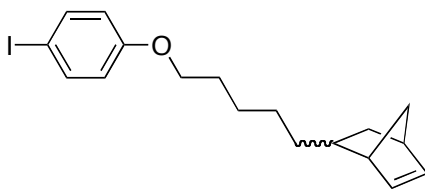


5-Bromomethyl bicyclo[2.2.1] hept-2-ene (6).⁵⁴⁻⁵⁵ A thick-wall glass tube was charged with dicyclopentadiene (35.0 g, 265 mmol) and allyl bromide (64.06 g, 529.5 mmol). The mixture was heated at 195 °C for 4 h. At 1 atmosphere, low boiling point starting materials were distilled out at 175 °C. The desired product was fractionally distilled *twice*

at 25 mmHg from 91 °C to 94 °C to yield an isomer mixture of product (50.13 g, 51%). The ratio between *endo* and *exo* isomers was approximately 83% to 17%. The ¹H spectrum was in agreement with previously reported spectrum.⁵⁵

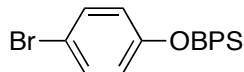


5-(5-Bromopentyl) bicyclo[2.2.1] hept-2-ene (8).⁵⁴ 5-bromomethyl norbornene (36.94 g, 197.5 mmol) was added to an oven-dried flask containing magnesium turnings (11.98 g, 492.8 mmol) and anhydrous THF (250 mL). The reaction was initiated with heat. An ice bath was used to control the exothermic reaction until it stabilized. The reaction stirred at room temperature for 24 h. 1,4-Dibromobutane (93.5 mL, 790 mmol) was added to an oven-dried Schlenk round bottom. The flask was charged with anhydrous THF (200 mL) followed by LiCuCl₄ (20 mL, 83 mmol). The reaction mixture was cooled to 0 °C. Norbornene methyl magnesium bromide was transferred dropwise by cannula. After complete transfer of the Grignard reagent, the reaction stirred at room temperature for 24 h. The reaction mixture was added to diethyl ether (100 mL) and washed with saturated aqueous NH₄Cl (100 mL). The aqueous layer was extracted with ether (3 × 200 mL). The combined organic phases were washed with saturated aqueous NaCl (150 mL) and water (3 × 200 mL) then dried over MgSO₄. The clear, yellow liquid recovered after rotary evaporation was distilled at 140 °C at 1 atmosphere. A clear, colorless liquid was obtained after distillation (66.51 g, 56%). The ¹H spectrum was in agreement with previously reported spectrum.⁵⁴



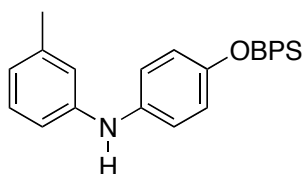
5-[5-(4-Iodophenoxy)pentyl] bicyclo[2.2.1] hept-2-ene (9). 5-(5-bromopentyl)

norbornene (4.915 g, 20.21 mmol), 4-iodophenol (3.785 g, 17.13 mmol), potassium carbonate (4.768 g, 34.50 mmol), and 17.0 mL of anhydrous DMF were added to a 100 mL round bottom flask and stirred at room temperature for three days. The reaction mixture was poured into a separatory funnel containing 100 mL of distilled water. The product was extracted into ethyl acetate. The organic layer was washed with 3 × 50 mL portions of ice-cold water and with 50 mL of saturated aqueous NaCl. The solvent was removed under reduced pressure to obtain a clear, light brown oil. The crude product was purified by column chromatography on silica gel, eluting with hexanes. The solvent was removed under reduced pressure to obtain a clear, colorless oil. Mass recovered was 5.358 g (81% yield). ^1H NMR (300 MHz, CDCl_3): δ 7.52 (d, J = 9.1 Hz, 2 H), 6.65 (d, J = 9.1 Hz, 2 H), 6.10 (dd, J = 5.6, 3.0, 2.7 Hz, 1 H), 5.90 (dd, J = 5.6, 3.0, 2.7 Hz, 1 H), 3.88 (t, J = 6.6 Hz, 2 H), 2.74 (m, 2 H), 1.95 (m, 2 H), 1.75 (m, 2 H), 1.34 (m, 3 H), 1.21 (m, 2 H), 1.18 (m, 2 H), 1.07 (m, 2 H). ^{13}C NMR (75 MHz, CDCl_3): δ 158.81, 137.97, 136.81, 132.22, 116.80, 84.10, 68.08, 49.59, 45.43, 42.54, 38.72, 34.71, 32.47, 29.20, 28.43, 26.29. EI-MS (70eV) m/z : M^+ 383 (23), 316 (100), 220 (74), 66 (49).



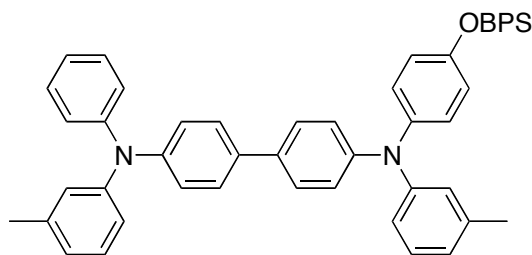
(4-Bromophenoxy)-tert-butyldiphenylsilane (11).⁴⁶ To a 500 mL round bottom flask, 4-bromophenol (6.051 g, 34.96 mmol) was added to anhydrous DMF (260 mL). Imidazole (4.763 g, 69.96 mmol) was added to the stirring solution before *tert*-

butyl(chloro)diphenylsilane (10.0 mL, 38.5 mmol) was added by syringe. The reaction mixture was allowed to stir at room temperature until all 4-bromophenol was consumed. The clear, colorless solution was diluted with distilled water. The aqueous layer was then extracted with 3 × 200 mL hexanes. The combined organic layers were dried over MgSO₄, and the solvent was removed under reduced pressure to reveal either a clear, colorless oil or a light yellow oil. Column chromatography on silica gel eluting with 3:1 hexanes: dichloromethane further purified the product (8.905 g, 62%). ¹H NMR (500 MHz, CDCl₃): δ 7.69 (d, *J* = 6.7 Hz, 4 H), 7.43 (t, *J* = 7.4 Hz, 2 H), 7.37 (app. t, *J* = 7.5 Hz, 6.9 Hz, 4 H), 7.17 (d, *J* = 8.9 Hz, 2 H), 6.63 (d, *J* = 8.9 Hz, 2 H), 1.20 (s, 9 H).

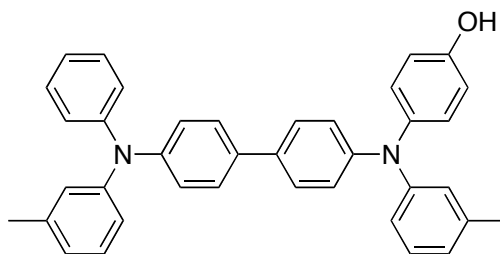


[4-(*tert*-Butyldiphenylsilyloxy)-phenyl]-*m*-tolyl amine (12).⁵¹ **2** (1.495 g, 3.634 mmol) was added to a Schlenk tube containing anhydrous toluene (10 mL), Pd₂(dba)₃ (0.057 g, 0.062 mmol), DPPF (0.069 g, 0.12 mmol), and sodium *tert*-butoxide (0.878 g, 9.14 mmol). *m*-Toluidine (0.55 mL, 5.1 mmol) was then slowly added to the stirring reaction mixture. The reaction was sealed under inert atmosphere, heated to 100 °C, and stirred until **2** was consumed. The desired product was isolated after column chromatography on silica gel with 10:1 hexanes: ethyl acetate as eluent. A yellow-brown slightly fragrant viscous liquid was recovered (1.432 g, 90%). ¹H NMR (500 MHz, CD₂Cl₂): δ 7.79 (d, *J* = 6.6 Hz, 4 H), 7.50 (t, *J* = 7.4 Hz, 2 H), 7.44 (dd, *J* = 7.5 Hz, 6.9 Hz, 4 H), 7.10 (t, *J* = 7.8 Hz, 1 H), 6.90 (d, *J* = 8.8 Hz, 2 H), 6.76 (d, *J* = 8.9 Hz, 2 H), 6.75 (br s, 1 H), 6.72 (br d, *J* = 8.0 Hz, 1 H), 6.68 (br d, *J* = 8.0 Hz, 1 H), 5.52 (br s, 1 H), 2.30 (s, 3 H), 1.16 (s, 9 H). ¹³C NMR (125 MHz, CD₂Cl₂): δ 151.0, 145.1, 139.5, 136.8,

136.0, 133.5, 130.3, 129.4, 128.1, 121.3, 120.9, 120.6, 116.9, 113.3, 26.7, 21.6, 19.7. EI-MS (70 eV) m/z : M^+ 437 (82), 380 (100), 302 (13), 273 (22), 190 (44).

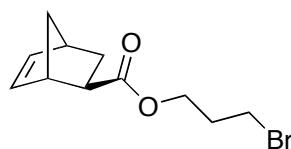


***N, N'*-(*m*-Tolyl)-*N*-[4-(*tert*-butyldiphenylsilanyloxy)-phenyl]-*N'*-phenyl-1,1'-biphenyl amine (**13**).⁵¹** $\text{Pd}_2(\text{dba})_3$ (0.223 g, 0.244 mmol), DPPF (0.270 g, 0.487 mmol), and sodium *tert*-butoxide (3.435 g, 35.74 mmol) were added to 38 mL of anhydrous toluene in a Schlenk tube. **4** (5.924 g, 14.30 mmol) was added to the stirring catalyst mixture followed by **3** (7.405 g, 16.92 mmol), which was dissolved in 10 mL of anhydrous toluene. The reaction vessel was sealed under nitrogen and heated to 100° C until TLC showed consumption of **4**. The crude mixture was purified on a silica plug with 300:1 hexanes: ethyl acetate before further purification by two column chromatography attempts using 300:1 hexanes: ethyl acetate. An off-white solid (3.803 g, 35%) was recovered after removing solvent. ^1H NMR (500 MHz, CD_2Cl_2): δ 7.79 (d, J = 6.6 Hz, 4 H), 7.52 – 7.41 (m, 10 H), 7.31 (d, J = 7.4 Hz, 1 H), 7.29 (d, J = 7.4 Hz, 1 H), 7.20 (t, J = 7.8 Hz, 1 H), 7.16 – 7.10 (m, 5 H), 7.06 (t, J = 7.3 Hz, 1 H), 7.02 (d, J = 8.7 Hz, 2 H), 6.99 (br s, 1H), 6.94 (d, J = 8.1 Hz, 1 H), 6.94 (d, J = 8.1 Hz, 1 H), 6.92 (d, J = 8.8 Hz, 2 H), 6.89 (br s, 1 H), 6.85 (d, J = 8.1 Hz, 1 H), 6.83 (d, J = 7.6 Hz, 1 H), 6.77 (d, J = 8.9 Hz, 2 H), 2.31 (s, 3 H), 2.28 (s, 3 H), 1.17 (s, 9 H). ^{13}C NMR (125 MHz, CD_2Cl_2): δ 152.5, 148.2 [2], 148.0, 147.6, 147.1, 141.4, 139.7, 139.4, 136.0, 135.0, 134.0, 133.4, 129.6, 129.4, 129.2, 128.1, 127.4, 127.3, 127.2, 125.5, 124.5, 124.4 [2], 124.2, 123.5, 123.0 [2], 122.0, 121.0, 120.9, 26.7, 21.5 [2], 19.7.



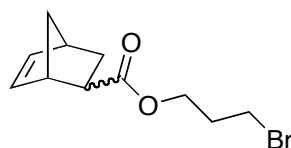
***N, N'*-(*m*-Tolyl)-*N*-[4-hydroxy-phenyl]-*N'*-phenyl-1,1'-biphenyl amine (14).⁴⁶ 13**

(3.635 g, 4.719 mmol) was dissolved in 107 mL of THF. *tert*-Butyl ammonium fluoride (2.4 mL, 8.3 mmol) was then added by syringe. The reaction vessel was capped and allowed to stir at room temperature for 15 hours. THF was removed by rotary evaporation before the desired product was extracted into ethyl acetate. The organic layer was washed with water (3 × 75 mL) then saturated aqueous NaCl (1 × 75 mL). The alcohol was further purified by column chromatography on silica gel eluting with 10:1 hex: ethyl acetate. A yellow, highly viscous liquid was obtained (2.669 g, 106%). ¹H NMR (500 MHz, CD₂Cl₂): δ 7.50 (d, *J* = 11.5 Hz, 2 H), 7.47 (d, *J* = 10 Hz, 2 H), 7.31 (d, *J* = 7.5 Hz, 1 H), 7.30 (d, *J* = 7.5 Hz, 1 H), 7.21 – 7.04 (m, 12 H), 6.99 (br s, 1 H), 6.94 (m, 2 H), 6.90 (br t, *J* = 7.0 Hz, 2 H), 6.86 – 6.82 (m, 3 H), 2.31 (s, 3 H), 2.29 (s, 3 H). ¹³C NMR (125 MHz, CD₂Cl₂): δ 152.7, 148.3, 148.2, 148.0, 147.7, 147.1, 141.1, 139.7, 139.5, 135.0, 134.0, 129.6, 129.4, 129.3, 128.0, 127.4 [2], 125.5, 124.5, 124.4, 124.3, 124.2, 123.5, 123.0 [2], 122.0, 120.8, 116.6, 21.5 [2].

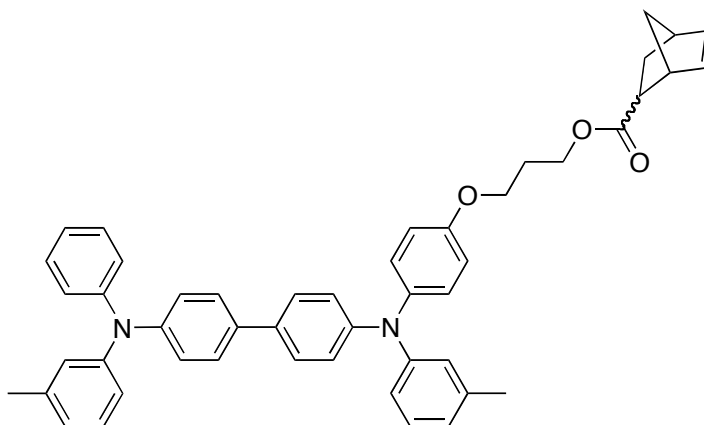


***exo*-3-Bromopropyl bicyclo[2.2.1] hept-5-ene-2-carboxylate (15).⁴⁹** To a pump-filled flask were added *exo*-norbornene-carboxylic acid (1.508 g, 10.91 mmol), 3-bromo-1-propanol (0.98 mL, 11 mmol), and DMAP (0.054 g, 0.44 mmol). Anhydrous THF (15 mL) was then added to dissolve the reactants. The flask was cooled to 5 °C before the addition of DCC (3.085 g, 14.95 mmol). The reaction was stirred at 50 °C for 24 h. The products were extracted into diethyl ether. The combined organic layers were washed

with saturated NaHCO₃ and with brine. The organic layer was filtered to remove urea precipitate and dried over MgSO₄. The solvent was removed by rotary evaporation. **15** was isolated on a silica gel plug eluting with 50:1 hexanes: ethyl acetate. A clear, yellow liquid was recovered (0.481 g, 17%). ¹H NMR (500 MHz, CDCl₃): δ 6.13 – 6.08 (m, 2 H), 4.21 (t, *J* = 6.0 Hz, 2 H), 3.45 (t, *J* = 7 Hz, 2 H), 3.01 (br s, 1 H), 2.91 (br s, 1 H), 2.18 (m, 3 H), 1.89 (dt, *J* = 11.5 Hz, 8.0 Hz, 1 H), 1.49 (app. d, *J* = 8.5 Hz, 1 H), 1.35 (m, 2 H). ¹³C NMR (125 MHz, CDCl₃): δ 176.1, 138.1, 135.7, 62.1, 46.7, 46.4, 43.1, 41.6, 31.7, 30.3, 29.4.



3-Bromopropyl bicyclo[2.2.1] hept-5-ene-2-carboxylate (16).⁴⁹ To a pump-filled flask were added *endo/exo*-norbornene-carboxylic acid (1.2 mL, 9.8 mmol), 3-bromo-1-propanol (1.0 mL, 11 mmol), and DMAP (0.122 g, 0.999 mmol). Anhydrous THF (25 mL) was then added to dissolve the reactants. The flask was cooled to 5 °C before the addition of DCC (2.271 g, 11.01 mmol). The reaction was stirred at room temperature for 24 h. The precipitate was filtered before extracting the ester into diethyl ether. The combined organic layers were washed with saturated NaHCO₃ then with brine. The organic layer was dried over MgSO₄, and the solvent was removed by rotary evaporation. *endo/exo*-Propylester norbornene was isolated on a silica gel plug eluting with 10:1 hexanes: ethyl acetate. A clear, colorless liquid was recovered (1.732 g, 68%, 80:20 *endo/exo*). ¹H NMR (500 MHz, CDCl₃): δ 6.15 (dd, *J* = 3.0 Hz, 1 H, *endo*), 6.11 – 6.06 (m, 2 H, *exo*), 5.88 (dd, *J* = 3.0 Hz, 1 H, *endo*), 4.18 (t, *J* = 3.0 Hz, 2 H, *exo*), 4.15 – 4.08 (m, 2 H, *endo*), 3.44 (t, *J* = 6.5 Hz, 2 H, *exo*) 3.42 (t, *J* = 6.5 Hz, 2 H, *endo*), 3.16 (br s, 1 H, *endo*), 2.99 (br s, 1 H, *exo*), 2.93 – 2.90 (m, 1 H, *endo*), 2.87 (br s, 2 H, *endo* + *exo*), 2.20 – 2.08 (m, 5 H, *endo* + *exo*), 1.89 – 1.84 (m, 2 H, *endo* + *exo*), 1.47 (br d, *J* = 8.5 Hz, 1 H, *exo*), 1.41 – 1.31 (m, 4 H, *endo* + *exo*), 1.24 (br d, *J* = 8.0 Hz, 1 H, *endo*).



3-(4-((4'-(Phenyl (*m*-tolyl) amino) biphenyl-4-yl) (*m*-tolyl amino) phenoxy) propyl bicyclo[2.2.1] hept-5-ene-2-carboxylate (17). **14** (0.937 g, 1.76 mmol) was added to a pump-filled Schlenk tube and dissolved in anhydrous DMF (22 mL). K₂CO₃ (0.363 g, 2.63 mmol) and 3-bromopropyl-5-norbornene-2-carboxylate (0.986 g, 3.81 mmol) then were added to the flask. The reaction was stirred at room temperature for 24 h. The desired ester TPD was extracted into ethyl acetate, and the combined organic layers were washed (water, brine) and dried (MgSO₄). The desired monomer was isolated by SEC, and the residual solvent was removed under reduced pressure. A brown, glassy solid was recovered (0.158 g, 47%, 74:26 *endo/exo*). ¹H NMR (500 MHz, CD₂Cl₂): δ 7.46 – 7.41 (m, 6 H, *endo* + *exo*), 7.28 – 7.24 (m, 3 H, *endo* + *exo*), 7.17 – 7.00 (m, 16 H, *endo* + *exo*), 6.94 (br s, 2 H, *endo* + *exo*), 6.91 – 6.84 (m, 7 H, *endo* + *exo*), 6.81 (d, *J* = 7.0 Hz, 2 H, *endo* + *exo*), 6.17 (m, 1 H, *endo*), 6.13 (m, 2 H, *exo*), 5.88 (m, 1 H, *endo*), 4.26 (t, *J* = 6.5 Hz, 2 H, *exo*), 4.19 (m, 2 H, *endo*), 4.05 (m, 4 H, *endo* + *exo*), 3.18 (br s, 1 H, *endo*), 3.02 (br s, 1 H, *exo*), 2.90 (br s, 2 H, *endo* + *exo*), 2.26 (s, 4 H, *endo* + *exo*), 2.25 (s, 4 H, *endo* + *exo*), 2.22 (m, 1 H, *exo*), 2.12 (m, 3 H, *endo* + *exo*), 1.90 (m, 1 H, *endo* + *exo*), 1.49 (d, *J* = 8.5 Hz, 1 H, *exo*), 1.42 – 1.33 (m, 4 H, *endo* + *exo*). ¹³C NMR (125 MHz, CD₂Cl₂): δ 176.4, 174.8, 156.0, 148.3, 148.1, 147.7, 147.2, 141.2, 139.7, 139.5, 138.4, 138.1, 136.1, 135.1, 134.0, 132.7, 129.6, 129.5, 129.3, 127.7, 127.5, 127.4, 125.5, 124.6, 124.4 [2], 124.3, 123.5, 123.1, 123.0, 122.0, 120.9, 115.8, 65.2 [2], 61.6, 61.3, 60.7, 50.0,

47.04, 46.7, 46.2, 43.7, 43.53, 43.0, 42.1, 30.7, 29.5, 29.2 [2], 21.6 [2], 21.2. EI-MS (70eV) m/z: M⁺ 710 (5), 644 (100), 531 (27), 113 (9).

References

- (1) Jabbour, G.E.; Shaheen, S.E.; Morrell, M.M.; Anderson, J.D.; Lee, P.;
Thayumanavan, S.; Barlow, S.; Bellmann, E.; Grubbs, R.H.; Kippelen, B.;
Marder, S.; Armstrong, N.R.; Peyghambarian, N. *IEEE J. Quantum. Electron.*
2000, *36*, 12–17.
- (2) Tang, C.W.; VanSlyke, S.A. *Appl. Phys. Lett.* **1987**, *51*, 913–915.
- (3) Shi, J.; Tang, C.W. *Appl. Phys. Lett.* **1997**, *70*, 1665–1667.
- (4) Cornil, J.; Gruhn, N.E.; dos Santos, D.A.; Malagoli, M.; Lee, P.A.; Barlow, S.;
Thayumanavan, S.; Marder, S.R.; Armstrong, N.R.; Brédas, J.-L. *J. Phys. Chem.*
A **2001**, *105*, 5206–5211.
- (5) Maldonado, J.-L.; Bishop, M.; Fuentes-Hernandez, C.; Caron, P.; Domercq, B.;
Zhang, Y.-D.; Barlow, S.; Thayumanavan, S.; Malagoli, M.; Brédas, J.-L.;
Marder, S.R.; Kippelen, B. *Chem. Mater.* **2003**, *15*, 994–999.
- (6) Fujikawa, H.; Ishii, M.; Tokito, S.; Taga, Y. *Mater. Res. Soc. Symp. Proc.* **2000**, *621*,
Q3.4.1–Q3.4.11.
- (7) Kraft, A.; Grimsdale, A.C.; Holmes, A.B. *Angew. Chem. Int. Ed.* **1998**, *37*, 402–428.
- (8) Fong, H.H.; Lun, K.C.; So, S.K. *Mater. Res. Soc. Symp. Proc.* **2002**, *725*, P8.1.1–
8.1.6

- (9) Podzorov, V.; Menard, E.; Borissov, A.; Kiryukhin, V.; Rogers, J.A.; Gershenson, M.E. *Phys. Rev. Lett.* **2004**, *93*, 086602-1–086620-4.
- (10) Jurchescu, O.D.; Popincius, M.; van Wees, B.J.; Palstra, T.M. *Adv. Mater.* **2007**, *19*, 688–692.
- (11) Carrad, M.; Gonclave-Conto, S.; Si-Ahmed, L.; Adès, D.; Siove, A. *Thin Solid Films* **1999**, *352*, 189–194.
- (12) Kijima, Y.; Asai, N.; Tamura, S. *Jpn. J. Appl. Phys.* **1999**, *38*, 5274–5277.
- (13) Bellmann, E.; Shaheen, S.E.; Thayumanavan, S.; Barlow, S.; Grubbs, R.H.; Marder, S.R.; Kippelen, B.; Peyghambarian, N. *Chem. Mater.* **1998**, *10*, 1668–1676.
- (14) Goodbrand, H.B.; Hu, N.-X. *J. Org. Chem.* **1999**, *64*, 670–674.
- (15) Li, J.; Ma, C.; Tang, J.; Lee, C.-S.; Lee, S. *Chem. Mater.* **2005**, *17*, 615–619.
- (16) Shaheen, S.E.; Jabbour, G.E.; Kippelen, B.; Peyghambarian, N.; Anderson, J.D.; Marder, S.R.; Armstrong, N.R.; Bellmann, E.; Grubbs, R.H. *Appl. Phys. Lett.* **1999**, *74*, 3212–3214.
- (17) Cocchi, M.; Fattori, V.; Virgili, D.; Sabatini, C.; Di Marco, P.; Maestri, M.; Kalinowski, J. *Appl. Phys. Lett.* **2004**, *84*, 1052–1054.
- (18) Santerre, F.; Bedja, I.; Dodelet, J.P.; Sun, Y.; Lu, J.; Hay, A.S.; D'Iorio, M. *Chem. Mater.* **2001**, *13*, 1739–1745.

- (19) Hosokawa, C.; Kawasaki, N.; Sakamoto, S.; Kusumoto, T. *Appl. Phys. Lett.* **1992**, *61*, 2503–2505.
- (20) Kim, D.U.; Tsutsui, T.; Saito, S. *Polymer* **1995**, *36*, 2481–2483.
- (21) Adachi, C.; Hibino, S.; Koyoma, T.; Taniguchi, Y. *Jpn. J. Appl. Phys.* **1997**, *36*, L827–L830.
- (22) Liu, Y.; Ma, H.; Jen, A.K.Y. *Chem. Mater.* **1999**, *11*, 27–29.
- (23) Kisselev, R.; Thelakkat, M. *Macromolecules* **2004**, *37*, 8951–8958.
- (24) Liou, G.-S.; Huang, N.-K.; Yang, Y.-L. *Polymer* **2006**, *47*, 7013–7020.
- (25) Liao, L.; Cirpan, A.; Ding, L.; Karasz, F.E.; Pang, Y. *J. Polym. Sci., Part A: Polym. Chem.* **2006**, *44*, 2307–2315.
- (26) Sommer, M.; Thelekkat, M. *Eur. Phys. J. Appl. Phys.* **2007**, *36*, 245–249.
- (27) Bellmann, E.; Shaheen, S.E.; Grubbs, R.H.; Marder, S.R.; Kippelen, B.; Peyghambarian, N. *Chem. Mater.* **1999**, *11*, 399–407.
- (28) Liang, F.; Pu, Y.-J.; Kurata, T.; Kido, J.; Nishide, H. *Polymer* **2005**, *46*, 3767–3775.
- (29) Jiang, G.; Wu, J.; Yao, B.; Geng, Y.; Cheng, Y.; Xie, Z.; Wang, L.; Jing, X.; Wang, F. *Macromolecules* **2006**, *39*, 7950–7958.
- (30) Liou, G.-S.; Hsiao, S.-H.; Huang, N.-K.; Yang, Y.-L. *Macromolecules* **2006**, *39*, 5337–5346.

- (31) Shi, W.; Fan, S.; Huang, F.; Yang, W.; Liu, R.; Cao, Y. *J. Mater. Chem.* **2006**, *16*, 2387–2394.
- (32) Domercq, B.; Hreha, R.D.; Zhang, Y.-D.; Larribeau, N.; Haddock, J.N.; Schultz, C.; Marder, S.R.; Kippelen, B. *Chem. Mater.* **2003**, *15*, 1491–1496.
- (33) Sato, Y.; Kanai, H. *Mol. Cryst. Liq. Cryst.* **1994**, *253*, 141–143.
- (34) Hreha, R.D.; Haldi, A.; Domercq, B.; Barlow, S.; Kippelen, B.; Marder, S.R. *Tetrahedron Lett.* **2004**, *60*, 7169–7176.
- (35) Borsenberger, P.M.; Pautmeier, L.; Richert, R.; Bässler, H.; *J. Chem. Phys.* **1991**, *94*, 8276–8281.
- (36) Bässler, H. *Phys. Status Solidi (b)* **1993**, *175*, 15–56.
- (37) Van der Auweraer, M.; De Schryver, F.C.; Borsenberger, P.M.; Fitzgerald, J.J. *J. Phys. Chem.* **1993**, *97*, 8808–8811.
- (38) Benedicto, A.D.; Novak, B. M.; Grubbs, R.H. *Macromolecules* **1992**, *25*, 5893–5900.
- (39) Lee, J.C.; Parker, K.A.; Sampson, N.S. *J. Amer. Chem. Soc.* **2006**, *128*, 4578–4579.
- (40) Schueller, C.M.; Manning, D.D.; Kiessling, L.L. *Tetrahedron Lett.* **1996**, *37*, 8853–8856.
- (41) Amir-Ebrahimi, V.; Corry, D.A.; Hamilton, J.G.; Thompson, J.M.; Rooney, J.J. *Macromolecules* **2000**, *33*, 717–724.

- (42) Wolfe, J.P.; Wagaw, S.; Buchwald, S.L. *J. Amer. Chem. Soc.* **1996**, *118*, 7215–7216.
- (43) 5-(Bromomethyl) bicyclo[2.2.1] hept-2-ene was synthesized, purified, and characterized by Dr. Jian-Yang Cho.
- (44) Meyers, A.; Weck, M. *Macromolecules* **2003**, *36*, 1766–1768.
- (45) Unpublished data.
- (46) Smith, A.B.; Barbosa, J.; Wong, W.; Wood, J.L. *J. Amer. Chem. Soc.* **1996**, *118*, 8316–8328.
- (47) Ahmed, S.R.; Bullock, S.E.; Cresce, A.V.; Kofinas, P. *Polymer* **2003**, *44*, 4943–4948.
- (48) Mayo, P.; Tam, W. *Tetrahedron* **2002**, *58*, 9513–9525.
- (49) Burd, C.; Weck, M. *Macromolecules* **2005**, *38*, 7225–7230.
- (50) Pangborn, A.B.; Giardello, M.A.; Grubbs, R.H.; Rosen, R.K.; Timmers, F.J. *Organometallics* **1996**, *15*, 1518–1520.
- (51) Wolfe, J.P.; Rennels, R.A.; Buchwald, S.L. *Tetrahedron* **1996**, *52*, 7525–7546.
- (52) Suzuki, H.; Nakamura, K.; Goto, R. *Bull. Chem. Soc. Jpn.* **1966**, *39*, 128–131.
- (53) R.D. Hreha. Studies on the Synthesis and the Transport Properties of Organic Materials. Ph.D. Thesis, University of Arizona, Tuscon, AZ, 2003.

(54) Stubbs, L.P.; Weck, M. *Chem. Eur. J.* **2003**, *9*, 992–999.

(55) Prepared by Dr. Jian-Yang Cho following the literature procedure.

CHAPTER 3

SYNTHESIS AND CHARACTERIZATION OF NORBORNENE-FUNCTIONALIZED 1,10-PHENANTHROLINE MONOMERS

Introduction

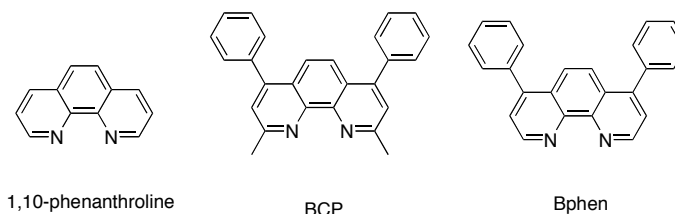


Figure 3.1. Structures of commercially available phenanthroline derivatives.

1,10-Phenanthroline is the parent molecule of a class of molecules used as hole blocking materials for organic light-emitting diodes (OLEDs). 2,9-Dimethyl-4,7-diphenyl-1,10-phenanthroline, which is also known in the literature as bathocuproine (BCP), is a common hole blocking material (HBM) in OLED devices.¹⁻³ The molecule is well suited as an HBM because its molecular orbitals are ideally positioned to transport electrons from the cathode while preventing holes from migrating to the cathode. The lowest unoccupied molecular orbital (LUMO) energy is approximately 3.0 eV below vacuum, so BCP has been used as an electron transport layer (ETL).^{1,3,4} BCP has also been doped into *tris*(8-hydroxyquinoline) aluminum (Alq₃) for use as an ETL because the LUMOs closely align with each other.⁴ The energy level of the highest occupied molecular orbital (HOMO) is sufficiently low in energy to block hole injection from many of the materials commonly used for the emissive layer. The HOMO is deep, 6.7 eV below vacuum, and this characteristic of BCP helps to confine holes in the emission layer (EL) where they can recombine with electrons.^{1,4}

Since BCP can block holes, devices incorporating BCP often exhibit higher luminous efficiencies and power efficiencies (*i.e.*, they emit brighter light using less power) than similarly structured devices without a hole blocking layer.¹ The improvement is likely due to a higher rate of recombination of charges to produce photons compared to devices without BCP. Other features of BCP that make it ideal as a HBM are that it is not an emitter,⁴ it is not toxic, and it decreases the turn-on voltage for a device.¹ Wang *et al.* postulated that the turn-on voltage for their devices was lower than a comparable device without BCP because the LUMO of Alq₃ was better aligned energetically with the LUMO of BCP. The alignment facilitated transport from one layer to the other because the additional layer provided a lower energy barrier for electrons.

Recently, Bphen (bathophenanthroline or 4,7-diphenyl-1,10-phenanthroline) has been reported in the literature as a HBM.⁵⁻⁸ As with BCP, devices with Bphen showed improvement in luminous efficiencies and power efficiencies.^{5,7} However, both BCP and Bphen must be vapor deposited onto the device, and they have been reported to crystallize during device operation.^{1,7,8} Phenanthroline itself cannot be used as a HBM despite its low-lying HOMO because it also crystallizes,⁹ which often leads to phase separation. Thus, crystallization can lead to the devices requiring higher voltages to inject charges and becoming less efficient to operate.

Based on the preliminary information about phenanthroline, BCP, and Bphen, quantum-chemical calculations of several 1,10-phenanthroline derivatives (Figure 3.2) were performed by Dr. Karin Schmidt in the Bredas Research Group. The calculations showed that the methyl groups in the 2 and 9 positions act to destabilize the HOMO (*e.g.*, BCP and IV [Bphen]) while the phenyl groups do not appear to have any significant

contribution. Our criteria for selecting compounds to study further were that they have HOMO energies similar to or lower than BCP.

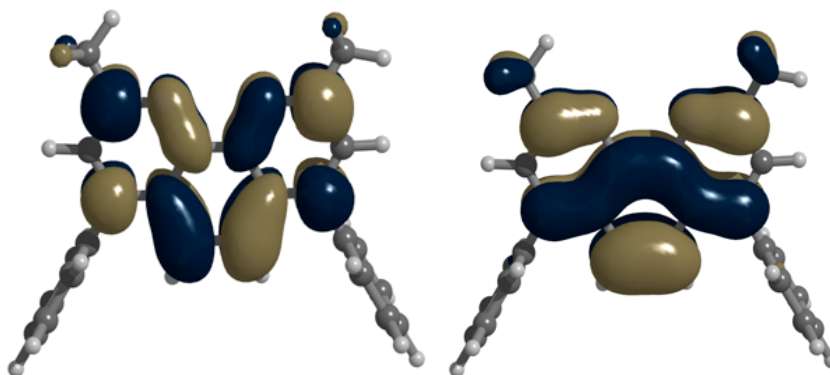


Figure 3.2 (a). Illustration of the HOMO (left) and LUMO (right) wavefunctions for bathocuproine.

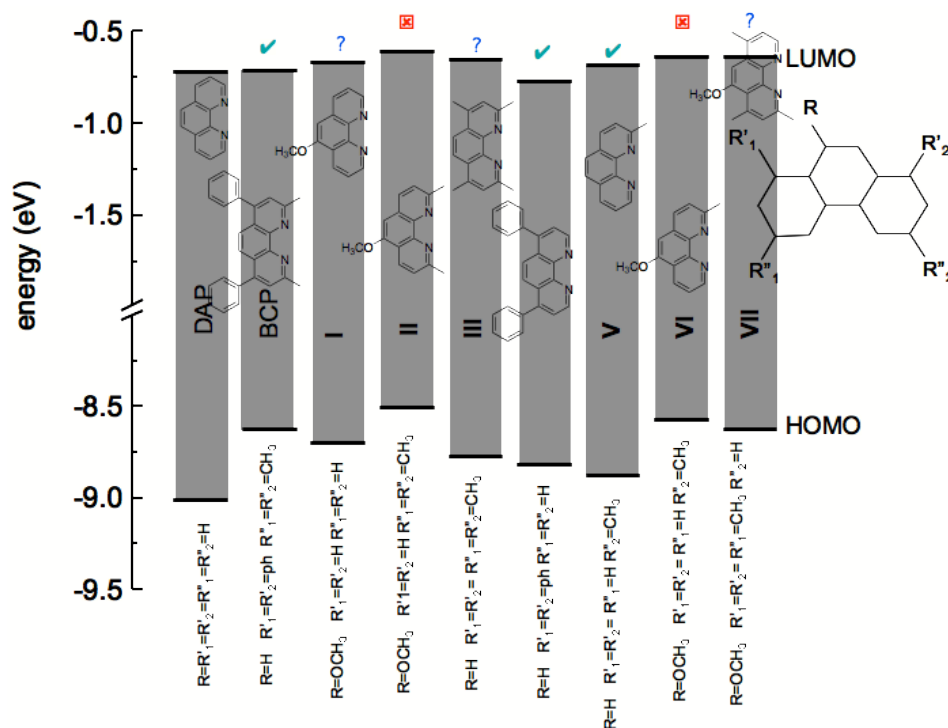


Figure 3.2 (b). Diagram of the AM1 quantum-chemical energy levels for 1,10-phenanthroline derivatives (courtesy of Dr. Karin Schmidt).

Because of the significant increase in LUMO energy, II and VI were not considered further. While I, III, and VII had HOMO energies lower than BCP, the LUMOs were somewhat destabilized. However, the LUMOs were believed to be at a

reasonable level to support electron transport. Based on the electron affinities of Alq₃ (3.25 eV)¹⁰ and BCP, it is our hypothesis that the increases in LUMO energies are small enough to not affect or minimally affect charge injection. BCP, Bphen, and 2-methyl-1,10-phenanthroline were deemed excellent candidates for initial studies.

Both BCP and Bphen are commercially available; however, they are expensive as starting materials for synthetic modifications on gram scales. For this reason, it is our desire to synthesize polymerizable HBMs based on 1,10-phenanthroline. The polymers are expected to be solution processible, thermally stable, non-emissive, and electronically stable. Because there is an incomplete body of work on 1,10-phenanthroline in the literature, we chose to attempt to determine whether the small molecules form radical anions of comparable stability to those of BCP and Bphen, are non-emissive, and are efficient hole blockers and electron transport materials.

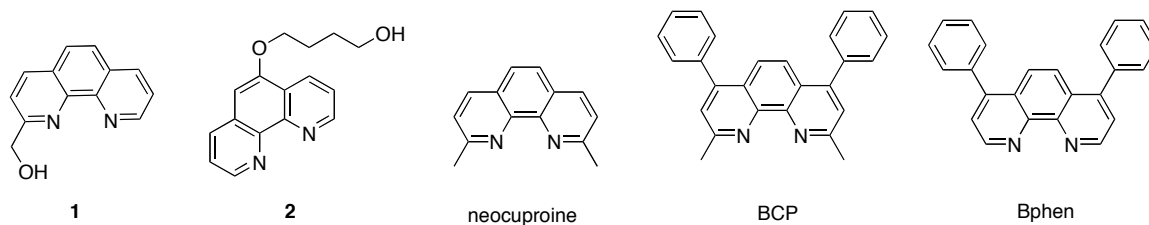


Figure 3.3. Structures of 1,10-phenanthroline derivatives for electrochemical studies.

The initial goals of our project were as follows:

- Synthesize 2-carbinol-1,10-phenanthroline (**1**) and 4-(1,10-phenanthrolin-5-yloxy)butan-1-ol (**2**)
- Determine if **1**, **2**, neocuproine (2,9-dimethyl-1,10-phenanthroline), BCP, and Bphen form stable radical anions using cyclic voltammetry.
- Use cyclic voltammograms of the five compounds to estimate HOMO and LUMO energies for comparison to computational data.

- Fabricate OLEDs using the small molecules and obtain information on efficiencies, turn on voltages, and device lifetime.

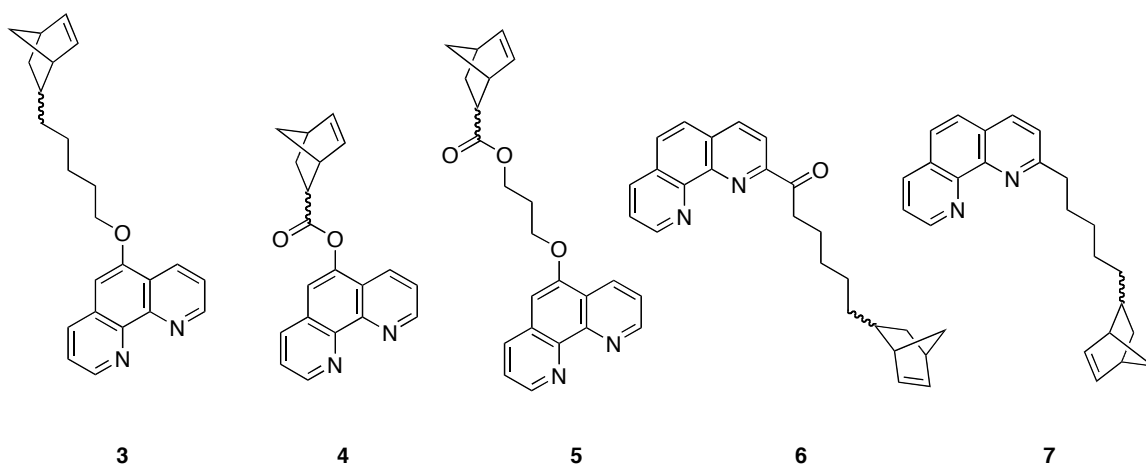


Figure 3.4. Structures of 1,10-phenanthroline based norbornene monomers.

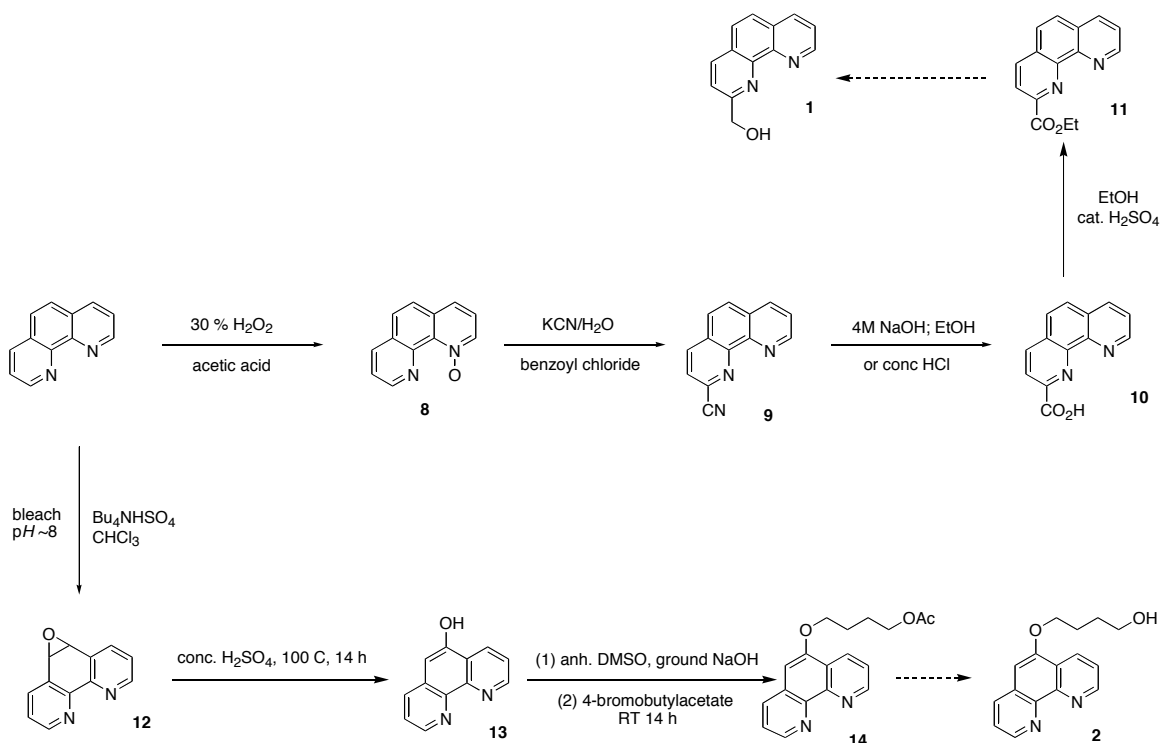
We have since decided to change the target molecules to four norbornene monomers **3–7** (Figure 3.4). The decision was based in part on synthetic difficulties and on electrochemical studies of several phenanthroline small molecules. 1,10-phenanthrolines are used to coordinate metals,^{11–15} so we anticipated that our phenanthrolines could coordinate to the metal centers of ROMP initiators. However, we chose to continue using norbornene as the polymerizable group because Dr. Feng Jing in our group ran trial polymerizations of norbornene by Grubbs’s initiators in the presence of 1,10-phenanthroline. From his results, it was observed that phenanthroline did not inhibit polymerization of norbornene when either the second- or third-generation catalyst was used.

Results and Discussion

The BCP project began with efforts to synthesize 2-carbinol-1,10-phenanthroline (**1**) and 4-(1,10-phenanthrolin-5-yloxy)butan-1-ol (**2**) following literature methods (Scheme 3.1).¹⁶⁻¹⁷

Synthesis of 2-Substituted-1,10-Phenanthrolines

The intermediate compounds leading to **1** were prepared with high purities in good yields. 1,10-Phenanthroline-1-oxide was prepared by dissolving 1,10-phenanthroline in glacial acetic acid and adding one portion of 30% hydrogen peroxide dropwise. The reaction was heated to 72 °C for 3, 4, or 6 hours before a second portion of



Scheme 3.1. Synthetic routes to 2-carbinol-1,10-phenanthroline and 4-(1,10-phenanthrolin-5-yloxy)butan-1-ol.

oxidant was added dropwise. The reaction continued for another 3, 6, or 8 hours. The reaction mixture was allowed to cool to room temperature before the pH was adjusted to

~10 using saturated aqueous KOH. The aqueous layer was extracted several times with CHCl₃, and the combined organic layers were dried over MgSO₄. The solvent was removed by rotary evaporation, and residual solvent was removed on a vacuum line. The crude solid was mustard yellow. The 1-oxide can be recrystallized from chlorobenzene to give pure compound. The only impurity visible by ¹H NMR was the starting material. Longer reaction times were tried to give sufficient time for the reaction to go to completion. While the reactions times of 10 or 14 hours did lead to higher conversion rates, the overall yield of the reaction decreased. Using a freshly opened bottle of hydrogen peroxide did not appear to help drive the reaction to completion in the 6 hours reported by Sun *et al.*¹⁶

To prepare 2-cyano-1,10-phenanthroline, either pure 1-oxide or crude 1-oxide was used. Neither the yields nor the purities of the resulting cyano compound seemed to be affected by the presence of 1,10-phenanthroline. Potassium cyanide and **8** were dissolved in water before benzoyl chloride was added dropwise to the solution. Using a syringe stopcock produced grainier final product, whereas manually adding via pipette produced more needle-like product. The reaction stirred at room temperature for 2 hours after the addition of benzoyl chloride. The precipitate was filtered with suction and washed with water to remove benzoic acid and excess potassium cyanide. The brown solid was recrystallized from either methanol or ethanol, and the pure compound was recovered in good yields.

Synthesizing the 2-carboxy derivative proved to be the most challenging because the work up was *pH* sensitive. Both an acidic and a basic hydrolysis of 2-cyano-1,10-phenanthroline were attempted without much success initially. Following Sun *et al.*, the

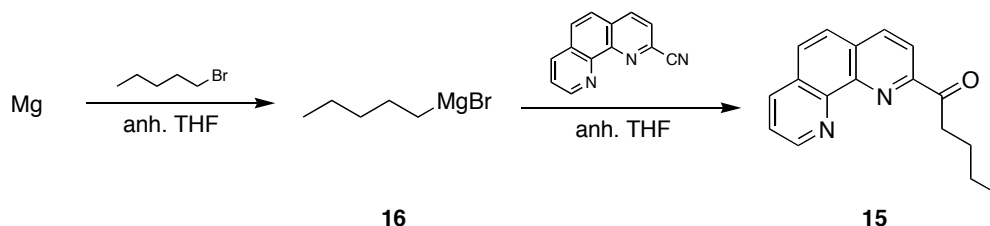
basic hydrolysis was performed by adding 4 M NaOH and 95 % ethanol to 2-cyano-1,10-phenanthroline and heating to reflux for 2 hours. Corey *et al.* reported the reaction was complete when the evolution of ammonia ceased,¹⁸ and the reaction was monitored for such an event. The reaction mixture was cooled to room temperature, and the pH was adjusted to 3 using concentrated HCl. An ice water bath was used to keep the flask cool during acidification, and nitrogen was blown intermittently into the flask to remove the resulting vapors. At pH 3, the reaction mixture was smooth and peach colored. The product was filtered and a clay-like precipitate remained. The color varied from tan to brick red, and it was dried under vacuum. Residual ethanol was removed in the vacuum oven at 47 °C. The product remained hydrated, as reported by Corey *et al.*¹⁸

Under acidic hydrolysis, **9** was refluxed in concentrated HCl for 6 hours. The reaction mixture was cooled to room temperature before adjusting the pH to 5 using aqueous sodium bicarbonate. No product was ever recovered despite seeing precipitate form during the work-up. Based on the challenges of isolating **10**, an alternative route was devised for 2-substitutions (*vide infra*).

2-Carboethoxy-1,10 phenanthroline (**11**) was synthesized from the carboxylic acid using standard Fischer esterification methods. The reaction was quenched with water, and the ester was extracted into dichloromethane. After the workup, a light yellow solid was recovered. It was nearly pure by ¹H NMR. When the reaction was scaled up, mixture of the acid and the ester resulted. Chromatographic and recrystallizing efforts to isolate the ester were unsuccessful.

Because of the challenges to isolate the carboxylic acid, synthesis of ketone **15** was proposed (Scheme 3.2) with the idea being to prepare a norbornene monomer. Zong

and Thummel reported 2-acetyl-1,10-phenanthroline,¹⁹ but it was thought best to use a pentyl group for its analogy to 1-bromopentyl norbornene (Figure 3.5). Thus, pentyl magnesium bromide was synthesized as a model for the norbornene.



Scheme 3.2. Synthetic route toward pentyl phenanthrolyl ketone from a nitrile and a Grignard reagent.

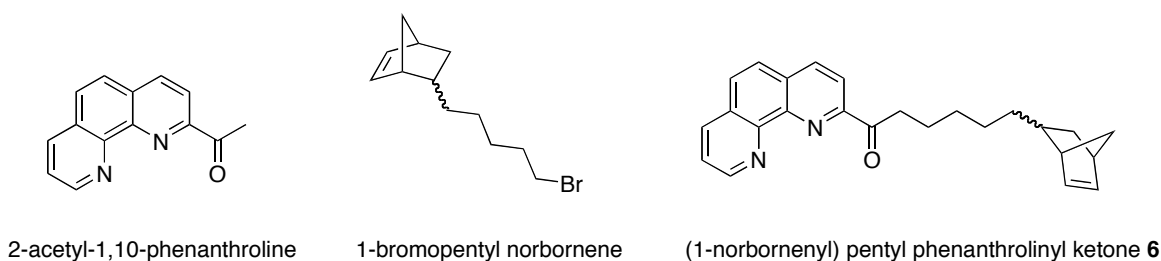


Figure 3.5. Structures related to the synthesis of a 2-substituted phenanthroline monomer.

Pentylmagnesium bromide **16** was prepared following a procedure from van Summeren *et al.*²⁰ Bromopentane was dissolved in anhydrous THF and transferred by cannula into a flask containing acid-washed and oven-dried magnesium turnings. The reaction was heated at 45 °C for 1 hour. Vigorous boiling was observed for about ten minutes, and it then subsided for the duration of time. The reaction was allowed to cool, and a white precipitate formed overnight as described by the authors. We speculated the precipitate were inorganic salt by-products of the reaction and the supernatant contained the desired Grignard reagent.

2-Cyano-1,10-phenanthroline was purged with nitrogen for 1 hour before the flask was charged with anhydrous THF. Most of the solute dissolved after stirring for 20

minutes. The flask was then cooled in a dry ice/acetone bath for 20 minutes. The Grignard solution, a brown liquid, was transferred dropwise to the nitrile over 40 minutes. The solution darkened in color during the addition of pentyl magnesium bromide. The reaction continued for 0.5 hour at $-78\text{ }^{\circ}\text{C}$ before the cooling bath was removed.

After 1 hour stirring at room temperature, the presumed imine intermediate was hydrolyzed to the ketone by slow addition of saturated aqueous NH_4Cl . A precipitate appeared then disappeared during hydrolysis. The organic layer was isolated, and the aqueous layer was extracted with THF. A dark brown crude liquid was recovered. Thin-layer chromatography using CH_2Cl_2 with and without NEt_3 provided a spot with the same R_f value in both eluents. A silica gel column was prepared in a pipette, and four 2 mL fractions were collected. The solvent was evaporated, and ^1H NMR of the four fractions indicated that only the second and the third fractions contained the desired phenanthrolinyl ketone. The first fraction contained solvent and an unidentified aliphatic species, while the final fraction contained only deuterated solvent.

Purification of the bulk crude phenanthrolinyl ketone (**15**) by silica plug was not successful. Fractions were collected, and the solvent was removed by rotary evaporation. The ^1H NMR showed the presence of many peaks, and it was not possible to clearly identify whether peak associated with the desired ketone were present. Moreover, there were no peaks consistent with the ketone in GC-MS analyses of the fractions.

Because we were able to isolate **15** on a small scale, it was our hypothesis that the ketone was not stable in air for more than a few days. **6** was prepared using the same procedure as the alkyl derivative (Scheme 3.3). When Grignard reagent **17** was

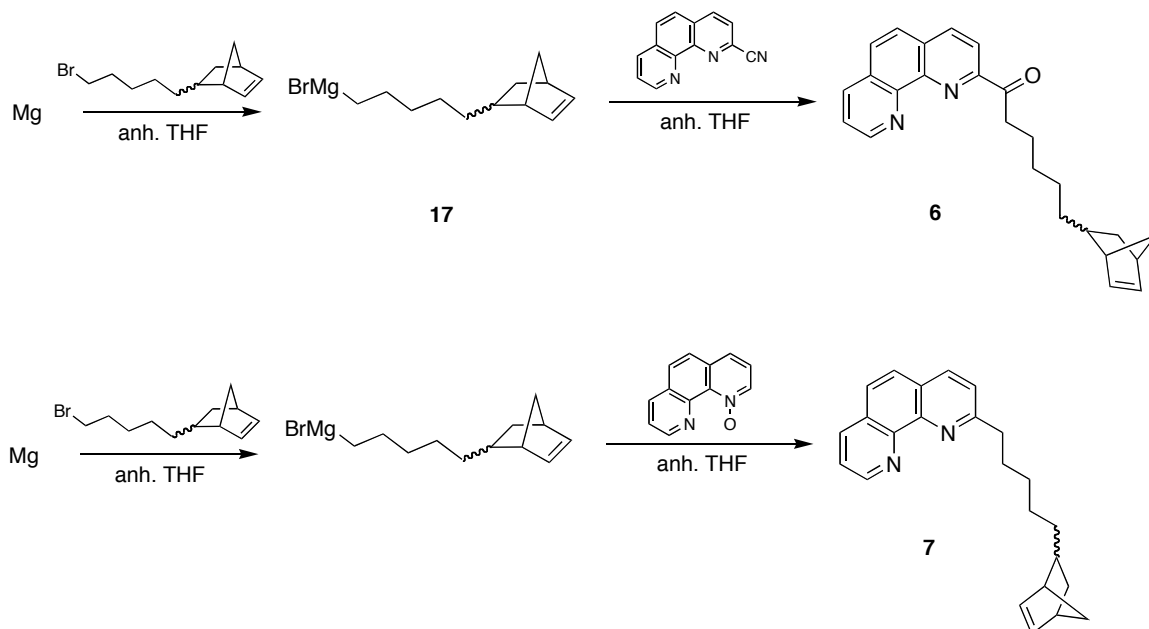
transferred to the nitrile solution, however, there was no observation of a dark blue color. The color changed to dark red. During the work-up, the emergence then disappearance of a precipitate was not seen when the Grignard coupling reaction was quenched with saturated aqueous NH_4Cl . The crude product was a similar semi-solid consistency as the pentyl analogue, but it was reddish brown instead of dark brown.

The crude material was chromatographed on silica gel, eluting with CH_2Cl_2 . Seven 500 mL fractions were collected. None of the fractions contained desired ketone based on GC-MS. Fraction 8 contained substantially more material than the other fractions, but there was neither the parent ion nor fragmentation consistent with the desired compound was observed in a mass spectrum.

The inability to recover **6** was unexpected. A new procedure to prepare 1-bromopentyl norbornene Grignard was attempted.²¹ The halide and catalytic iodine were deoxygenated in an oven-dried, pump-filled flask. The reaction was heated at 40 °C overnight. Dr. Xiaowei Zhan in our group reported that the reaction mixture changed from yellow to gray. The first trial produced a dark brown solid because the reagents were not adequately deoxygenated, and the second trial also failed to generate a stable Grignard reagent. The yellow color was observed, as was the presence of a white precipitate. In neither case was a gray color seen.

The addition of both benzaldehyde and benzyl bromide were used to test for the presence of the Grignard (Figure 3.6). Grignard reagents can either react with a carbonyl and reduce it to an alcohol or react with an alkyl halide and form the coupling product. One would expect that these products can be seen by GC-MS. In the case with benzaldehyde, we saw neither the alcohol nor the corresponding dehydration product.

With the benzyl bromide, peaks were observed that were consistent with the dimer product 1,10-di(bicyclo[2.2.1] hept-5-en-2-yl) decane. The dimer could have been formed by the presence of oxygen or by the Grignard reagent coupling with unreacted 1-



Scheme 3.3. Synthetic route to 2-substituted norbornene monomers.

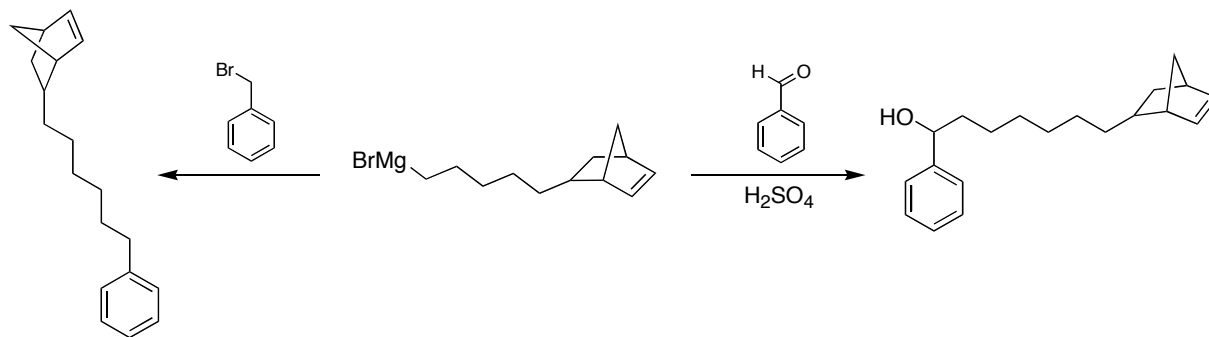


Figure 3.6. Expected products formed by reacting a Grignard reagent with benzyl bromide or benzaldehyde.

bromopentyl norbornene.

With the incomplete conversion of alkyl halide to Grignard reagent, it was no surprise that GC-MS spectra of **6** and 2-(5-(bicyclo[2.2.1] hept-5-en-2-yl) pentyl)-1,10-

phenanthroline (**7**) did not show desired product. The attempt to synthesize **7** was based on a literature preparation by Kato and Yamanaka.²² The authors reported the arylation of quinoline 1-oxide using phenylmagnesium bromide in anhydrous THF. They were able to isolate the desired 2-phenyl-1,10-phenanthroline in 95% yield using 5 equivalents of Grignard reagent and refluxing the solution for 4 hours. As stated previously, we do not have any data supporting the synthesis of 2-norbornenyl pentyl phenanthroline likely due to not forming the Grignard reagent necessary for alkylation.

Two reactions involving the carboxylic acid intermediate failed (Figure 3.7). In the *Bulletin of the Korean Chemical Society*, Cho and co-workers reported reducing

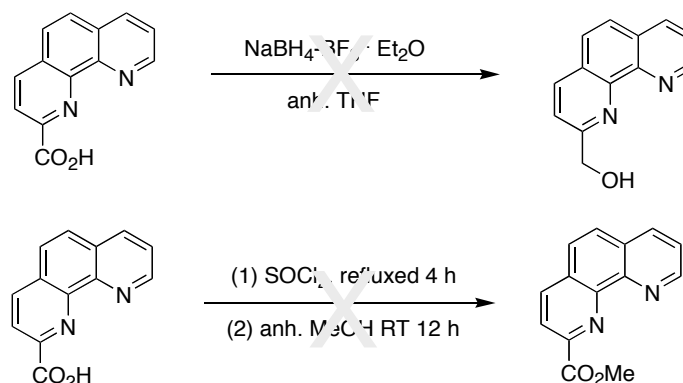


Figure 3.7. Reactions to reduce or to esterify 2-carboxy-1,10-phenanthroline.

a variety of aromatic carboxylic acids directly to their corresponding alcohols using $\text{NaBH}_4 \cdot \text{BF}_3 \cdot \text{Et}_2\text{O}$.²³ On a 500 mg scale, recovering the desired 2-carbinol was unsuccessful twice. A flask containing 2-carboxy-1,10-phenanthroline was purged with nitrogen for 20 minutes before being charged with anhydrous THF. Sodium borohydride and boron trifluoride etherate were added. The reaction was refluxed at 85 °C for about 45 minutes at which time a precipitate was present. The reaction was cooled in an ice bath to 0 °C before being slowly diluted with water. The mixture was stirred for ten

minutes, then dichloromethane was added. The mixture stirred for 1 hour at room temperature; it was washed with water and with brine. The organic layer was dried over MgSO_4 , filtered, and the solvent removed by rotary evaporation. A red-orange oil was recovered, but the ^1H NMR spectrum was not consistent with pure product. There were, however, two peaks at 4.65 and 4.85 ppm that may be attributable to the diastereotopic methylene protons. The amount of material recovered was less than 50 mg each time; the aqueous layers were extracted with diethyl ether in an effort to isolate more compound. From the ^1H NMR spectrum of the oil recovered from the aqueous layer, there were no peaks consistent with a phenanthroline.

Sun *et al.* reported the synthesis of 2-carbomethoxy-1,10-phenanthroline in good yields.¹⁶ Thionyl chloride and the carboxylic acid were refluxed under nitrogen until the solid dissolved and a red solution remained. On a 500 mg scale, this observation was seen after about 90 minutes. Thionyl chloride was distilled under vacuum, and anhydrous methanol was added to the flask. The reaction stirred at room temperature for 12 hours. The residue was eluted through basic alumina using methanol. Fractions containing an absorbent spot were isolated, and the solvent was removed by rotary evaporation. There was no conclusive evidence that the ester was synthesized. It was at this point the decision was made to find esterification conditions that avoided use of thionyl chloride. Using ethanol (*vide supra*) and sulfuric acid is a potential alternative.

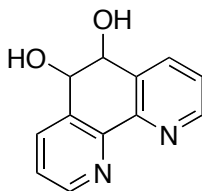
Synthesis of 2-Substituted-1,10-Phenanthrolines

Epoxidization of 1,10-phenanthroline with bleach was completed. Shen and Sullivan reported using Clorox[®] as the oxidant.²⁴ Bleach was diluted with water and cooled to 18 °C. The pH was adjusted to 8 using concentrated HCl. Phenanthroline and

tetrabutylammonium hydrogen sulfate dissolved in chloroform was added to the reaction mixture. The reaction was monitored by ^1H NMR, and the conversion was consistently completed in 2 hours using freshly opened bleach.

The majority of the bleach layer was decanted, and the organic phases were washed with water. Washing with water more than recommended by the authors resulted in a substantially lower yield. The crude solid was recrystallized from 5:1 chloroform: hexanes. In all cases, the filtrate had to be recrystallized at least once more to recover pure compound as white flakes.

An acid-catalyzed ring opening of 5,6-epoxy-1,10-phenanthroline to form 5-hydroxy-1,10-phenanthroline was performed. According to Slough *et al.*,¹⁷ the reaction was completed after 1 hour at 100 °C. Upon personal communication with the author, it was learned that the catalysis required 2 mL of concentrated H_2SO_4 per 300 mg of epoxide. Unfortunately, the reaction did not go to completion in one hour, two hours, or four hours although more epoxide was converted to **13** at longer durations. The by-product from the reaction was a non-aromatized 5,6-diol (Figure 3.8). This was a non-intuitive result because one would expect the elimination to be highly favored under the reaction conditions. Reacting the epoxide for 14 hours was found to be the optimal time for complete conversion to the aromatic 5-hydroxy-1,10-phenanthroline. Isolation of the



5,6-dihydro-5,6-dihydroxy-1,10-phenanthroline

Figure 3.8. Structure of by-product from incomplete conversion of epoxide **7**.

desired product on two- and five-gram scales proved successful as well.

In all cases, the acid-catalyzed ring opening was similar. Ground epoxide was added slowly to stirred concentrated sulfuric acid. The solution became clear yellow and viscous during the addition, and the epoxide was not always completely dissolved. During heating, however, the solution became less viscous. The epoxide went completely into solution. After heating for a given period of time, the reaction was allowed to cool to room temperature before being diluted with cold water. For the small-scale reactions, the work up was performed in a 50 mL resealable centrifuge tube in an ice/ CaCl_2 slurry at -3°C . The large-scale reactions were transferred to a beaker in a cryogenically cooled acetone bath kept at -7°C per Dr. Slough's suggestion. Reportedly, an insoluble black precipitate would form were the reaction mixture temperature to rise above 5°C .

6 M Aqueous NaOH was slowly added by pipette (or addition funnel) until the reaction was neutralized. As the mixture neared pH 7, it changed from clear yellow to opaque peach. Precipitate was visible starting at pH 5. It was challenging to neutralize the solution because one drop of acid from a pipette often increased the pH to 10. The visual clues do help one to know when to begin adding smaller volumes of base. Moreover, large scale work-ups were less sensitive because there was more product to neutralize and one drop of base did not result in a significant pH change at the neutralization point.

Centrifugation of the suspension followed by three resuspension/centrifugation cycles provided a pale yellow solid. This solid was again resuspended in water and frozen with liquid nitrogen. To remove water, the tube(s) were either placed on a lyophilizer for 16 hours or in a dessicator under vacuum for 36 hours. The weight of pure product recovered, however, was sometimes more than the theoretical yield. This

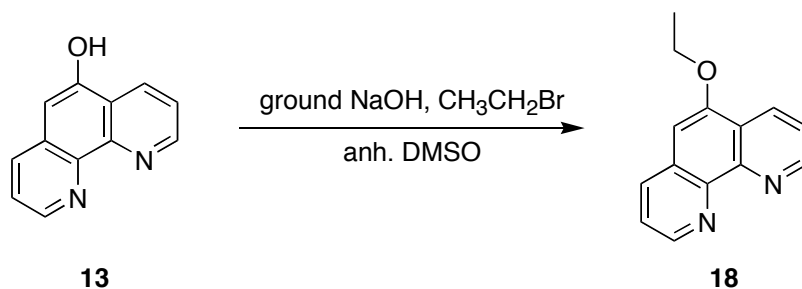
observation suggested that **13** was hygroscopic. Unlike with 2-carboxy-1,10-phenanthroline, the water was not quantified because the hydroxy substituted phenanthroline was only soluble in DMSO-*d*₆. The deuterated solvent is notorious for absorbing water even if an ampoule is used.

Assuming that **13** was hygroscopic, the product was purged with nitrogen for several hours prior to the alkylation step in anhydrous DMSO. To a stirred solution of anhydrous DMSO and 5-hydroxy-1,10-phenanthroline, ground NaOH was added. The solution turned from peach to bright orange as it stirred for 0.5 hour. 4-Bromobutyl-acetate was introduced via syringe, and the reaction continued at room temperature for 14 hours. The greenish brown solution was poured into ether and extracted against saturated NaCl. A clear, orange liquid was recovered. The desired acetate (**14**) was never isolated, though attempts were made to separate the reaction product by TLC. Slough *et al.*¹⁷ did not report purification methods because they used the crude material to deacetylate and form **2**.

Because we were unable to purify **14**, we synthesized 5-ethoxy-1,10-phenanthroline (**18**) to perform electrochemical studies as a model for 5-alkoxy-substituted phenanthrolines. The etherification route involved 5-hydroxy-1,10-phenanthroline and bromoethane (Scheme 3.4). Previous reports on the synthesis of 5-methoxy-1,10-phenanthroline were from either 5,6-epoxy-1,10-phenanthroline,²⁴ 8-amino-6-methoxy-quinoline,²⁵ or 5-chloro-1,10-phenanthroline²⁶ (Figure 3.9). This route has fewer steps than the other literature procedures,

The first norbornene functionalized 1,10-phenanthrolines were synthesized (Scheme 3.5). To our knowledge, there are no other such compounds in the literature.

1,10-Phenanthroline-5-yl-bicyclo[2.2.1] hept-5-ene-2-carboxylate **4** was synthesized from 5-hydroxy-1,10-phenanthroline and *endo*/*exo*-norbornene-2-carboxylate using



Scheme 3.4. Synthetic route for 5-ethoxy-1,10-phenanthroline.

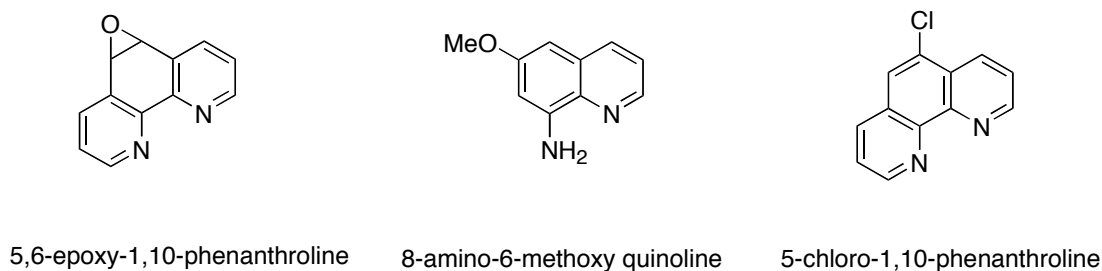
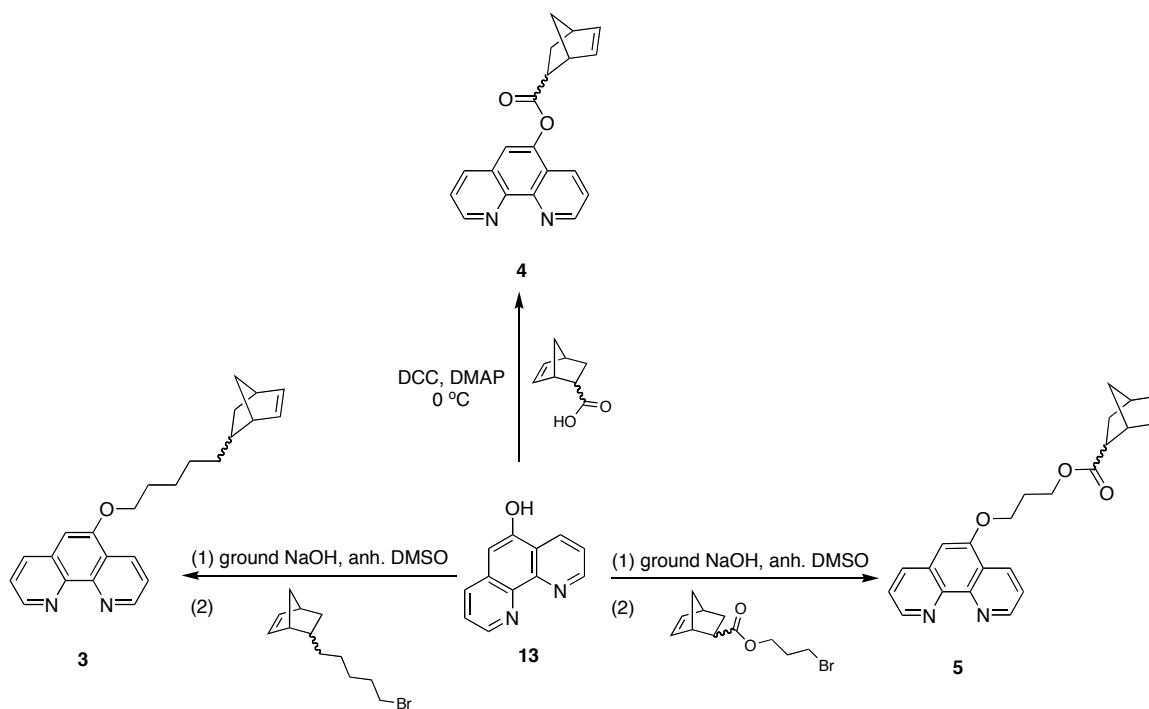


Figure 3.9. Structures of starting materials reported in the literature used to synthesize 5-methoxy-1,10-phenanthroline.



Scheme 3.5. Synthetic route to 5-substituted-1,10-phenanthrolines.

dicyclohexylcarbodiimide (DCC) and DMAP in anhydrous THF. 5-Hydroxy-1,10-phenanthroline, DMAP, and the carboxylic acid were added to an oven-dried, pump-filled flask, and the contents were purged with nitrogen for 0.5 hour. Anhydrous THF from the solvent purification system was charged into the flask by pump-filled syringe. The phenanthroline was not very soluble in THF, and more solvent was added to increase solubility. The additional solvent did not appear to help, however. The contents of the flask were cooled to 0 °C in an ice bath and DCC was introduced into the reaction mixture. The reaction was allowed to gradually return to room temperature, and it stirred overnight. After three hours, the reaction color was pink. The reaction was monitored by TLC, and pink precipitate was observed after the consumption of carboxylic acid.

The dicyclohexylurea precipitate was filtered, and diethyl ether was added to the filtrate. The organic layer was washed with saturated aqueous NaHCO₃ and with saturated aqueous NaCl before being dried over MgSO₄. The solvent was removed by rotary evaporation, and a light yellow solid was recovered as the crude product in low yield (30%). Spectra (¹H NMR and mass) were collected, and they were consistent with desired carboxylate product being the main product. The low yield was attributed mainly to the poor solubility of the starting phenanthroline substrate in THF.

Following the procedure used to synthesize **14** (*vide supra*), 4-(1,10-phenanthroline-5-yl)oxy) pentyl norbornene **3** was prepared. 1-Bromopentyl norbornene was used as the halide. The reaction was repeated twice, and the second attempt was thirteen times the original scale. 5-Hydroxy-1,10-phenanthroline was added to an oven-dried, pump-filled flask, and it was purged with nitrogen for 0.5 hour. Anhydrous DMSO and ground NaOH were added to the flask. The reaction turned bright orange almost

immediately after the base was introduced. The reagents stirred for an additional 0.5 hour prior to the addition of the halide. The reaction stirred at room temperature overnight.

When the phenanthroline was consumed, the reaction mixture was poured into ether. Slough *et al.*¹⁷ reported washing with water, but the layers emulsified rather than separated. Thus, the organic layer was washed twice with saturated aqueous NaCl. The organic layer was dried over Na₂CO₃/MgSO₄ and filtered. The solvent was removed by rotary evaporation. A clear, light brown viscous liquid was recovered, and it crystallized at room temperature. The crude mixture was purified by column chromatography on silica gel, and the product was collected in two fractions. The ¹H NMR spectra contained the expected phenanthroline and alkyl norbornene peaks; however, the aliphatic region integration was higher by three protons. The ¹³C NMR spectrum was inconclusive. It contained the expected number of peaks, but the aromatic: aliphatic ratio was incorrect. The mass spectra of the compounds were consistent with the presence of desired ether monomer, but there were fragment peaks that could not be attributed to the monomer. The sample has been sent for elemental analysis.

Electrochemical Studies

With many phenanthroline derivatives in hand, we sought to determine the relative stability of the radical anions. Bathophenanthroline (Bphen) and bathocuproine (BCP) have been used successfully as hole-blocking/electron-transporting layers in organic light emitting diodes; we wanted to see if the radical anions of substituted phenanthrolines showed comparable electrochemical stability to these.

Cyclic voltammograms were collected using 0.1 M Bu₄NPF₆ in both anhydrous THF and anhydrous acetonitrile. The scan rate was 50 mV/s and the potential was swept

from -2500 mV to 900 mV to view the redox potentials of ferrocene (an internal standard) and the compounds of interest. Scanning only the first reduction did not improve the reversibility of the peaks, so data was collected until the solvent began to breakdown (Table 3.1). A representative voltammogram is shown in Figure 3.10. In THF, 2-cyano-1,10-phenanthroline shows quasi-reversible reduction peaks around -1.6 V and -2.2 V versus $\text{FcCp}_2^{+/0}$.

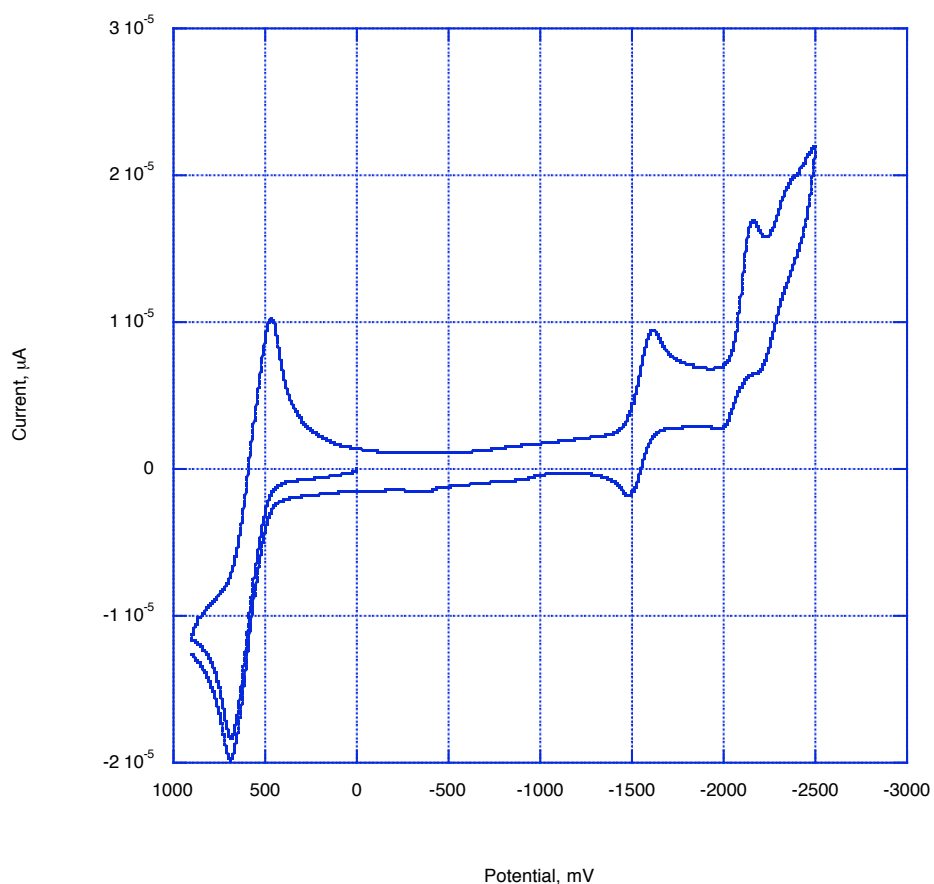


Figure 3.10. Cyclic voltammogram in THF of 2-cyano-1,10-phenanthroline vs. AgCl/Ag pseudoreference using 0.1 M Bu_4NPF_6 as electrolyte at a scan rate of 50 mV s^{-1} .

The redox process did not appear to be fully reversible because the current for reduction (i_{pc}) and the current for oxidation (i_{pa}) were not equal. On the other hand, in acetonitrile, most 1,10-phenanthroline derivatives showed no i_{pa} . Therefore, only the reduction peak potential (E_{pc}) was reported.

While it is of interest to see multiple reductions from several of the phenanthroline derivatives, we are only interested in the first reduction for applicability in devices. Thus, a graph depicting the first reductions of the molecules is shown in Figure 3.11.

Table 3.1. Redox potentials of 1,10-phenanthroline derivatives vs. $FeCp_2^{+/-}$ using 0.1 M Bu_4NPF_6 as electrolyte at a scan rate of 50 $mv\ s^{-1}$.

Compound	$E_{1/2}$ in THF (V)	$E_{1/2}$ in MeCN (V)
Phenanthroline	-2.58, -2.89	-2.36, -2.63
Neocuproine	-2.56	-2.47
Bathophenanthroline	—	-2.23, -2.47 ^a
Bathocuproine	—	-2.51 ^a
1,10-Phenanthroline-1-oxide	-2.34, -2.66, -2.90	-2.18, ^a -2.42, ^a -2.65 ^a
2-Cyano-1,10-phenanthroline	-2.13, -2.65	-2.08, -2.40, ^a -2.66 ^a
2-Carboethoxy-1,10-phenanthroline	—	-2.06, -2.39, -2.69

^a E_{pc} potential.

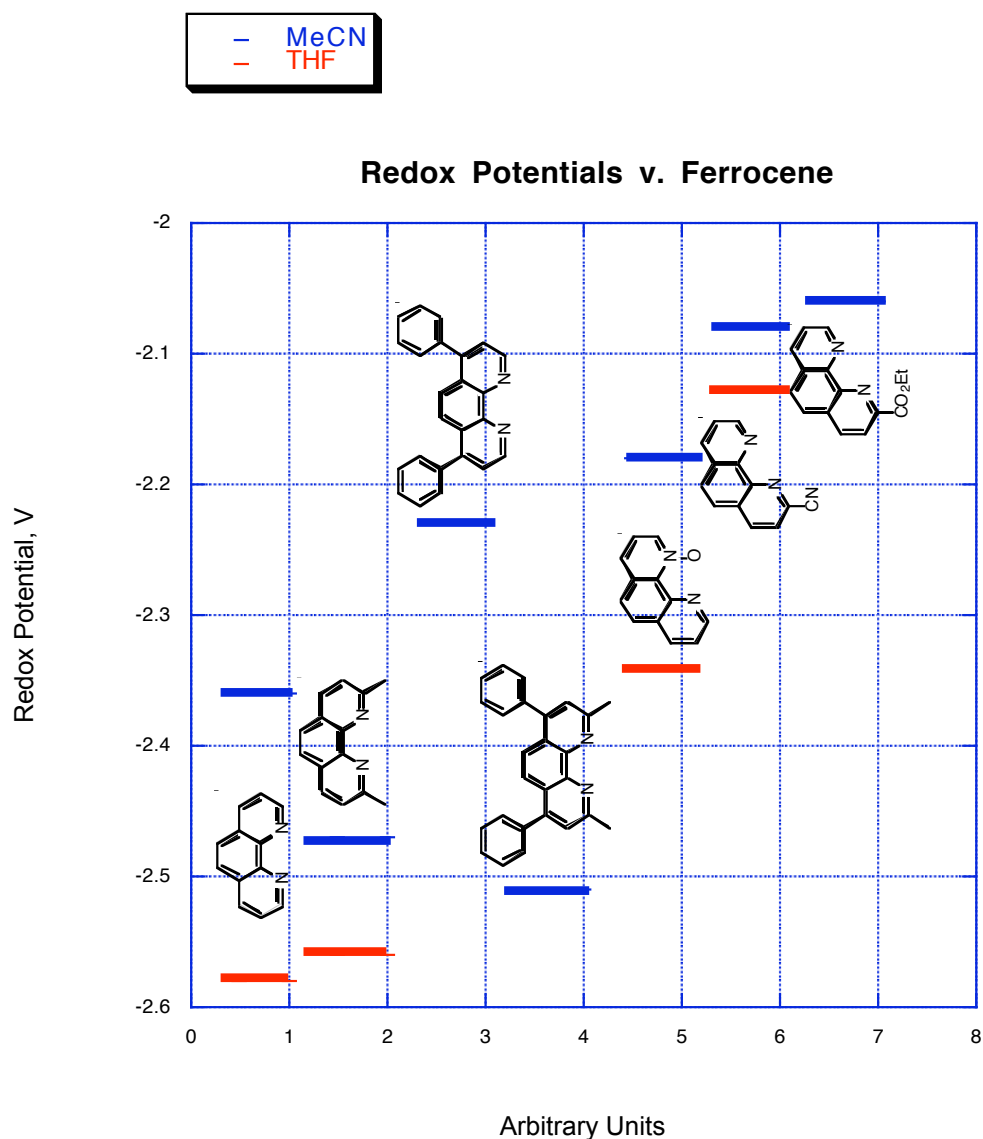


Figure 3.11. Graph plotting the first reduction potentials of 1,10-phenanthroline derivatives in both MeCN and THF.

Generally, the redox process is more reversible in THF than in acetonitrile. This suggests that the radical anion may be more stable in THF on the time scale of the experiment. The derivatives substituted in either the one or two position were easier to reduce than the commercially available phenanthrolines. The observation was expected considering the electron withdrawing nature of the substituents.

Interestingly, and perhaps importantly, neither Bphen nor BCP voltammograms appear any more (or less) reversible in acetonitrile than do those of the other phenanthroline derivatives. In fact, the only truly reversible peak was the first reduction of 2-cyano-1,10-phenanthroline in THF. With the exception of BCP and neocuproine in acetonitrile, the relative redox potentials for commercially available compounds (*i.e.*, phenanthroline–bathocuproine in Table 3.1) were consistent with other experimental data in the literature and with the results of the quantum-chemical calculations.

One would expect both Bphen and BCP to be easier to reduce than phenanthroline because the calculated LUMO energy is lower in these derivatives (Figure 3.2 (b)) likely due to the slight electron-withdrawing nature of the phenyl rings. One can see that the electron-donating methyl groups destabilize the LUMO of BCP, making it somewhat harder to inject an electron relative to Bphen. Thus, from a molecular orbital perspective, it is logical to conclude the ease of reduction to be Bphen < BCP < phenanthroline. Our data, however, show the redox potential for BCP in acetonitrile to be 0.15 V *harder* to reduce than phenanthroline while Bphen is expectedly easier to reduce than phenanthroline. Solvation effects may also play a role in the experimental values we observed.

It is known in the literature that BCP, Bphen, and neocuproine are in fact easier to reduce than phenanthroline.^{27–28} It is more difficult to ascertain the relative redox potentials of Bphen and BCP or neocuproine because the potentials were measured using different conditions. In 1973, two groups reported the redox potentials of neocuproine and Bphen along with phenanthroline for comparison. Both Musumeci *et al.* and Gürtler *et al.* used a polarography technique to obtain their data versus a saturated calomel

electrode (SCE). The redox potential for neocuproine was re-referenced to the more commonly reported ferrocene/ferrocenium couple,²⁹ but the potential for Bphen was not re-calculated because of the concentration of the electrolyte. The concentration definitely affects redox potentials; however, the factor cannot be quantified at this time with the information at hand. We can tell from Table 3.2, however, that the relative ease of reduction should be BCP³⁰ < neocuproine < phenanthroline. Whether Bphen is easier to reduce than neocuproine remains to be seen, though from molecular orbital theory, this is expected to be the case.

Neocuproine is not represented in Figure 3.2 (b); however, the experimental data in the literature is counter-intuitive. Methyl groups are electron-donating. If electron-withdrawing groups like a nitrile or an oxide make phenanthroline easier to reduce, then

Table 3.2. Redox potentials of 1,10-phenanthroline derivatives reported in the literature.

Compound	E _{1/2} vs SCE (V) in MeCN	E _{1/2} vs FeCp ₂ ⁺⁰ (V) in MeCN
Phenanthroline	-2.070, ^a -1.99 ^b	-2.54 ^a
Neocuproine	-2.055 ^a	-2.52 ^a
Bathophenanthroline	-1.89 ^b	—
Bathocuproine	—	-2.39 ^c

^aRedox potentials from Gürtler *et al.* using 0.8 M Et₄NClO₄. ^bRedox potentials from Musumeci *et al.* using 0.1 M Bu₄NClO₄. ^cRedox potential vs FeCp₂⁺⁰ from Ono *et al.* using 0.1 M Bu₄NClO₄ in DMF.

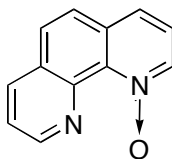
we expect electron-donating groups to make phenanthroline harder to reduce. Consider BCP and Bphen: the methyl groups destabilize both the HOMO and the LUMO of BCP. Even in the case of V, one methyl in the 2 position of phenanthroline increases the LUMO energy. Therefore, one would expect a second methyl to further increase the energy of the LUMO. But according to experimental data, the second methyl does not destabilize the energy level as much as the first methyl group. Perhaps providing an axis

of symmetry stabilized the LUMO. Theoretical calculations of synthesized molecules (*e.g.*, neocuproine) may give further insight into the experimental observation.

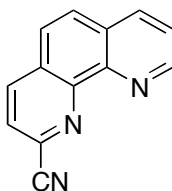
Future work in this project will focus on isolating pure monomers, determining the absorption and emissive properties of the small molecules and monomers, finding more precise energy levels of our phenanthroline derivatives by ultraviolet photoelectron spectroscopy (UPS),³¹ and evaluating the electron transport and hole blocking abilities of our derivatives.

Experimental

All reagents were purchased from Sigma/Aldrich, Acros, or EM Science and were used without further purification unless otherwise noted. Air sensitive reactions were conducted under a nitrogen atmosphere using Schlenk and vacuum line techniques. Schlenk flasks were oven dried overnight at 120°C and cooled on a vacuum line by pump-filling prior to use. Anhydrous solvents were taken from a solvent purification system or transferred from sealed containers via cannula. ³² ¹H, ¹³C, and COSY nuclear magnetic resonance spectra of pure compounds were recorded on either a Varian 300 MHz or a Bruker 500 MHz NMR spectrometer and referenced to residual proton solvent peaks. All mass spectra were obtained from the Georgia Institute of Technology BioAnalytical Mass Spectrometry Facility. Elemental Analyses were conducted at Atlantic Microlab, Inc. in Norcross, Georgia. Electrochemical measurements were performed under nitrogen using either deoxygenated acetonitrile or tetrahydrofuran and 0.1 M Bu₄NPF₆ as electrolyte. A BAS potentiostat, a glassy carbon working electrode, a platinum auxiliary electrode, and a non-aqueous AgCl/Ag pseudoreference electrode were used.

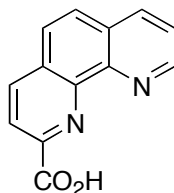


1,10-Phenanthroline 1-oxide (8).¹⁶ To a flask containing 1,10-phenanthroline (25.015 g, 138.81 mmol) and glacial acetic acid (28.5 mL), 30% hydrogen peroxide (16 mL) was added dropwise. The reaction was stirred at 72 °C for 4 h before the final portion (16 mL) of 30% hydrogen peroxide was added dropwise. The reaction continued for 6 h. The desired product was extracted into chloroform (4 × 400 mL). The solvent was removed by rotary evaporation at 50 °C. Residual solvent was removed overnight at 50 °C and high vacuum (4×10^{-2} mbar). A mustard yellow solid was recovered and not further purified (16.916 g, 62 %). The isolated solid was 86% pure by ¹H NMR. The other peaks corresponded to 1,10-phenanthroline. ¹H NMR (500 MHz, CD₂Cl₂): δ 9.22 (dd, J = 4.3 Hz, 2.0 Hz, 1H), 8.64 (dd, J = 6.3 Hz, 1.5 Hz, 1H), 8.29 (dd, J = 8.3 Hz, 2.0 Hz, 1H), 7.82 (q, J = 25 Hz, 9.0 Hz, 2H), 7.76 (dd, J = 8.0 Hz, 1.0 Hz, 1H), 7.69 (dd, J = 8.3 Hz, 4.5 Hz, 1H), 7.47 (dd, J = 8.0 Hz, 6.5 Hz, 1H).

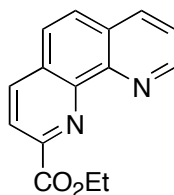


2-Cyano-1,10-phenanthroline (9).¹⁶ Crude 1,10-phenanthroline 1-oxide was added to a flask containing potassium cyanide (11.144 g, 171.13 mmol). The compounds were dissolved in distilled water (89.5 mL), and benzoyl chloride (12 mL) was added dropwise to the solution being stirred. After 2 h, the resulting precipitate was filtered at suction, washed with water, and dried. The brown grainy solid was recrystallized from either methanol or ethanol. The pure compound was a light brown solid (8.082 g, 69%). ¹H

NMR (500 MHz, CD₂Cl₂): δ 9.22 (dd, J = 4.3 Hz, 2.0 Hz, 1H), 8.43 (d, J = 8.5 Hz, 1H), 8.34 (dd, J = 8.3 Hz, 2.0 Hz, 1H), 7.99 (d, J = 5.0 Hz, 1H), 7.98 (d, J = 4.5 Hz, 1H), 7.88 (d, J = 9.0 Hz, 1H), 7.75 (dd, J = 8.3 Hz, 4.5 Hz, 1H).

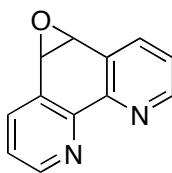


2-Carboxy-1,10-phenanthroline (10).¹⁸ To a flask containing 2-cyano-1,10-phenanthroline (2.000 g, 9.698 mmol) was added 95% ethanol (20 mL) and 1.6 g NaOH dissolved in 10 mL distilled water. The reaction mixture was stirred at reflux for 2 h (the evolution of ammonia ceased) before being cooled to room temperature. The solution was adjusted to pH 3 using concentrated HCl. The precipitate was filtered and collected as a tan clay-like solid. It was dried under high vacuum (4×10^{-2} mbar) for 5 h. The recovered mass was 2.092 g (96% yield) ¹H NMR (500 MHz, DMSO-*d*₆): δ 9.16 (dd, J = 4.0 Hz, 2.0 Hz, 1H), 8.66 (d, J = 8.0 Hz, 1H), 8.54 (dd, J = 8.0 Hz, 2.0 Hz, 1H), 8.35 (d, J = 8.0 Hz, 1H), 8.10 (q, J = 21 Hz, 8.5 Hz, 2H), 7.83 (dd, J = 8.3 Hz, 4.0 Hz, 1H).

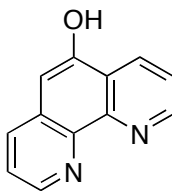


2-Carboethoxy-1,10-phenanthroline (11). A round bottom flask fitted with a stir bar was charged with 2-carboxy-1,10-phenanthroline (0.154 g, 0.687 mmol) and absolute ethanol (1.5 mL). The reaction was catalyzed with concentrated H₂SO₄ and placed immediately on the reflux condenser. The reaction was refluxed overnight for 12 h under a nitrogen atmosphere. The reaction was quenched with water (1 mL) and extracted into

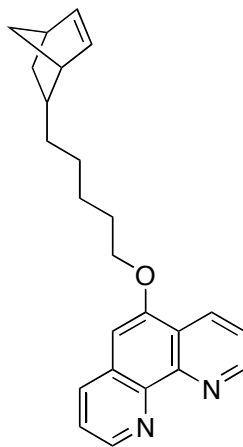
CH₂Cl₂ (2 × 10 mL). The combined organic layers were washed with brine (10 mL), dried over MgSO₄ and filtered. The solvent was removed by rotary evaporation, and a pale yellow solid was recovered (0.017 g, 10%) ¹H NMR (500 MHz, CDCl₃): δ 9.17 (dd, *J* = 4.0 Hz, 2.0 Hz, 1H), 8.58 (d, *J* = 8.5 Hz, 1H), 8.49 (d, *J* = 8.5 Hz, 1H), 8.38 (dd, *J* = 8.0 Hz, 2.0 Hz, 1H), 7.93 (q, *J* = 19.5 Hz, 9.0 Hz, 2H), 7.77 (dd, *J* = 8.0 Hz, 4.5 Hz, 1H), 4.12 (q, *J* = 14.0 Hz, 7.0 Hz, 2H). 1.26 (t, *J* = 7.5 Hz, 3H).



5,6-Epoxy-1,10-phenanthroline (12).²⁴ Clorox[®] bleach (1800 mL) was diluted with distilled water (1200 mL) and allowed to cool to 18 °C. The pH then was adjusted to ~8 using concentrated HCl. To the stirring solution was added 1,10-phenanthroline (10.221 g, 56.717 mmol) and tetrabutylammonium hydrogen sulfate (4.429 g, 13.04 mmol) dissolved in 1000 mL of chloroform. The pH of the mixture remained between 8 and 9 during the reaction. The epoxidation was monitored by ¹H NMR until all the phenanthroline reacted. The majority of the aqueous layer was decanted, and the organic layer was washed with distilled water (3 × 1000 mL). The solvent was removed by rotary evaporation. The yellow/orange crude product was recrystallized from 5:1 chloroform: hexanes. The purified solid was recovered as white flakes (5.295 g, 48%). ¹H NMR (500 MHz, CD₂Cl₂): δ 8.85 (dd, *J* = 4.8 Hz, 2.0 Hz, 2H), 8.03 (dd, *J* = 7.5 Hz, 2.0 Hz, 2H), 7.42 (dd, *J* = 7.8 Hz, 5.0 Hz, 2H), 4.63 (s, 2H). The ¹H NMR spectrum was consistent with that reported by Shen and Sullivan.²⁴

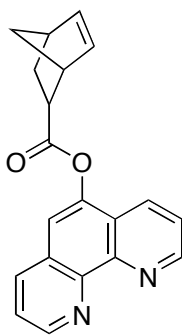


5-Hydroxy-1,10-phenanthroline (13).¹⁷ 5,6-epoxy-1,10-phenanthroline (1.922 g, 9.796 mmol) was slowly added to stirring concentrated H₂SO₄ (16.5 mL). The reaction was heated at 100 °C under nitrogen overnight for 14 h. The viscous solution was diluted with cold water (50 mL) and transferred to a beaker. Using a Cryostat chiller, the reaction was kept between 5 °C and 7 °C during neutralization. 6M NaOH was used to adjust the reaction to pH 7. The slurry was transferred to 50 mL centrifuge tubes. The suspension was centrifuged and the supernatant decanted. The solid was resuspended in water (15 mL) and centrifuged three times before being resuspended, frozen in liquid nitrogen, and placed under vacuum for 36 h. A pale yellow solid was recovered (1.900 g, 99%). The ¹H NMR spectrum was consistent with that reported by Slough *et al.*¹⁷



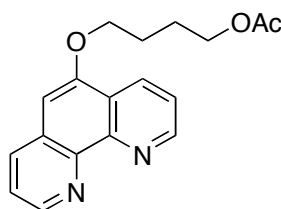
4-(1,10-Phenanthrolin-5-yloxy) pentyl norbornene (3).¹⁷ 5-hydroxy-1,10-phenanthroline (1.266 g, 6.452 mmol) was added to a pump-filled flask and purged with nitrogen for 0.5 h. The flask was charged with anhydrous DMSO (13 mL) followed by the addition of ground NaOH (0.307 g, 0.766 mmol). The solution was stirred for 0.5 h,

and 1-bromopentyl norbornene (2.529 g, 10.40 mmol) was added by syringe. The reaction stirred overnight at room temperature and was monitored by TLC. When the starting phenanthroline was consumed, the reaction was poured into diethyl ether (325 mL) and extracted against saturated aqueous NaCl (150 mL). The organic phase was washed with saturated aqueous NaCl (150 mL), and it was dried over Na₂CO₃/MgSO₄. The solvent was removed by rotary evaporation. The desired ether was chromatographed on a silica plug using CH₂Cl₂ then 4:1 CH₂Cl₂:MeOH as eluents. After rotary evaporation, a brown crystalline solid was recovered (1.595, 69%). ¹H NMR (500 MHz, CD₂Cl₂): δ 9.19 (dd, *J* = 4.3 Hz, 2.0 Hz, 1H), 9.01 (dd, *J* = 4.3 Hz, 2.0 Hz, 1H), 8.70 (dd, *J* = 8.3 Hz, 2.0 Hz, 1H), 8.09 (dd, *J* = 8.3 Hz, 2.0 Hz, 1H), 7.64 (dd, *J* = 8.3 Hz, 4.5 Hz, 1H), 7.55 (dd, *J* = 8.0 Hz, 4.5 Hz, 1H), 6.94 (s, 1H), 6.12 (dd, *J* = 6.0 Hz, 3.0 Hz, 1H), 6.09 (dd, *J* = 5.5 Hz, 3.0 Hz, 1H), 6.03 (dd, *J* = 5.8 Hz, 3.0 Hz, 1H), 5.94 (dd, *J* = 5.5 Hz, 3.0 Hz, 1H), 4.25 (t, *J* = 6.5 Hz, 2H), 2.78 (br s, 1H), 2.76 (br s, 1H), 2.05 – 1.94 (m, 3H), 1.87 – 1.83 (m, 1H), 1.65 – 0.8 (m, 10H), 0.52 (ddd, *J* = 11.3 Hz, 4.3 Hz, 3.0 Hz). EI-MS (70eV) *m/z*: M⁺ 358 (40), 292 (60), 196 (100), 66 (21). ¹³C was inconsistent with the desired structure.



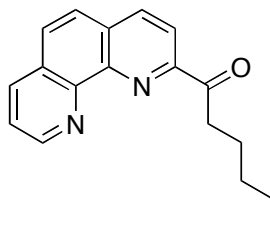
1,10-Phenanthroline-5-yl bicyclo[2.2.1] hept-5-ene-2-carboxylate (4).³³ To a pump-filled flask, *endo/exo*-5-norbornene-2-carboxylic acid (0.06 mL, 0.5 mmol), 5-hydroxy-

1,10- phenanthroline (0.106 g, 0.540 mmol), and a catalytic amount of DMAP were added. These reactants were purged with nitrogen for 0.5 h before the addition of anhydrous THF (0.94 mL). The reaction flask was cooled in an ice bath to 0 °C, and DCC (0.108 g, 0.523) was added. The solution was allowed to gradually warm to room temperature, and it stirred overnight. The reaction was monitored by TLC, and the pink precipitate was filtered when all the acid was consumed. The filtrate was poured into ether, and the organic layer was washed with saturated aqueous NaHCO₃ (10 mL) then with saturated aqueous NaCl (10 mL). The organic layer was dried over MgSO₄, and the solvent was removed by rotary evaporation. A light yellow solid was recovered as crude product (0.045 g, 30%). **EI-MS (70eV) m/z: M⁺ 316 (3), 223 (18), 196 (100), 66 (31).** *¹H NMR and MS spectra were consistent with desired monomer; however, there were significant impurities that two column chromatography attempts did not remove. These impurities prevented me from assigning peaks to the norbornene moiety.*

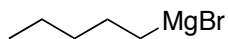


4-(1,10-Phenanthrolin-5-yloxy) butyl acetate (14).¹⁷ 5-hydroxy-1,10-phenanthroline (0.185 g, 0.933 mmol) was added to a two-necked flask and purged with nitrogen for 1 h. To this solid was added anhydrous DMSO (1.9 mL) and ground NaOH (0.039 g, 0.98 mmol). The bright orange mixture was stirred for 0.5 h and 4-bromobutyl acetate was added dropwise. The reaction stirred overnight for 14 h under nitrogen. The solution was poured into ether (50 mL) and extracted against brine (2 × 20 mL). The combined organic layers were dried over MgSO₄, filtered, and the solvent removed under reduced pressure.

A clear, dark orange liquid was recovered as crude product. *The ^1H NMR peaks for desired acetate could not be assigned from the complicated crude spectrum.*



Pentyl phenanthrolinyl ketone (15).²⁰ Pentyl magnesium bromide (18.5 mL) was transferred dropwise to a flask containing a stirred solution of 2-cyano-1,10-phenanthroline (1.849 g, 9.010 mmol) and anhydrous THF (100 mL) at $-78\text{ }^{\circ}\text{C}$. After the addition of Grignard reagent, the reaction stirred at $-78\text{ }^{\circ}\text{C}$ for 0.5 h and at room temperature for 1 h. Saturated aqueous NH_4Cl (50 mL) was added slowly to the solution. The organic layer was separated, and the aqueous layer was extracted with THF (70 mL). The combined organic layers were washed with saturated NaCl ($2 \times 70\text{ mL}$). The organic layer was dried over $\text{Na}_2\text{CO}_3/\text{MgSO}_4$ and filtered. The solvent was removed by rotary evaporation. The ketone was purified by chromatography, though impurities remained. *The chromatography of the bulk material was unsuccessful, and a ^1H NMR spectrum suitable for publication was never obtained.*



Pentyl magnesium bromide (16).²⁰ Pentyl bromide (4.6 mL, 37 mmol) was dissolved in anhydrous THF (30 mL). The solution was transferred to magnesium turnings and heated at $45\text{ }^{\circ}\text{C}$ for 1 h. White precipitate was allowed to settle from the reaction mixture overnight. The supernatant was used for subsequent Grignard reactions.

References

- (1) Wang, Y.-M.; Teng, F.; Zhou, Q.-C.; Wang, Y.-S. *Appl. Surf. Sci.* **2006**, *252*, 2355–2359.
- (2) Veinot, J.G.C.; Marks, T.J. *Acc. Chem. Res.* **2005**, *38*, 632–643.
- (3) Kim, Y.; Im, W. B. *Phys. Stat. Sol. (A)* **2004**, *201*, 2148–2153.
- (4) Wu, Z.; Yang, H.; Duan, Y.; Xie, W.; Liu, S.; Zhao, Y. *Semicond. Sci. Technol.* **2003**, *18*, L49–L52.
- (5) Kanno, H.; Giebink, N.C.; Sun, Y.; Forrest, S.R. *Appl. Phys. Lett.* **2006**, *89*, 023503-1–023503-3.
- (6) Kondakov, D. Y. *J. Appl. Phys.* **2006**, *99*, 024901-1–024901-4.
- (7) Choy, W.C.H.; Hui, K.N.; Fong, H.H.; Liang, Y.J.; Chui, P.C. *Thin Solid Films* **2006**, *509*, 193–196.
- (8) Kan, Y.; Wang, L.; Gao, Y.; Duan, L.; Wu, G.; Qiu, Y. *Synth. Met.* **2004**, *141*, 245–249.
- (9) Kim, T.-S.; Kim, D.-H.; Im, H.-J.; Shimada, K.; Kawajiri, R.; Okubo, T.; Murata, H.; Mitani, T. *Sci. Technol. Adv. Mater.* **2004**, *5*, 331–337.
- (10) Mahapatro, A.K.; Agrawal, R.; Ghosh, S. *J. Appl. Phys.* **2004**, *96*, 3583–3585.
- (11) Meadows, K.A.; Liu, F.; Sou, J.; Hudson, B.P.; McMillin, D.R. *Inorg. Chem.* **1993**, *32*, 2919–2923.
- (12) Liu, F.; Meadows, K.A.; McMillin, D.R. *J. Amer. Chem. Soc.* **1993**, *115*, 6699–6704.
- (13) Guo, X.-Q.; Castellano, F.N.; Li, L.; Szmecinski, H.; Lakowicz, J.R.; Sipior, J. *Anal. Biochem.* **1997**, *254*, 179–186.

- (14) Yam, V.W.; Lo, K.K. *Coord. Chem. Rev.* **1999**, *184*, 157–240.
- (15) McMillin, D.R.; McNett, K.M. *Chem. Rev.* **1998**, *98*, 1201–1219.
- (16) Sun, W.-H.; Jie, S.; Zhang, S.; Zhang, W.; Song, Y.; Ma, H.; Chen, J.; Wedeking, K.; Frölich, R. *Organometallics* **2006**, *25*, 666–677.
- (17) Slough, G.A.; Krchnák, V.; Helquist, P.; Canham, S.M. *Org. Lett.* **2004**, *6*, 2909–2912.
- (18) Corey, E.J.; Borror, A.L.; Foglia, T. *J. Org. Chem.* **1965**, *30*, 288–290.
- (19) Zong, R.; Thummel, R.P. *Inorg. Chem.* **2005**, *44*, 5984–5986.
- (20) van Summeren, R.P.; Moody, D.B.; Feringa, B.L.; Minnaard, A.J. *J. Amer. Chem. Soc.* **2006**, *128*, 4546–4547.
- (21) Zhan, X., Georgia Institute of Technology, Atlanta, GA, Final Report, 2006.
- (22) Kato, T.; Yamanaka, H. *J. Org. Chem.*, **1965**, *30*, 910–913.
- (23) Cho, S.-D.; Park, Y.-D.; Kim, J.-J.; Falck, J.R.; Yoon, Y.-J. *Bull. Korean Chem. Soc.* **2004**, *25*, 407–409.
- (24) Shen, Y.; Sullivan, P. *Inorg. Chem.* **1995**, *34*, 6235–6236.
- (25) Zacharias, D.E. and Case, F.H. *J. Org. Chem.* **1962**, *27*, 3878–3882.
- (26) Druey, J.; Schmidt, P. *Helv. Chim. Acta*, **1950**, *33*, 1080–1087.
- (27) Musumeci, S.; Rizzarelli, E.; Fragalà, I.; Sammartano, S.; Bonomo, R.P. *Inorg. Chim. Acta* **1973**, *7*, 660–664.
- (28) Gürtler, V.O.; Dietz, K.P.; Thomas, P.Z. *Anorg. Allg. Chem.* **1973**, *396*, 217–226.
- (29) Connelly, N.G.; Geiger, W.E. *Chem. Rev.* **1996**, *96*, 877–910.
- (30) Ono, K.; Yanase, T.; Ohkita, M.; Saito, K.; Matsushita, Y.; Naka, S.; Okada, H.; Onnagawa, H. *Chem. Lett.* **2004**, *33*, 276–277.

- (31) Hill, I.G.; Kahn, A. *J. Appl. Phys.* **1999**, *86*, 4515–4519.
- (32) Pangborn, A.B.; Giardello, M.A.; Grubbs, R.H.; Rosen, R.K.; Timmers, F.J.
Organometallics **1996**, *15*, 1518–1520.
- (33) Burd, C.; Weck, M. *Macromolecules* **2005**, *38*, 7225–7230.

CHAPTER 4

CONCLUSIONS

We successfully synthesized three novel norbornene-functionalized TPD monomers (Chapter 2) and six phenanthroline intermediates for norbornene-functionalized monomers (Chapter 3) using the side-chain monomer approach. Our compounds showed promise as potential hole transporting and electron transporting/hole blocking materials for OLEDs.

The electrochemical studies provided evidence that our TPD monomers and phenanthroline intermediates behaved similar to or better than the parent compounds. The phenoxy functionality of the TPD monomers had an insignificant affect on the electronic and spectroscopic properties of the TPD skeleton. Thus, the polymers are expected to increase the T_g of the hole transport layer. The device stability of OLEDs will likely improve while minimally affecting the color light emitted from the devices and the device turn-on voltages.

Phenanthroline small molecules we synthesized were easier to reduce than phenanthroline and commonly used derivatives BCP and Bphen while forming similar quasi-reversible reduction peaks. The observation suggests that devices incorporating norbornene-functionalized derivatives of these small molecules may require lower operating voltages and improve luminance and power efficiencies.

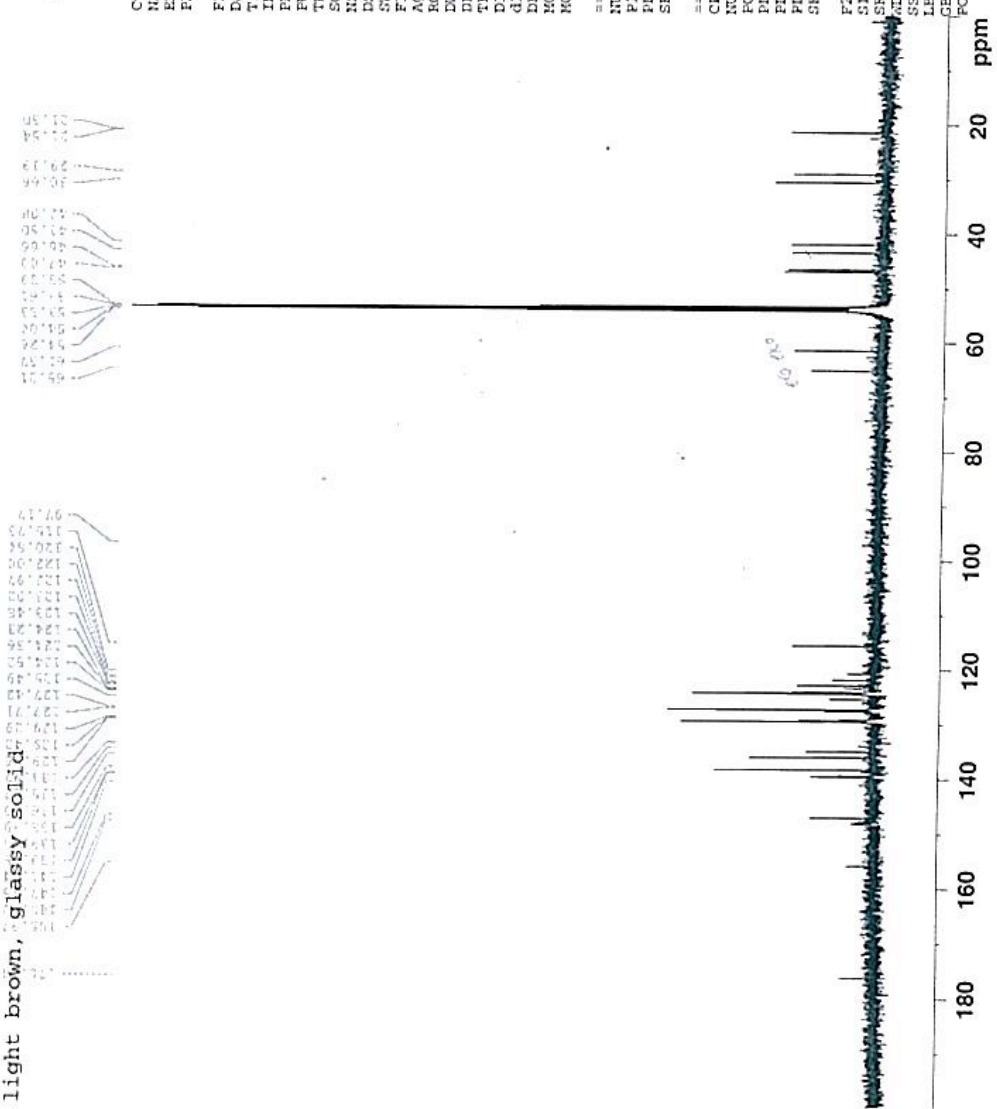
The research in this thesis includes syntheses of novel TPD monomers and a previously unexplored approach to understanding how phenanthroline-based small molecules may contribute to OLED performance parameters (*i.e.*, external quantum efficiency, device lifetime, color purity, etc.). Future work on these projects includes

device fabrication and testing as well as determining parameters like HOMO-LUMO energies, charge carrier mobilities, spectroscopic details (*e.g.*, absorbance, fluorescence), and morphological stabilities of small molecules/monomers and the corresponding polymers.

¹H NMR AND ¹³C NMR SPECTRA OF NOVEL TPD ESTERS



LMM-III-053-D *exo-mor-ester-TPD*
 light brown, glassy solid



```

Current Data Parameters
NAME      LMM-III-053-D
EXPNO     5
PROCNO    1

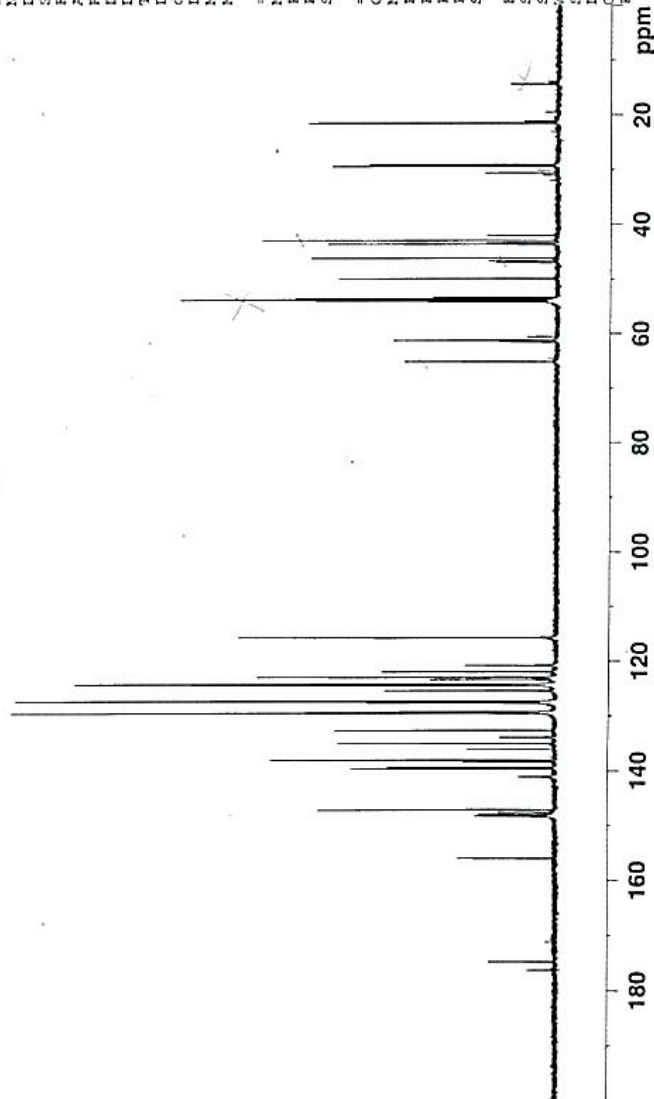
F2 - Acquisition Parameters
Date_     20070820
Time      9.33
INSTRUM   spect
PROBHD    5 mm Multinucl
PULPROG   zgpg30
TD        65536
SOLVENT   CDCl3
NS         1000
DS         4
SFO1      30010.029 Hz
FIDRES    0.458222 Hz
AQ         1.091244 sec
RG         3251
DE         16.650 usec
TE         6.00 usec
TH         298.0 K
D1         2.00000000 sec
d11        0.03000000 sec
DELTA     1.89999998 sec
MCREST    0.00000000 sec
MCNEX     0.01500000 sec

===== CHANNEL f1 =====
NUC1       13C
P1         15.50 usec
PL1        -6.00 dB
SFO1      125.7703643 MHz

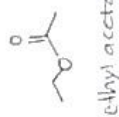
===== CHANNEL f2 =====
CTDPRG2   waltz16
NUC2       1H
P2         68.00 usec
PL2        0.00 dB
PL12       18.00 dB
PL13       120.00 dB
SFO2      500.1320005 MHz

F2 - Processing parameters
SI         32768
SF         125.7577390 MHz
WDW         EM
SSB         0
LB         1.00 Hz
GB         0
PC         1.40
  
```

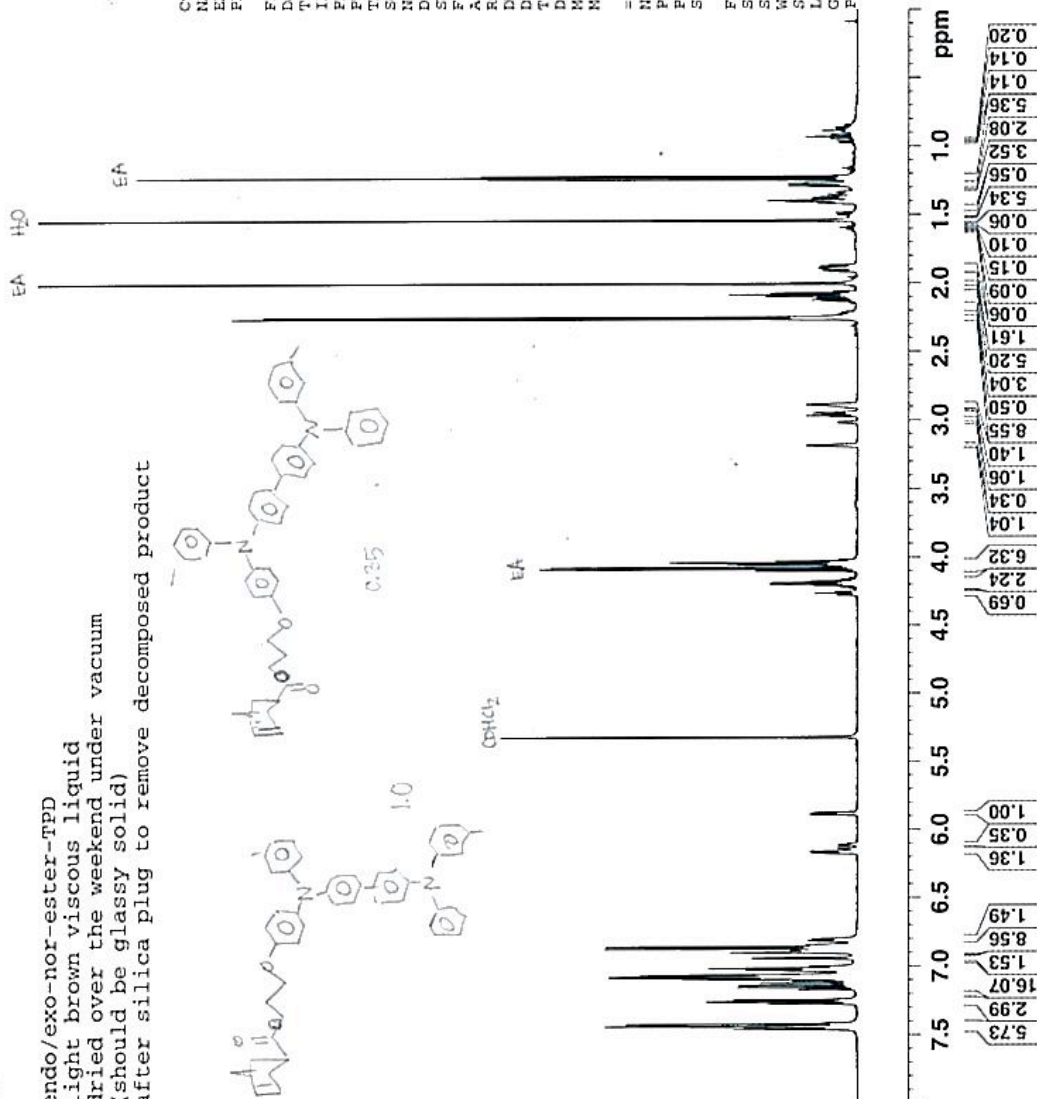
F2 - Processing parameters	
SI	32768
SF	125.7577390 MHz
WDW	EM
SSB	0
LB	1.00 Hz
GB	0
PC	1.40



endo/exo-nor-ester-TPD
light brown viscous liquid
dried over the weekend under vacuum
(should be glassy solid)
after silica plug to remove decomposed product



Current Data Parameters
NAME LHM-III-075-D
EXPNO 1
PROCNO 1
F2 - Acquisition Parameters
Date_ 20060821
Time 14.59
INSTRUM spect
PROBHD 5 mm Multinucl
PULPROG zg30
TD 65536
SOLVENT CD2Cl2
NS 16
DS 2
SWH 10000.000 Hz
FIDRES 0.152588 Hz
AQ 3.2768500 sec
RG 322.5
DM 50.000 usec
DE 6.00 usec
TE 298.0 K
D1 1.00000000 sec
MCREST 0.00000000 sec
MCNPK 0.01500000 sec
===== CHANNEL f1 =====
NUC1 1H
P1 8.80 usec
PL 0.00 dB
SFO1 500.1330885 MHz
F2 - Processing parameters
SI 32768
SF 500.1300207 MHz
WDW EM
SSB 0
LB 0.30 Hz
GB 0
PC 1.00



25% exo